Design and Analysis of Green Mission-Critical Fiber-Wireless Broadband Access Networks

by

Ahmad Dhaini

A thesis
presented to the University of Waterloo
in fulfillment of the
thesis requirement for the degree of
Doctor of Philosophy
in
Electrical and Computer Engineering

Waterloo, Ontario, Canada, 2011

I hereby declare that I am the sole author of this thesis. This is a true copy of the thesis, including any required final revisions, as accepted by my examiners.

I understand that my thesis may be made electronically available to the public.

Abstract

In recent years, the ever-increasing environmental friendliness concern has made energy efficiency in telecom networks as an important theme in their operations. Meanwhile, mission-critical (MC) services and systems (such as healthcare, police, and firefighting) have been acquiring special attention from telecom designers and operators. The currently deployed MC network technologies are indigent in terms of bandwidth capacity, and thus they are not able to support the emerging MC multimedia applications. Therefore in this thesis, we first explore the possibility of provisioning the MC services over the integration of fiber-wireless (FiWi) technologies, which has been considered as a promising candidate for the deployment of high-speed and mobile broadband access networks. We then investigate the energy efficiency problem in the FiWi integration, which consists of WiMAX in the wireless plane, and of Ethernet Passive Optical Network (EPON) – the most popular variant of the next-generation PON (NG-PON) technology, in the optical plane. In WiMAX, the energy saving protocol has been extensively investigated and standardized. Conversely, it has been recently studied in NG-PON, which currently consumes the least power among all the high-speed access networks. However, NG-PON has notably matured in the past few years and is envisioned to massively evolve in the near future. This trend will increase the power requirements of NG-PON and make it no longer coveted. Therefore we address the energy efficiency problem in NG-PON. The accomplishments of the thesis can be briefly summarized as follows.

Firstly, a novel mission-critical FiWi architecture on broadband access networks (namely MC-FiWiBAN) is introduced, where layer-2 virtual private networks (VPNs) are created and each presents a bundle of service requirements to the respective users that connect wirelessly to the base stations. The VPN requirements are stipulated in the service level agreement, and should be fulfilled via a suite of effective bandwidth management solutions. For achieving this, we propose two novel VPN-based admission control (AC) schemes and a dynamic bandwidth

allocation (DBA) mechanism to provide per-stream quality-of-service (QoS) protection and bandwidth guarantee for real-time flows. The first AC scheme is a measurement-based mechanism which admits a flow if enough bandwidth is available to accommodate its data rate in the optical and wireless domains. The second AC scheme is delay-based and it admits a flow if its expected delay is less than the maximum delay requirement, so as to increase the network utilization. The expected delay is measured through a new generic analytical model which applies to both the optical and wireless domains. The DBA is performed via a common medium access control protocol working in both domains as well.

Secondly, the most promising technique to save energy in NG-PON has been to allow the optical network unit (ONU) to go into *sleep* mode. This nonetheless still wastes energy due to the overhead time caused by switching from the *sleep* mode to the *active* mode. To address this problem, we propose a novel green bandwidth allocation (GBA) framework, which aims to explore the maximum design dimensions and achieve the best possible power saving while maintaining the QoS requirements for each type of service. With the batch-mode transmission enabled in the downstream and upstream channels, the ONU can go into the sleep mode for a certain amount of time before waking up to send/receive a batch of buffered traffic. To determine the maximum ONU sleep time without impairing the required QoS, we develop an analytical model which extracts an expression for the maximum ONU sleep time based on the delay requirements of all supported services.
With GBA, the ONU may access the shared media directly upon waking up, which can cause a collision if the sleep times of all ONUs are not well scheduled. We address this problem and propose a novel sleep time sizing mechanism, namely Sort-And-Shift (SAS), which sorts and shifts the sleep times of potentially colliding ONUs until the collision is eliminated while ensuring maximum energy saving.

For each of the aforementioned contributions, we conduct extensive simulations to demonstrate the effectiveness and advantages of the proposed solutions.

Acknowledgements

First and foremost, I wish to express my sincere thanks and gratitude to my thesis supervisor, Prof. Pin-Han Ho, for his expert guidance, help, and support throughout my research work. Professor Ho's boundless enthusiasm and persistent commitment to high quality research have extremely contributed to this thesis.

I would also like to thank my collaborators, Prof. Xiaohong Jiang and Prof. Gangxiang Shen, for their constructive comments on major parts of this work.

I must also thank my colleagues and friends Jean-Paul, Marko, James, Emad, as well as my kind office-mates Amir and Helen for their friendships and discussions who have taught me many things during my studies.

I thank all the staff members in the Electrical and Computer Engineering (ECE) Department for their kind and warm assistance. I also thank the Faculty of Engineering and Computer Science at University of Waterloo, for their superb teaching environment.

I thank Prof. Johnny Wong, Prof. Zhou Wang, and Prof. Paul Ward for serving on my thesis examining committee, and for their kind and constructive comments. I am also very thankful to Prof. Suresh Subramaniam for serving as the external thesis examiner and for his great observations and comments. It is a great honor to have you all as my thesis committee.

My warmest appreciation goes to all my great friends for their support and love during my Ph.D. studies. The list is too long to be accommodated ◡̈. However, I must especially thank Michelle, Jalal, Imad, Benjamin, Khoder, Sandra, and Hussein for always being there for me. Words cannot describe how lucky and honored I am to have you guys in my life.

My deepest gratitude and love go to my dear sisters, brother, father, and dearly beloved mother whom with their endless giving love and support throughout my life made everything possible.

Last but not least, I thank God for providing me with the faith, will, and energy to achieve my goals in life.

Dedication

To my dearly beloved family

Contents

List of Tables

List of Figures

Chapter 1

Introduction

Over the past decade, major work has been done in the areas of broadband access networks[1]. Specifically, optical and wireless access networks have significantly improved the Internet access for private and public users by increasing their capacities while offering end-user mobility. Access networks and equally mission-critical networks have been exposed under substantial challenges due to the ever-increasing bandwidth needs, the asymmetric backbone capacity and the "anytime-anywhere" Internet access demand. Moreover, the tremendous growth of Internet traffic has drawn a deep attention to the aggravating lag of access networks' capacities in meeting the users' requests and requirements.

Recently, energy efficient networks have become a crucial requirement in the fight against global warming and the control of operational expenses. Meanwhile, network operators and users have increased their interests in environment-friendly technologies. As a result, standardization bodies and equipment vendors have launched various projects to provide energy efficient solutions in the near future. Particularly, decreasing the power consumption of access networks has become an urgent requirement, as these networks constitute the largest part of the Internet and connect a big amount of active devices.

[1]Broadband refers to a transmission speed of 1.54 million bits per second or more using a single medium that has two or more channels carrying information at once.

In the following sections, we discuss each of these aforementioned themes while highlighting the related challenges that motivate the thesis. We then introduce our contributions and the organization of the thesis.

1.1 Internet Traffic Growth

The Internet has become phenomenally popular and the number of users requiring broadband access and willing to pay for it, has been increasing steadily despite the drops in the global economy [1]. A massive growth in the number of people requiring broadband access is forecasted. Most of the development in broadband networks based on the optical and wireless technologies has been achieved as a result of an active and stimulating role of governmental agencies. These agencies strive to implement policies that can increase the computer literacy rates amongst its citizens [2].

Studies show that data traffic is increasing at an exponential rate and has already surpassed voice traffic [2]. Market research shows that after upgrading the broadband connection, a significant increase in the amount of users that are online have been witnessed ($35 \sim 40\%$). The voice traffic, which used to be requested in small amounts, have been increasing at a rate of $8 \sim 9\%$ per annum [2]. This trend is expected to continue in the future, especially with the new emerging bandwidth-intensive and real-time applications envisioned to monopolize the users' activities over the Internet.

1.2 The First Mile Evolution

The first mile[2] (or "last mile" as called by some telecommunications operators), has been a major bottleneck between the high-capacity Local Area Networks (LANs)

[2] *First Mile*: Mile or Km that connects the service provider central offices to businesses and residential subscribers (also known as the access network).

and the subscriber home network. The huge amount of bandwidth carried by the backbone has to reach the users premises through the access network. This asymmetry of capacities generates a problem, known as the bandwidth *bottleneck problem.*

1.2.1 Wired Access Networks

The wired broadband technologies that are widely deployed to provide services in the last mile are Digital Subscriber Loop (DSL) and Cable Modem (CM). DSL is ubiquitous and is capable of offering general web browsing and e-mail services. However, it is not able to support the emerging media-rich broadband services. Moreover due to signal distortion, the physical area that a Central Office (CO) can cover with DSL is limited to distances less than 18000 ft. In general, network operators do not provide DSL services to subscribers located more than 12000 ft from the CO due to the potentially increased cost. Although other variants of DSL (e.g., VDSL, ADSL2, and G.SHDSL) providing higher data rates have been considered, these technologies are expensive and still pose network reach limitations. On the other hand, CM can only provide Internet access at low speeds and is incapable of offering services over large distances with high reliability.

To alleviate these bandwidth bottlenecks, optical fibers have penetrated deeper into the first mile with a great promise to offer fiber to the home (FTTH) and fiber to the building (FTTB). Consequently, many telecom companies (e.g., NT&T and Verizon) have started to switch to the fiber technology by employing promising network solutions such as Next-Generation Passive Optical Network (NG-PON) [3].

NG-PON (or simply PON) is a point-to-multipoint (P2MP) access network with no active elements in the signals path from source to destination. The only interior elements used in PON are passive such as optical fiber, splices, and splitters. NG-PON is viewed by many as an attractive and cost-effective solution for the access network bottleneck and as the final frontier of optical FTTX networks, where they may interface with a number of wireless access technologies.

The term NG-PON became popular with the famous Ethernet PON (EPON) which takes advantage of inexpensive and ubiquitous Ethernet equipment, and offers a transmission speed of 1 *Gbps*. Before EPON, other standardized NG-PON versions such as Broadband PON (PON) also called Asynchronous Transfer Mode (ATM) PON (APON), existed. However, the proliferation of bandwidth-hungry applications such as voice over Internet Protocol (VoIP), standard and high-definition television (HDTV), video conferencing (interactive video), and data traffic with strict quality-of-service (QoS) requirements, has greatly contributed to the rapid advancement of NG-PON. Consequently, higher speed versions emerged such as Gigabit EPON (G-EPON), Gigabit PON (GPON) which also supports ATM, Wavelength Division Multiplexing PON (WDM-PON), and Long-Reach PON (LR-PON). LR-PON mainly extends the reaching ability of PONs and like WDM-PON, employs multiple wavelengths in the optical channel. Currently, the term NG-PON1 is used for the *evolutionary* growth of EPON/GPON, which supports coexistence with EPON/GPON on the same optical distribution network (ODN); and the term NG-PON2 represents the *revolutionary* change of NG-PON with no requirement in terms of coexistence with EPON/GPON on the same ODN [3].

1.2.2 Wireless Access Networks

Wireless and mobile technologies have presented themselves as a powerful tool to break the barriers of time and space. With the introduction of high-bandwidth digital communication technologies, it is possible to deliver audio, video, and waveform data to wherever and whenever needed. Satellite-based solutions and those based on second-generation (2G) and third-generation (3G) mobile technology, as well as global systems for mobile communications (GSM) appeared, enabling the delivery of remote services in mobile environments as well as communications to geographic zones inaccessible by fixed networks.

With the successful penetration and the tremendous success of wireless technologies in the telecommunications arena, the idea of a broadband wireless system as a

next-generation access network became viable through the introduction of Worldwide Interoperability for Microwave Access (WiMAX)[3], and Long Term Evolution (LTE)[4] networks. These networks offer wireless broadband access in the last mile with a rich variety of deployment scenarios and transmission speeds.

1.2.3 Fiber-Wireless Access Networks: The Next Evolutionary Step

Recently, the integration of EPON and WiMAX has been presented as the next evolutionary step toward the convergence to a high-speed, wireless, and cost-effective fiber-wireless (FiWi) broadband access network [4, 5, 6]. More attractively, EPON and WiMAX perfectly match in terms of capacity hierarchies and design premises. EPON for instance, supports a total of 1 *Gbps* bandwidth, shared by typically $8 \sim 32$ remote optical network units (ONUs). On average, each ONU accesses ≈ 70 *Mbps* bandwidth, which matches the total capacity offered by a WiMAX base station (BS) over a 20 MHz channel. In addition, the integration enables integrated resource allocation and packet scheduling paradigms that help ameliorate the performance level of emerging QoS applications, as well as improve the overall network throughput. Furthermore, the integration can help realize fixed mobile convergence (FMC) by supporting mobility in the broadband network access, thereby significantly reducing network design and operational costs [4, 7].

In spite of its numerous advantages, the integration of EPON and WiMAX requires addressing many research challenges and issues that are critical in pushing this promising network into practical deployment (e.g., traffic mapping, bandwidth allocation, handover, addressing, packet forwarding, and many more).

[3]http://www.wimaxforum.org/home/
[4]http://www.3gpp.org/LTE

1.3 Mission-Critical Networks Evolution

Mission-critical (MC) systems and organizations such as healthcare, police, and firefighting, rely heavily on the underlying telecommunications infrastructure to conduct their daily tactical and emergency operations. In recent years, the MC sector has witnessed the proliferation of diverse multimedia applications such as remote patient monitoring, 2-way video/audio-conferencing, 3D geographical mapping and positioning, enhanced telemetry, and live surveillance video broadcasting. All these technological advancements are expected to force the MC service providers (SPs) to migrate from simple data services to *triple-play* (data, voice, and video) or even *quadruple-play* services (triple-play services plus mobile) on a single infrastructure in order to offer state-of-the-art MC service support.

Public Safety and Disaster Relief (PSDR) networks are particularly designed to guarantee a reliable, continuous, secure, and flexible MC service. Since 1997, the TErrestrial Trunked RAdio (TETRA) standard [8] (which is predominant in Europe, Middle East and Africa, and in Asia Pacific) and the ASTRO-25 standard (which is equally predominant in the Americas) have become the de-facto standards for PSDR communications, and have been employed by senior market players (e.g., Motorola, Nokia, and Lucent-Alcatel) in their deployment of MC networks in rural and urban areas. More interestingly, TETRA networks have successfully penetrated other large markets such as transportation, utilities, and oil/gas services (as recently announced in Qatar) [9]. The current two major TETRA releases (TETRA-1 and TETRA-2) developed by the European Telecommunications Standards Institute (ETSI), provide radio capabilities endorsing network controlled services and direct mobile-to-mobile communications, with a wide range of functionalities such as group calls, fast call-setup, encryption/decryption, real-time localization, and grade-of-service connections [8]. However, the access capability offered by TETRA, which focuses on voice plus data (V+D) services only, is not sufficient to satisfy the bandwidth requirements of the emerging multimedia PSDR applications. The transmission rates of these applications are peculiarly higher than the 28.8

kbps TETRA maximum data bit rate. Furthermore, the available MC network resources (e.g., wireless radio bands) in most parts of the world are unable to satisfy the increasing MC bandwidth requirements, which has motivated the MC SPs to investigate the feasibility of employing public networks to support the emerging PSDR applications [10].

In May 2000, Project MESA [11] was introduced to define a new platform and a set of MC requirements that aim at forming an advanced PSDR telecommunication network with an improved bit rate of 2 Mbps. In 2007, Motorola announced MOTOA^4 [12], a suite of proprietary network solutions leveraging the ubiquity of the IEEE 802.11n to form a wireless outdoor mesh wide area network. MOTOA^4 operates at high data bit rates of 300 Mbps and offers full ASTRO interoperability. However, its deployment has been restricted to urban areas only.

Although the evolution of public networks has significantly contributed to the advancement of the MC telecommunications sector, a big gap still exists between public networks and MC networks. The current MC network technolgies are unable to cope with the emerging MC requirements and demands. Therefore, new architectures and solutions are required to support these services. The new architectures should be able to meet the unique MC network requirements (which are detailed in the next chapter) and at the same time provide the MC users with high-speed and mobile Internet access in urban and rural areas.

1.4 Energy Efficiency in Access Networks

In order to meet the expected global energy demand in year 2035, power production must increase by almost 49%, which is not feasible [13]. Meanwhile, the bare necessity for ensuring sustainability requires reducing global green house gas emissions at large quantities. Recent studies have revealed shocking facts regarding the energy consumption in modern telecommunications networks. According to Bell Labs, today's networks consume 10,000 times more energy than the absolute mini-

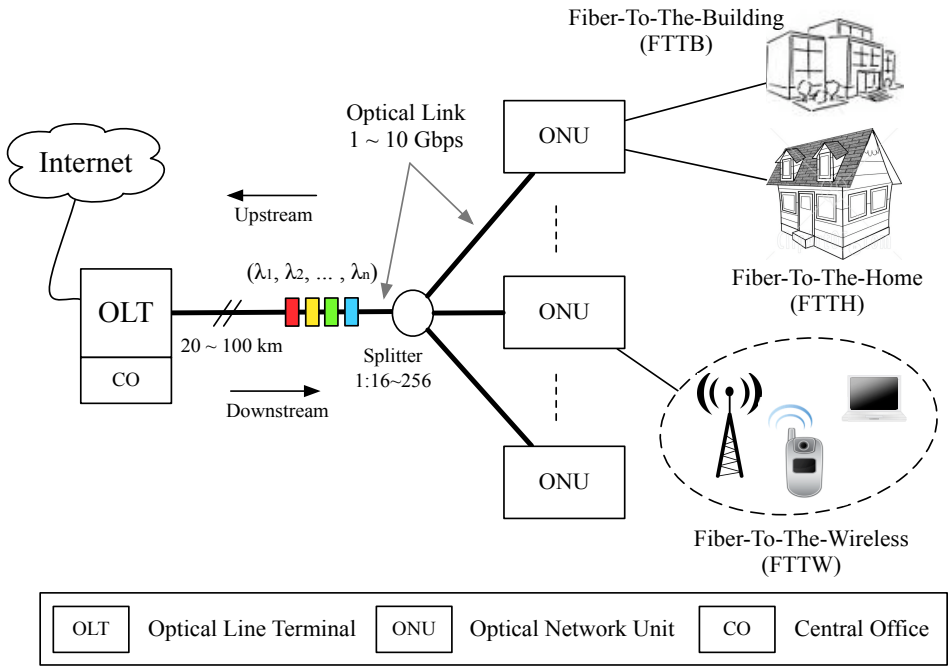

Figure 1.1: Evolution of the NG-PON P2MP architecture: Higher transmission rates, higher split ratios, more ONUs, longer reach abilities and multiple wavelengths.

mum required. The Internet currently consumes about 0.4% of the total electricity consumption in broadband-enabled countries and is foreseen to reach 1% with the data transmission rate increase trend [14]. These appalling numbers have triggered tremendous efforts and collaborations between industry and academia to undertake this challenging problem [15, 16]. Consequently in 2010, GreenTouch [14] – a consortium of leading Information and Communications Technology (ICT) industry, academic, and non-governmental research experts, was launched aiming to make communications networks, within five years, 1,000 times more energy efficient. A joint effort to achieve these theoretical limits would not only reduce the estimated 2% of the world's carbon emissions ICT contributes directly, but would also lower the 98% contributed by all the other sectors touched directly and indirectly by ICT [14].

Energy efficiency has long been studied in wireless technologies such as wireless sensor networks where the network elements have limited power supply. In advanced access network technologies such as WiMAX, the energy saving mecha-

nism has already been standardized [17], and Ethernet networks have also received their share of attention in the research community [18, 19]. Conversely, energy efficiency in optical Internet Protocol (IP) networks has recently been studied [20, 21], although these networks constitute a big portion of the modern Internet infrastructure. Consequently, many strategies have aimed at re-engineering the current optical communication system in order to save energy while maintaining the desired network performance [22].

Recent studies show that NG-PON consumes the least power among all the broadband access technologies [20]. However, its evolution is expected to significantly increase its energy consumption [3]. As illustrated in Fig. 1.1, NG-PON is envisioned to support very high data rates (up to 10 *Gbps*), long reach abilities (up to 100 *km*) and very high split ratios (up to 1 : 256), thereby provisioning a large number of active devices in very wide areas. To date, only few techniques have been proposed to address this problem that is currently being standardized [23, 24]. Among those, putting the ONU into sleep mode has been the most promising technique. However, intelligent protocols and mechanisms are still required to manipulate the sleep period of the ONU to achieve maximum energy saving without impairing the users' requirements.

1.5 Thesis Motivation and Contributions

The first aim of our work is to take advantage of the public network evolution to provide state-of-the-art MC service support in urban and rural areas. Specifically, the contributions of the thesis in this subject are summarized as follows:

1. We propose a new emergency-aware mission-critical fiber-wireless broadband access network architecture (namely, MC-FiWiBAN), to support MC services over FiWi access networks. MC-FiWiBAN employs the EPON-WiMAX integration as the underlying infrastructure in order to provide the MC systems with the luxury of high-bandwidth and user-mobility. To offer security and

customized network control for the MC users, we propose to construct layer-2 virtual private networks (VPNs) over the integration. To the best of our knowledge, this is the first work that considers the support of layer-2 VPNs over EPON or WIMAX, and over the EPON-WIMAX integration as well. With MC-FiWiBAN, we also define and present new techniques to address important MC netwok requirements such as fault tolerance and error recovery.

2. We attempt to provide effective solutions to the resource management and QoS assurance problems - two of the key issues that arise in the VPN construction over a shared network infrastructure. A resource allocation framework, so-called WiMAX-V**P**ON, is presented to offer guaranteed QoS for MC services as defined in the VPN service level agreement (SLA). Particularly, WiMAX-V**P**ON comprises the following:

   (a) A new QoS-provisioning paradigm that fairly distributes the EPON-WIMAX bandwidth among the VPNs.

   (b) A novel measurement-VPN-based admission control scheme that admits a VPN flow if its data rate can be accommodated in both the optical and wireless domains.

   (c) A new delay-based admission control engine that admits a VPN flow if its expected end-to-end (from SS to OLT) average delay is less than the maximum delay requirement.

   (d) A novel VPN-based bandwidth allocation mechanism that operates in the optical and wireless domains, and which guarantees the bandwidth committed for each admitted flow.

The second aim of this work is to make the optical part of the FiWi integration (i.e., NG-PON or EPON) be energy efficient, thereby contributing to the ongoing efforts toward standardizing the energy saving mechanism in NG-PON. Specifically, the contributions of the thesis in this subject are summarized as follows:

1. We propose a novel green bandwidth allocation (GBA) framework, which leverages the sleep mode feature of the ONU to achieve the maximum possible energy saving. The salient feature of GBA is that the QoS requirements of all types of services are taken as a constraint when the sleep time is computed for every ONU. Further, due to its novel design in terms of batch-mode transmissions, more energy can be saved with the same amount of sleep time.

2. We address the problem that emerges when multiple ONUs are scheduled to access the shared media directly upon waking up from the sleep mode, without properly synchronizing their sleep times. This is a research issue that has not been investigated before. To resolve this problem, we propose a new sleep time sizing scheme, so-called Sort-And-Shift (SAS), which sorts and shifts the sleep time of the collided ONUs until the collision is eliminated. SAS saves the shifted sleep time portion as "credit" for the ONU in the next cycle so as to ensure that the ONU is fully granted with its allocated sleep time, thereby ensuring maximum energy saving.

1.6 Organization of The Thesis

The rest of the thesis is organized as follows. Chapter 2 presents an overview of the enabling technologies used in the integration, as well as the mission-critical systems. Several open research issues identified in the EPON-WiMAX integration are highlighted, and a review of the most relevant related work is also presented. This chapter also presents a literature survey on the energy efficiency techniques in NG-PONs. In Chapter 3, we present MC-FiWiBAN. The potential advantages and the related design issues are also exhibited. Chapter 4 presents the proposed WiMAX-V**P**ON framework. In Chapter 5, we present our GBA framework and the SAS mechanism. We finally conclude the thesis in Chapter 6 and we discuss potential future work.

Chapter 2

Background and Related Work

2.1 EPON-WiMAX Enabling Technologies

2.1.1 EPON: An Overview

EPON [25] represents the convergence of inexpensive and ubiquitous Ethernet equipment with low-cost fiber infrastructure. It has been standardized by the IEEE 802.3ah working group [26] and is considered the most famous variant of the NG-PON family.

Like any NG-PON technology, as illustrated in Fig. 1.1, EPON comprises one Optical Line Terminal (OLT) that connects a set of associated ONUs through a single fiber. The OLT resides in the provider's CO and connects the optical access network to the metropolitan area network (MAN) or wide area network (WAN). On the other hand, the ONU is usually located at either the curb (i.e., FTTC) or the end-user location (i.e., FTTB or FTTH), and provides broadband video, data, and voice services.

EPON systems deploy one channel for downstream traffic and another channel for upstream traffic. In the downstream, Ethernet frames are broadcasted by the OLT and are selectively received by each ONU. Alternatively in the upstream, multiple ONUs share the same transmission channel to transmit data and control

packets to the OLT. To prevent collisions, a medium access control (MAC) protocol is required to arbitrate the access of the ONUs to the shared media. EPON's current MAC supports Time Division Multiple Access (TDMA) [27]. Hence in every frame/cycle, each ONU is allocated a time slot, and the packets arriving from different subscribers are buffered until they are transmitted in the assigned transmission window (TW).

Multi-point Control Protocol (MPCP)

The OLT-ONUs communication is conducted via MPCP (multi-point control protocol). MPCP is a signaling access protocol that the OLT to gather information from different ONUs using MPCP's REPORT messages, and to allocate bandwidth to the ONUs using MPCP's GATE messages. Note that MPCP does not specify any particular bandwidth allocation mechanism. Instead, it is designed to facilitate the implementation of the bandwidth allocation schemes.

Dynamic Bandwidth Allocation (DBA)

The bandwidth allocation for the ONUs' incoming flows/packets on the upstream channel can be performed in the following two ways:

- **Inter-ONU scheduling**: Here, the OLT is responsible for arbitrating the transmission of the ONUs over the upstream shared media. This can either be done in a static fashion (i.e., static bandwidth allocation [SBA]) where the OLT assigns a fixed time slot for every ONU regardless of its bandwidth demands; or in a dynamic fashion (i.e., dynamic bandwidth allocation [DBA]) where the allocation is based on the ONUs' demands and other factors such as the QoS requirements and the SLA.
- **Intra-ONU scheduling**: Here, the ONU is responsible for allocating bandwidth for the packets of each classe of service (CoS) queue, to be transmitted

in the upstream TW that is assigned by the OLT through the employed DBA [28, 29].

Many DBA schemes have been proposed in the literature. These schemes mainly aim at either improving the statistical multiplexing in EPON or providing QoS assurance for all types of services. Interested readers are referred to reference [30] for a comprehensive survey on DBAs in EPON.

QoS Support in EPON

EPON networks support diverse applications with differentiated services (DiffServ). These services are typically aggregated into three main CoSs: 1) *Best Effort (BE) "data"* traffic, 2) *Assured Forwarding (AF)* traffic such as variable-bit-rate (VBR) video stream and 3) *Expedited Forwarding (EF)* traffic used to emulate point-to-point (P2P) connections or real time services, such as VoIP. The high priority class is *EF*, which is delay-sensitive and requires bandwidth guarantees. The medium priority class is *AF*, which is not delay-sensitive but requires bandwidth guarantees. The low priority class is *BE* which has no specific QoS requirements. According to the IEEE 802.3ah standard, each ONU can support up to eight priority queues or possibly eight different CoSs [27].

2.1.2 WiMAX: An Overview

The IEEE 802.16/WiMAX technology [17] was initially desgined to provide broadband wireless connectivity to fixed and mobile users in a wireless-MAN environment. However, the standard provides the flexibility for different deployment scenarios. Namely, WiMAX can either be deployed as a broadband wireless access (BWA) or as a wireless backhaul network. As illustrated in Fig. 2.1, The BWA WiMAX is a P2MP single-hop network with a single base station (BS) and multiple subscriber stations (SSs) or mobile stations (MSs). As backhaul, WiMAX is expected to transport traffic from the cellular edge to the core network through a

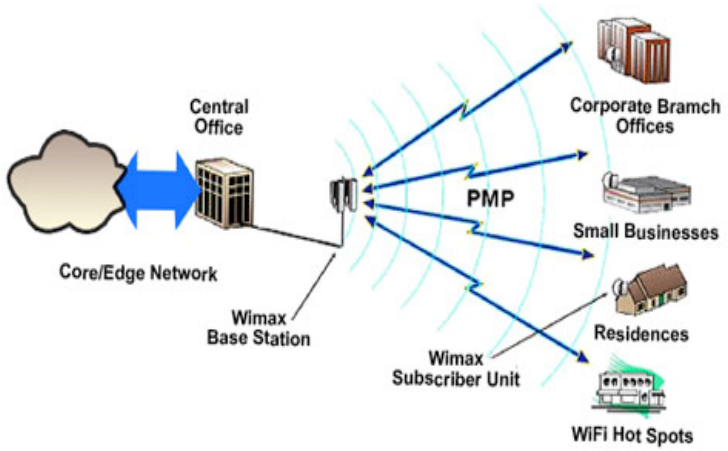

Figure 2.1: WiMAX P2MP architecture [http://www.conniq.com].

wireless mesh network made by the BS and SSs, as shown in Fig. 2.2. The IEEE 802.16 standard defines the physical (PHY) and MAC layers.

PHY Layer

PHY's air interface operates at $10-66\ GHz$ and $2-11$ GHz bands and supports data rates in the range of $32-130\ Mbps$, depending on the operation bandwidth (e.g., 20, 25, or 28 MHz) and the enabled modulation and coding schemes. The $10-66\ GHz$ band is used when the BS and the SS are in line-of-sight (LOS), and the $2-11\ GHz$ band is used when the BS and the SS are in non-line-of-sight (NLOS). The latter is supported through three different air interfaces:

- Single Carrier (SC) modulation (WirelessMAN-SCa).
- Orthogonal Frequency Division Multiplexing-based (OFDM) transmission (WirelessMAN-OFDM). Here, the MAC protocol is TDMA-based such that all the OFDM subcarriers are assigned to the same SS in the time domain.
- Orthogonal Frequency Division Multiple Access-based (OFDMA) transmission (WirelessMAN-OFDMA). Here, different groups of subcarriers may be assigned to different SSs.

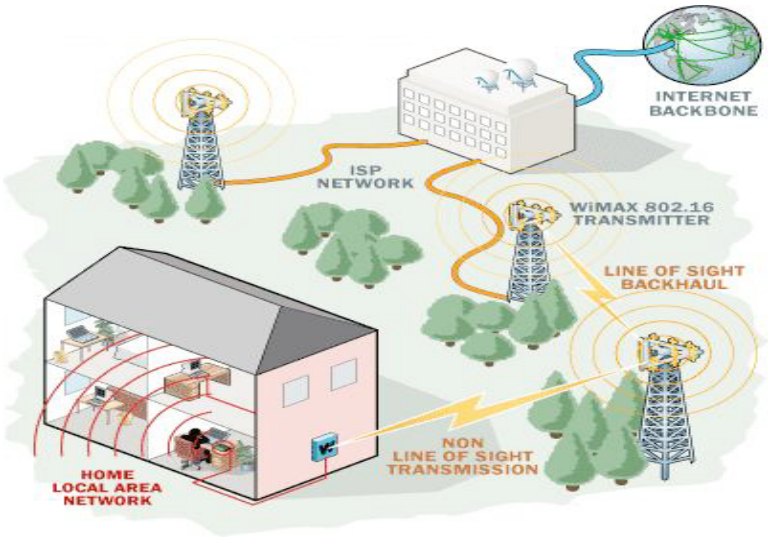

Figure 2.2: WiMAX mesh architecture [http://computer.howstuffworks.com].

OFDM is widely employed in modern broadband communication systems, due to its hardware implementation simplicity. On the other hand, OFDMA has been mainly employed in WiMAX to allow user mobility in NLOS environments. This is due to the fact that in mobile systems, the subchannelization scheme based on dispersed subcarrier allocation to subchannels is mandatory in all mobile WiMAX implementations, which can only be achieved using the OFDMA technology. When subcarriers assigned to one subchannel are distributed over the available bandwidth, frequency diversity can be achieved. This diversity is important because it can be used to make the transmission link more resistant against fast fading. Nevertheless, the resource management scheme over OFDMA systems becomes more complex.

MAC Layer

The main purpose of the IEEE 802.16 MAC is the management of radio resources for multiple accesses of different users. As shown in Fig. 2.3, it is divided into three sublayers: convergence sublayer, common MAC sublayer, and security sublayer. The primary task of the convergence sublayer is to classify each MAC service data unit (MSDU) and associate it with the proper MAC service flow and connection

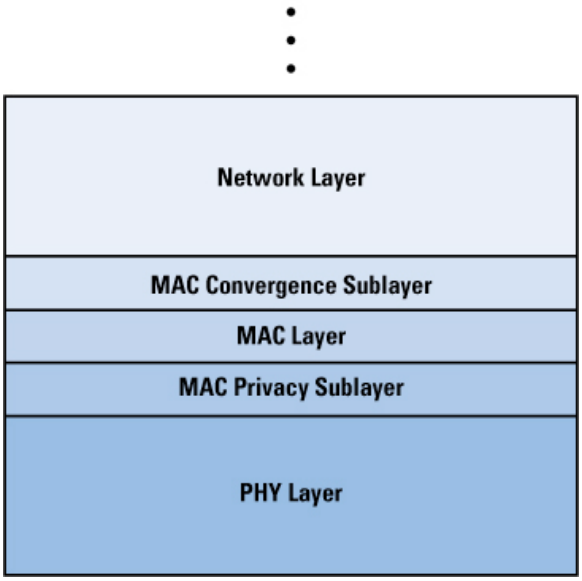

Figure 2.3: WiMAX protocol stack [http://www.cisco.com].

identifiers. The common MAC sublayer is independent of the transport layer protocol, and is responsible for the fragmentation and segmentation of each MSDU into MAC protocol data units (PDUs). The MAC also contains a separate security or privacy sublayer, which handles authentication, secure key exchange, and encryption matters.

The MAC portion of the standard is frequency-independent. More specifically, the IEEE 802.16/WiMAX MAC supports the PHY layer in frequency-division duplex (FDD) and time-division duplex (TDD) transmission modes:

- With the FDD mode, the uplink and downlink links use separate subcarriers, which allows the SSs to transmit and receive simultaneously.

- With the TDD mode, a MAC frame is divided into uplink (UL) and downlink (DL) sub-frames. The lengths of these sub-frames are determined dynamically by the BS and are broadcasted to the SSs through the downlink and uplink MAP messages (i.e., UL_MAP and DL_MAP) at the beginning of each frame. An illustration of a WiMAX OFDMA frame under the TDD mode is given in Fig. 2.4.

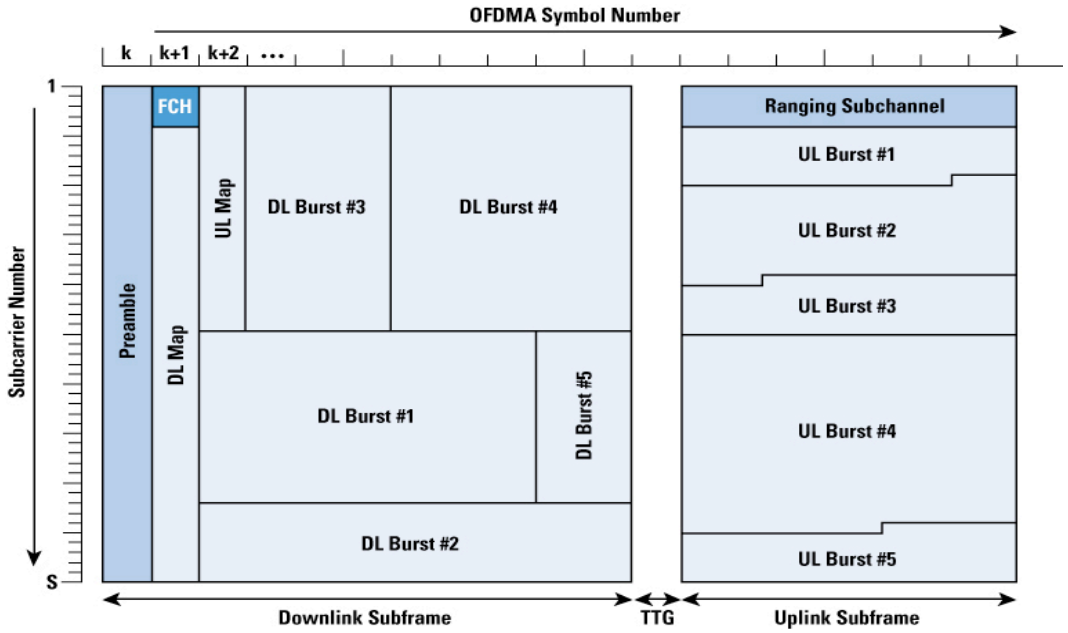

Figure 2.4: WiMAX OFDMA/TDD frame structure [http://www.cisco.com] (TTG is the guard time that seperates the uplink and downlink subframes, and FCH is the Frame Control Header).

TDD enables more flexible sharing of the available bandwidth than FDD. However for mesh-based WiMAX, TDD requires synchronization between multiple BSs in order to avoid interference among neighboring cells.

As in EPON, the IEEE 802.16 standard does not specify any bandwidth allocation scheme. However, it defines request and grant mechanisms to facilitate the implementation of the DBA. In specific, each SS can request bandwidth from the BS via the BW_Request PDU in two different modes:

1. Contention mode: Here, an SS transmits BW_Request PDUs during the contention period, and a backoff mechanism is used to resolve the contention among the BW_Request PDUs of different SSs.

2. Contention-free mode (i.e., polling): Here, an SS is periodically polled by the BS, and it responds by sending the BW_Request PDU.

The contention-free mode is more suitable for QoS-sensitive applications as it enables a "predictable" packet delay.

The bandwidth requests are always per-connection, and they can either be sent as stand-alone packets or they can be piggybacked with data packets. In addition, they can either be incremental or aggregate. An incremental bandwidth request means that the SS requires more bandwidth for an existing connection. An aggregate bandwidth request means that the SS is specifying in advance how much total bandwidth is needed for a connection. Most requests are incremental, but aggregate requests are occasionally used to correct the BS's perception of the SSs' needs.

WiMAX networks provision Integrated Services (IntServ) such that the bandwidth grants are specified by the BS in two ways: 1) Grant Per Connection (GPC) and 2) Grant Per Subscriber Station (GPSS). With GPC, the BS allocates bandwidth for every connection; whereas with GPSS, the BS allocates bandwidth for an SS in aggregate, and the SS is responsible for distributing the allocated bandwidth among its connections. GPC is more favorable if few users are connected to the SS at the expense of making the DBA scheme more complex. Conversely, GPSS is scalable and it reacts more quickly to the QoS needs of every connection. However, it requires an intelligent and "heavier" SS.

For multi-carrier air interfaces, the BS allocates OFDM subcarriers and power to the SSs/MSs based on the perfect knowledge of their channel state information (CSI). Every SS estimates its CSI and reports it to the BS at the beginning of each frame[1]. The BS then allocates the resources based on the information included in the CSI and broadcasts the allocation vector on a signaling channel at the beginning of the next frame.

Many DBA schemes have been proposed to perform power and bandwidth allocation in WiMAX. Interested readers are referred to reference [31] for a survey on DBAs in WiMAX.

[1]The CSI can also be incorporated in the BW_Request.

QoS Support in WiMAX

To support QoS in the MAC, The IEEE 802.16 standard defines five classes of service [17]:

- Unsolicited Grant Service (*UGS*): This service class enables fixed bandwidth allocation. That is once a UGS flow is admitted in the network, its bandwidth is allocated automatically in each specified period of time (could be in each frame). Like EF, this service is designed to provision CBR traffic with maximum sustained rate (MST) as an additional QoS requirement.

- Extended real-time Polling Service (*ertPS*)[2]: This service is designed to support VoIP with silence suppression (i.e., no traffic is sent during silent periods). With ertPS, the BS allocates the ertPS flow's MST in the active period and nothing is allocated during the silent period, thereby saving the control messaging overhead in the silent period. The QoS requirements of the ertPS service are similar to UGS's.

- Real-time Polling Service (*rtPS*): This service class is designed to support VBR traffic and is reported to the BS in every polling interval (PI). The QoS requirements are in terms of packet latency and throughput.

- Non-realtime Polling Service (*nrtPS*): This service class is for non-real-time VBR traffic (e.g., File Transfer Protocol [FTP]) with no delay requirements and only minimum throughput guarantees.

- *BE*: Same as BE in EPON, this service class requires neither delay nor throughput guarantees.

[2]ertPS is defined in the IEEE 802.16e version of the WiMAX standard.

2.2 EPON-WiMAX Integration: Challenges and Related Work

In this section, we first discuss the advantages of the EPON-WiMAX integration which make it an attractive solution. We then present an overview of the work related to resource management in EPON-WiMAX since it is the focus of our research. Fig. 2.5 depicts the taxonomy graph for the related work including the relation between the employed architectures and the challenges addressed in each of the references.

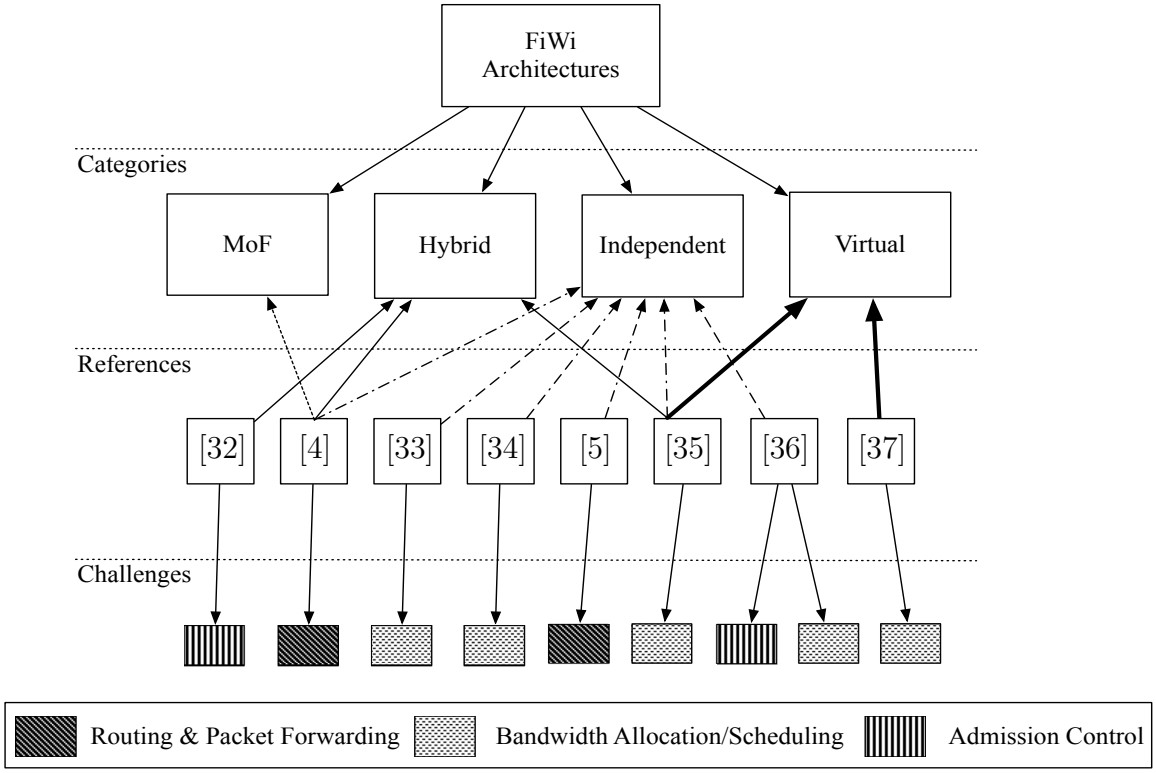

Figure 2.5: Taxonomy for the FiWi related work

2.2.1 Advantages of EPON-WiMAX

The integration of EPON and WiMAX has various advantages. The most important ones are summarized as follows:

1. *Cost Efficiency*: With the wireless/mobile characteristic of WiMAX, installing fiber all the way until the customers' premises is no longer required. This can significantly reduce the network's deployment and maintenance costs.

2. *Flexibility*: The "anytime-anywhere" feature that distinguishes wireless networks is also applicable to the integration. This is due to the fact that users are served through the wireless front-end of the hybrid network, thereby enabling a seamless wireless inter-connection for the users.

3. *Robustness*: FiWi networks are more robust than standalone wired networks such as EPON. In the case of a fiber link failure or cut, all the users served by a certain FiWi BS can immediately pair with a different reachable BS.

4. *Reliability and Load Balancing*: EPON-WiMAX does not suffer from congestion or information loss, due to the inherent reliability of optical networks. Moreover, hybrid networks can have better load balancing capabilities due to the wireless users' mobility.

5. *Fault Tolerence*: The EPON-WiMAX network's connectivity and its load balancing characteristics make it "self-organizing". This feature facilitates the implementation of robust routing and traffic forwarding techniques to recover from possible faults or failures.

2.2.2 EPON-WiMAX Architectures

The authors of [4] investigated candidate architectures for the EPON-WiMAX integration. As illustrated in Fig.2.6, the difference between these architectures is in the mounting procedure of the EPON's ONU and the WiMAX's BS, except if the Radio-over-Fiber (RoF) technology is used for the communication between the BS and SSs. The architectures are detailed below.

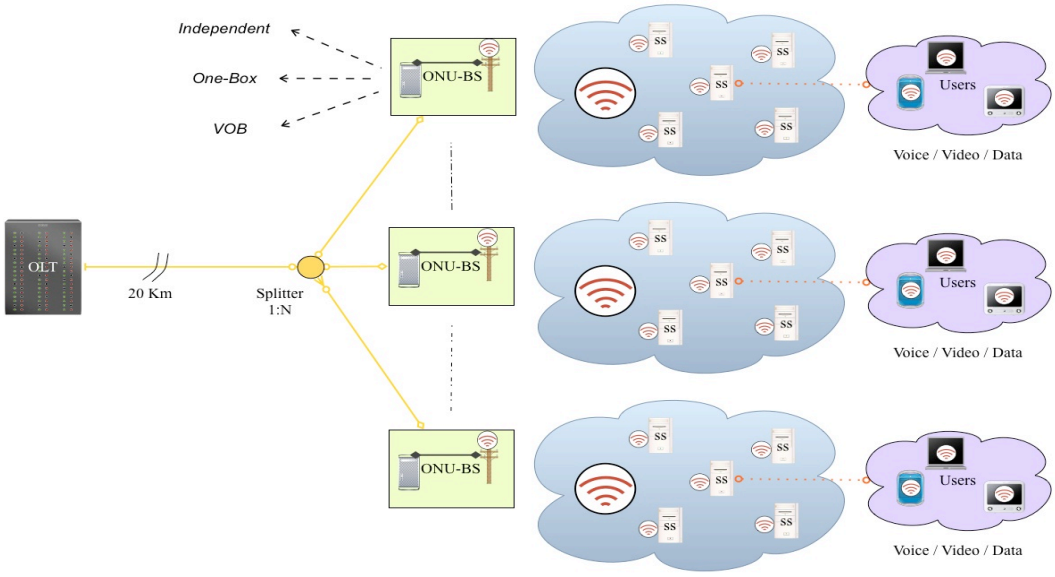

Figure 2.6: EPON-WiMAX architecture

Independent

In this architecture, EPON and WiMAX work independently. As a result, each ONU would consider a WiMAX BS as an end-user and can interconnect it through Ethernet (a common supported standard interface). The advantage of this architecture is that no amendment is required to the EPON and WiMAX standards. Nonetheless, the fact that those two networks operate autonomously makes the scheduling details in the wireless plane hidden from the ONU, especially in the uplink/upstream direction where packets are eventually destined to the OLT. Furthermore, the fact that two devices (ONU and BS) are required in the middle-end of the network, makes this architecture costly and thus less attractive.

Hybrid

In this architecture, the ONU and the BS are mounted in one box, so-called *ONU-BS*. It is designed to compensate for the drawbacks of the previous architecture by enabling *centralized* operation and management in the mounted box at the expense of additional hardware and software requirements. At the hardware level, three CPUs may be installed (i.e., CPU-1, CPU-2, and CPU-3). CPU-1 works on the

EPON-end of the integration and runs the MPCP, whereas CPU-3 handles the WiMAX-end of the network and runs the WiMAX control protocol. Finally, CPU-2 acts as the central controller of the ONU-BS and handles the communication between CPU-1 and CPU-3. At the software level, a unified bandwidth allocation and management paradigm is required to handle both the wired and wireless planes. Clearly, the "one-box" concept eliminates the problems stemming from the first architecture. Nonetheless, the fact that new devices will be required as opposed to using existing ones, might not be very appealing to companies looking to reduce their capital expenses. In addition, the DiffServ-IntServ heterogeneity of EPON and WiMAX requires modifying one of the MACs in order to provide a unified bandwidth allocation mechanism.

Unified Connection-Oriented

The purpose of this architecture is to enable an end-to-end ([E2E], i.e., from SS to OLT) connection-oriented DBA paradigm. To achieve so, instead of carrying Ethernet frames, WiMAX MAC PDUs containing multiple encapsulated Ethernet frames are used so as to enable fine-grained bandwidth allocation.

Microwave-over-Fiber (MOF)

In this architecture, a "dumb" antenna is connected to the EPON's ONU, responsible for relaying WiMAX radio signals to and from its associated microcell. Here, one optical subcarrier and another wireless subcarrier are used to transfer the signals from the wireless domain to the optical domain. The modulation of a WiMAX carrier frequency (e.g., 2.5 GHz) over an optical frequency is termed as microwave-over-fiber (MOF). The advantage of this architecture is the simplified handover operation for mobile users. Nonetheless, the optical beat interference between the upstream optical subcarrier signals can be very complex. As a result, separate wavelengths may be required for each ONU, which may require an unfavorable upgrade to WDM-PON.

Virtual

Recently, the authors of [37] addressed the disadvantages of both the *independent* and *hybrid* architectures and proposed a different approach for designing the ONU-BS communication while preserving the current EPON and WiMAX standards. Namely, they presented the concept of VOB (Virtual ONU-BS) in which the ONU and the BS are connected using Ethernet through a network *bridge* acting as an intermediate controller. The bridge handles the QoS mapping between both sets of queues and runs the control protocols in both domains. The three devices connected form the VOB. For consistency, we will refer to this architecture as *Virtual*.

2.2.3 Bandwidth Allocation and Admission Control

EPON and WiMAX networks are designed to deliver services for numerous multimedia and data applications. Hence, the integrated FiWi network is expected to deliver the same services with the same level of quality and performance. To enable these services, bandwidth allocation and admission control schemes are required.

Previous research efforts on WiMAX scheduling, resource allocation, and admission control in the downstream direction have been extensively reported [31], and the additional consideration of EPON on top of WiMAX has not brought up more issues due to broadcast-in-nature transmission in both systems. On the other hand, in the upstream direction, the EPON's ONUs and WiMAX's SSs launch packets in the shared media, respectively, and have to be synchronized such that the packets can be successfully transmitted to the corresponding OLT and BS. This is expected to fundamentally change the nature of the problem. Therefore, we focus on solutions pertaining to bandwidth allocation and admission control for EPON-WiMAX networks in the upstream direction. The following paragraphs give an overview on the state-of-the-art progress of the research topic.

Bandwidth Allocation

The authors of [37] proposed a simple uplink/upstream DBA scheme for the Virtual EPON-WiMAX architecture. In the optical domain (i.e., DBA computed at the OLT), the ONUs are granted the bandwidth with excess consideration[3]. In the wireless domain, (i.e., DBA computed at the VOB), best-effort traffic is granted a minimum portion of the total bandwidth and the real-time traffic is allocated the remaining bandwidth in a greedy manner such that the higher priority traffic is satisfied at the expense of lower priority if not enough bandwidth is available to accommodate all CoSs. However, the DBA allocates bandwidth per-class rather than per-connection and thus it can neither offer bandwidth guarantees nor QoS protection for the admitted services.

The authors of [35] discussed different EPON-WiMAX architectures and presented a centralized SBA mechanism that operates over an architecture similar to the Virtual architecture (so-called hybrid ONU-BS [HOB]). Although the proposed scheme minimizes the E2E packet delay, it does not provide any bandwidth guarantees or QoS protection for each service flow. Moreover, the SBA mechanism neither exploits the available resources nor enables statistical multiplexing [27].

The authors of [34] presented a hybrid optical-wireless network based on the Independent architecture, where the ONU can either be connected to a WiMAX BS, a 3G network node, or a Wireless-LAN (WLAN) access point (AP). They have also proposed a simple uplink bandwidth allocation scheme where the allocation is only based on the application type (either light or heavy FTP, or video) and source (WLAN, WiMAX, or 3G).

The authors of [33] proposed a game theory-based intra-ONU scheduler to fairly schedule the transmission of upstream traffic which is categorized as either Ethernet-based (i.e., wired connection) or WiMAX-based (i.e., wireless connection).

[3]The excess bandwidth is what remains in every cycle from lightly-loaded ONUs (i.e., ONUs requesting bandwidth less than their minimum bandwidth guaranteed). This bandwidth gets distributed to highly-loaded ONUs (i.e., ONUs requesting bandwidth more than their minimum bandwidth guaranteed) such that the distribution depends on the employed DBA [38].

Moreover, Interleaved Polling with Adaptive Cycle Time (IPACT) [27] is employed as the DBA at the OLT. Again no QoS guarantee is provided.

Admission Control (AC)

In order to support the QoS of real-time traffic streams, one needs in addition to efficient DBA and precise service differentiation, an intelligent AC mechanism which helps making the decision on the admission of a traffic flow. The AC scheme should be developed so as to help the system meet the QoS requirements without sacrificing the upstream channel utilization. Furthermore, maintaining fairness according to the given operational policy is another important goal of an AC mechanism.

The authors of [36] proposed a queue-length based AC framework, where an analytical model was developed to measure the expected packet delay in the assigned time slot. It is found that although the queuing delay at the ONU-BS serves as an index on the usage of the network resources, there are other system parameters that are also important and should not be ignored in the admission rules, such as the scheduling policies and channel condition experienced by each flow. In addition, the rejection of a flow should not only be based on its expected packet delay, but should also consider the situation where the cycle size is dynamic and is DBA-dependent. Namely in some cycles, extra bandwidth could be spent on a requested flow to accommodate its delay constraints. Furthermore, the proposed framework has not rigorously provided precise E2E QoS protection to the already admitted flows nor discussed how the uplink bandwidth allocation is computed.

The authors of [32] proposed a simple QoS-Aware framework for the Independent EPON-WiMAX architecture. Here, an AC and an upstream bandwidth allocation schemes are presented such that the decision whether to admit a flow is based on the bandwidth availability, bounded by a threshold. As for the upstream bandwidth allocation, it simply allocates bandwidth to a reported real-time flow in the assigned transmission window. This scheme does not exploit the available bandwidth through any DBA mechanism. In addition, the authors adopted the strict

priority (SP) intra-ONU scheduler, which may cause BE traffic starvation[4] [39].

2.2.4 Routing and Packet Forwarding

The authors of [4] addressed the packet forwarding problem in the integrated EPON-WiMAX architecture. They suggested to install an IP access router (AR) at the mounted ONU-BS to forward the incoming traffic to local SSs at the expense of creating a bottleneck caused by the round-trip-time (RTT) spent to forward the packets. This problem can be solved via employing a layer-2 Ethernet bridge. However, it may require an additional AR to ensure secure data transfer.

The authors of [5] installed a set of Independent EPON-WiMAX architectures (so-called Wireless Optical Broadband Area Network [WOBAN]) in the Davis, California area, to form a FiWi mesh network. They mainly tackled the network planning and routing challenges due to the anycast nature of the wireless upstream direction, which allows an SS to communicate with any other SS in the same or in a neighboring EPON-WiMAX network.

2.2.5 QoS Support in EPON-WiMAX

Although the EPON-WiMAX integration consists of two heterogeneous networks, the QoS support can be straightforward given the similarity between the type of services supported in both networks. Table 2.1 summarizes the QoS support in EPON and WiMAX, and shows how the CoS mapping can be done in the integration.

2.3 Mission-Critical Systems

Different from public systems, MC systems require a set of unique services and network requirements. In this section, we briefly overview different types of multi-

[4]The SP scheduler services the highest priority queue until it is empty, and then moves to the next highest priority queue, and so on. It is possible that if there is enough high priority traffic, the lower priorities never get scheduled.

Table 2.1: QoS support in EPON-WiMAX

Traffic	EPON	WiMAX	Applications	QoS Requirements
CBR	EF	UGS	Voice, P2P	Delay, Jitter & Bandwidth guarantee
VBR	AF	rtPS	Video streaming	Delay & Bandwidth guarantee
		nrtPS		
		ertPS	Voice with silence suppression	
BE	BE	BE	E-mail, Web-browsing	N/A

media services envisioned to extensively appear in such systems. We also highlight the main network requirements for ensuring robust MC service support.

2.3.1 Mission-Critical Services

With the emerging multimedia MC services, PSDR users can establish audio/video calls or share images and other miscellaneous mission-critical information. These services (illustrated in Fig. 2.7) possess stringent QoS and security requirements that need to be fulfilled via an effective network solution. Typically, an MC service may belong to one of the following categories:

- **Emergency** (*asynchronous*): A one-way message (or flow of short length) that is triggered by an emergency event (e.g., fire event, criminal pursuit, or an alarm by a health monitoring system) and that requires an immediate delivery/broadcast.

- **Real-time** (*synchronous*): It can be as simple as telephone calls or as complex as a sophisticated virtual-reality robotic surgery. It can also be used for monitoring of long-term care agents by establishing video-conferencing.

- **Store-and-Forward** (*asynchronous*): It supports delivery of non-emergency MC data (e.g., images, bio-signals, etc.) to specialists for e-consultation, evaluation or other purposes. It does not require interactive communications

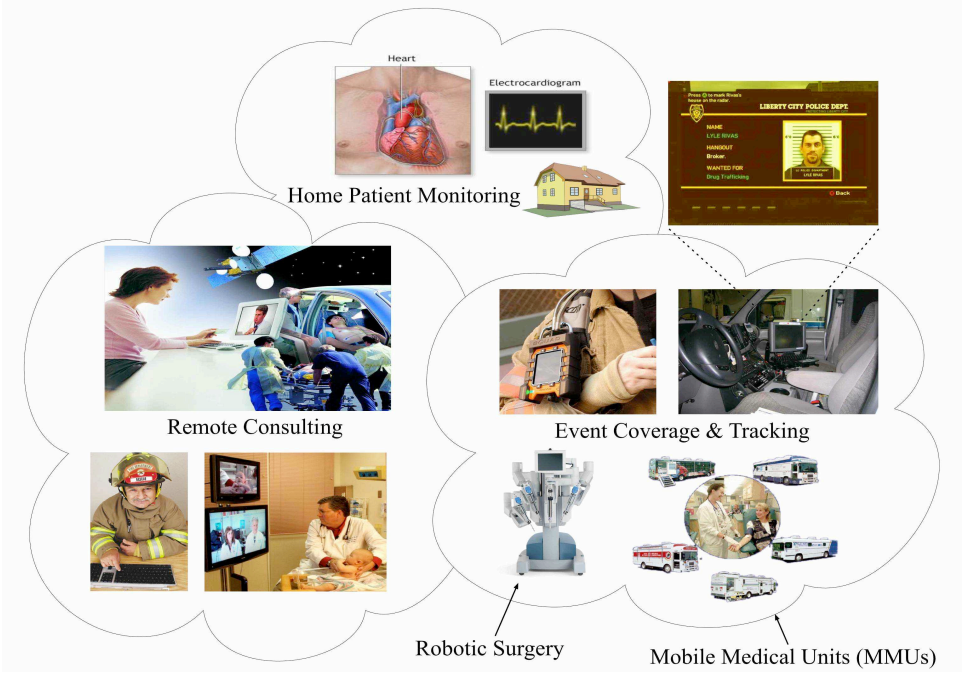

Figure 2.7: Envisioned mission-critical services and applications

between involved parties in real-time; however, high data integrity and bandwidth guarantees are crucially required.

2.3.2 Mission-Critical Network Requirements

A typical MC network is illustrated in Fig. 2.8. In this example, the MC headquarters connects to rural MC centers using a wired link (e.g., DSL), and to mobile units such as ambulances and police cars, as well as home-care patients (e.g., for electrocardiogram [ECG] monitoring) using a wireless link (e.g., sattelite, GSM, 3G, IEEE 802.11, or WiMAX). Mobile units can communicate MC data with the headquarters' database through its intranet. They can also establish audio/video-conferencing with remote experts for consultations and diagnosis.

In addition to security and reliability, an MC network must fulfill the following salient requirements:

- **Operability**: The ability to establish and sustain communications between different MC units during an MC event.

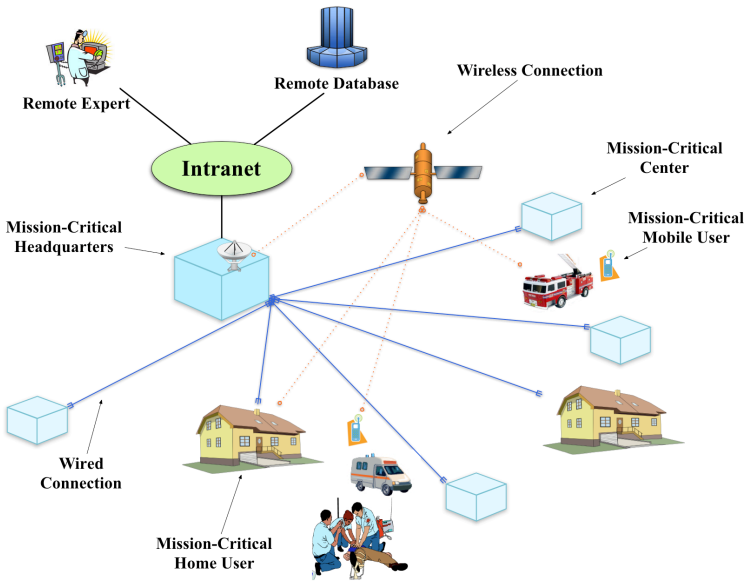

Figure 2.8: Illustration of a typical mission-critical network

- **Interoperability**: The ability of all MC units (from all levels and disciplines) to communicate among each others as authorized and as needed, regardless of their network capabilities.

- **Continuity of Communications**: The ability to maintain communications, even in the event of a network failure.

It is therefore imperative that any employed network solution must sustain these network requirements to perpetuate the diverse QoS requirements of MC services[5].

2.4 Energy Efficiency Techniques in NG-PON

Although extensively studied in wireless networks, energy saving in NG-PON has not yet matured and is currently being standardizd [23, 24, 49]. In the following sections we provide a literature survey on the energy saving techniques in NG-PONs. As depicted in the taxonomy graph in Fig. 2.9, these techniques can be

[5]In 2005, the U.S. Department of Homeland Security (DHS) has activated a communications program, so-called Safecom (`http://www.safecomprogram.gov`), that aims at improving emergency responses through wireless communications. Safecom also lists the same features as emergency requirements.

Table 2.2: Comparison between different ONU architectures

ONU Architecture	**Laser Turn-on Time**	**Clock Recovery Time**	**Sync. Time**	**Total Overhead**	**Active Power Consumption**	**Sleep Power Consumption**	**Doze Power Consumption**
STD-ONU	600 ns	N/A	N/A	600 ns	3.85 W	N/A	N/A
GR-ONU-1/A	600 ns	2 ms (**A**ggressive)	0.125 ms	2.125 ms	3.85 W	0.75 W	1.7 W
GR-ONU-1/C		5 ms (**C**onservative)		5.125 ms			
GR-ONU-2	600 ns	$10 - 50$ ns	0.125 ms	0.125 ms	3.85 W	1.08 W	1.7 W
GR-ONU-3	600 ns	0 ms	0.125 ms	0.125 ms	3.85 W	1.28 W	1.7 W

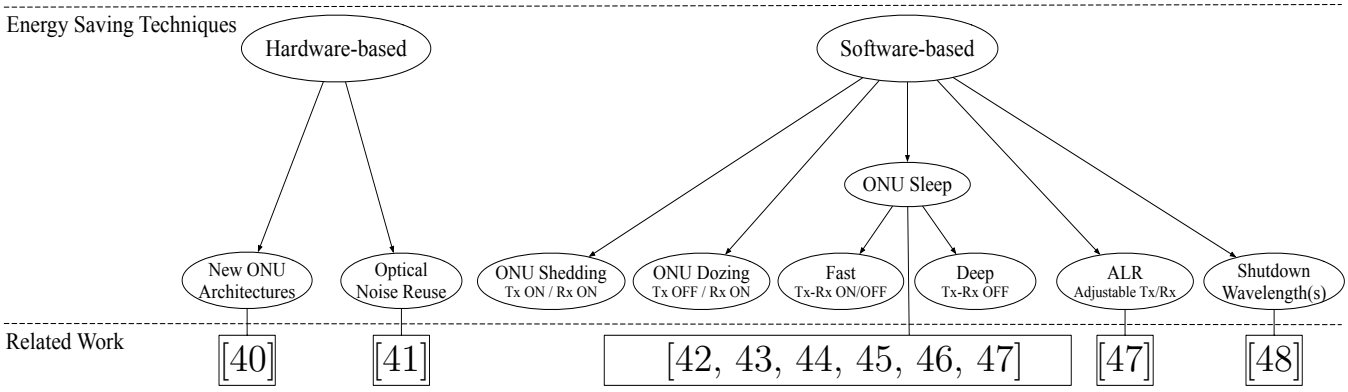

Figure 2.9: Taxonomy for the energy saving techniques in NG-PONs

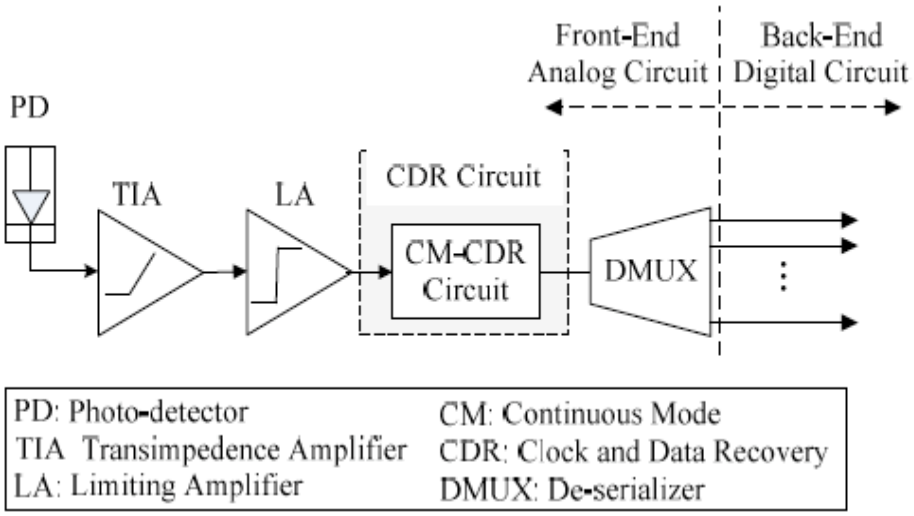

Figure 2.10: Legacy ONU architecture

categorized as either hardware- or software-based, and can be employed under any NG-PON technology, unless specified differently.

2.4.1 Hardware-based Techniques

Hardware-based techniques can be via new ONU architectures and/or optical noise reuse.

Table 2.3: Power consumption comparison between different ONU architectures

ONU Architecture	**Front-End Analog Circuit**					**Back End Digital Circuit**
	PD	**TIA**	**LA**	**CM-CDR**	**DMUX**	
STD-ONU	negligible	0.1 W	0.1 W	0.33 W	0.47 W	2.85 W
GR-ONU-1	off	off	off	off	off	0.75 W
GR-ONU-2	off	off	off	0.33 W	off	0.75 W
GR-ONU-3	negligible	0.1 W	0.1 W	0.33 W	off	0.75 W

New ONU Architectures

The legacy IEEE 802.3ah standard ONU (STD-ONU), depicted in Fig. 2.10 [40], does not support sleep mode. To remedy this deficiency, new ONU architectures were proposed in [40]. Table 2.2 exhibits these ONUs and highlights the disparity between the attributes of each architecture vs. STD-ONU which always consumes maximum energy[6]. Details on the hardware power consumption for every ONU architecture are also given Table 2.3 (the data is collected from [24, 40]). We briefly describe these architectures as follows:

- **Green ONU-1 (GR-ONU-1):** It basically comprises the same architecture as STD-ONU, yet with enabled sleep mode functionality (using its embedded timer). The advantages of GR-ONU-1 is that it requires no new ONU manufacturing, meanwhile it can save maximum energy by turning off most of its hardware when going into the sleep mode. However, the high overhead time that it carries (which is the time spent by the ONU to switch from the sleep mode to the active mode and mainly consists of the laser turn-on time, clock recovery time, and synchronization period), creates a tradeoff between maximum energy saving and network performance.

- **Green ONU-2 (GR-ONU-2):** This ONU basically keeps some of its hardware on, such that a very short overhead time is caused at the expense of

[6]The data is collected from [23, 24, 40, 50]. The ONU power consumption in the active and sleep modes is model-dependant; other types might consume differently.

slightly higher energy consumption while in the sleep mode.

- **Green ONU-3 (GR-ONU-3):** This architecture mainly focuses on eliminating the overhead time by shutting down the minimum hardware required to put the ONU into sleep. However as expected, the energy consumption in the sleep mode will be higher.

These architectures do not work independently. They rely on the existence of software-based protocols that manipulate their sleep functionalities (as we will see later). Clearly, GR-ONU-2 is considered with the best technical merits over the other types of ONUs due to its very short overhead time and slightly higher energy consumption. Nevertheless, the design and installation costs might decelerate its deployment. GR-ONU-1 on the other hand, although subject to longer overhead time and hence possibly impaired QoS level in the power saving mode, has been widely deployed as the mainstream of the NG-PON industry in past decade [3]. To reduce the impact of long overhead time in GR-ONU-1, it is necessary to design a mechanism that can intelligently manipulate the sleep mode operation. The mechanism should be general to possibly be operated on any envisioned ONU architecture in the future.

Optical Noise Reuse

The extension of the network reach in NG-PON (e.g, in LR-PON, NG-PON1, and NG-PON1), may result in significant optical signal losses. Furthermore, the closely adjacent wavelengths are subject to Rayleigh backscattering effects that can disrupt the feeder fiber of the power splitter, leading to throughput degradation. Equipping the ONU with a semiconductor optical amplifier (SOA) has been, so far, the most widely employed solution to this problem; however SOA notably increases the power consumption. To resolve this issue, the authors of [41] proposed a new technique that mainly reuses the optical noise of the amplifier as pumping power for all network nodes. This ultimately allows for more simultaneously provisioned users at lower or equal energy costs.

2.4.2 Software-based Techniques

Software-based techniques can be via the following five methods.

ONU Power Shedding

With power shedding [23], the ONU simply turns off some of its devices and reduces power usage by engaging into a different mode of services and functions, while leaving the optical link in full function. As such, power shedding can only achieve minimum energy savings though the best possible system performance can be ensured.

ONU Dozing

ONU dozing only turns off the transmitter for a substantial amount of time (typically during the periods where no upstream traffic is available), while the receiver is always on [23]. Although ONU dozing can save the OLT from buffering the downstream traffic and from performing downstream bandwidth allocation, it does not exploit the option of turning off the receiver when no downstream traffic is available.

ONU Sleep

ONU sleep reflects the state where both the transmitter and receiver are off for a substantial period of time [23]. This technique is further categorized as follows:

- **Deep Sleep:** Under this mode, the ONU's transmitter and receiver are turned off when there is no upstream and downstream traffic. Although this can achieve maximum energy reduction, it might cause performance degradation due to possible dropping of the incoming/outgoing packets. This mode can be particularly employed when, for example, the ONU is not in use, or when the loss of some applications' traffic can be tolerated.

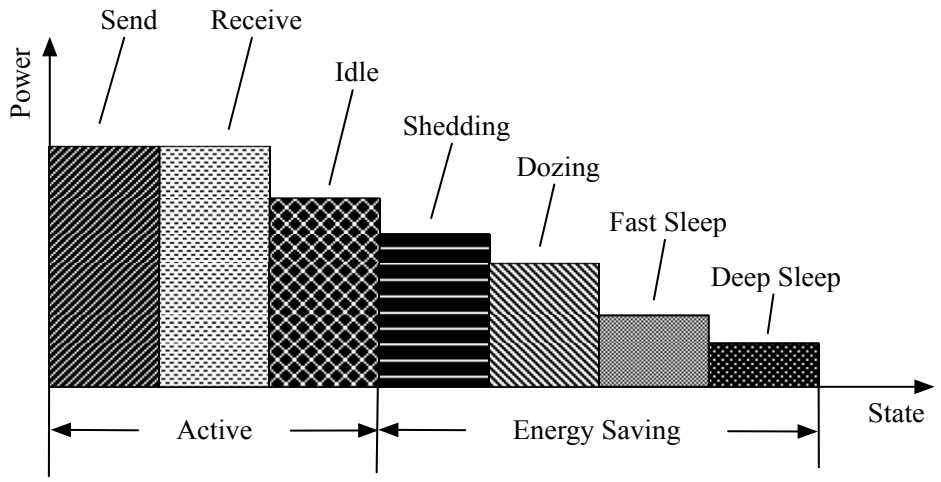

Figure 2.11: ONU power consumption under different active and energy-saving states.

- **Fast/Cyclic Sleep:** Under this mode, the ONU state alternates between the sleep state (i.e., when the transceiver is completely turned off) and the active state (i.e., when the transceiver is turned on). The active period and the subsequent sleep period form the *sleep cycle*. The system performance of this technique mainly depends on the assigned sleep period and the DBA scheme used in the active period.

These three software-based techniques enable the ONU to go into new energy-saving states. The ONU power consumption under different active and energy-saving states is shown in Fig. 2.11. Clearly, the ONU sleep mode can save more energy than all other techniques. It has also been considered the most promising energy saving strategy in NG-PONs [51], and has been extensively studied and explored under current research endeavours. The authors of [42] proposed a new energy-aware MAC protocol that performs slotted SBA for upstream and downstream traffic when the system is operating at low loads. The OLT constantly monitors the system throughput and puts the system into energy saving mode whenever the traffic load is below a certain threshold. Since the ONU wakes up and sleeps with a pre-defined period for data transmission/receiving, the scheme cannot handle any possible QoS constraint. Further, it assumes an infinite ONU buffer that can

accommodate all incoming traffic during the sleep period, which may introduce significant packet delay.

As observed in Table 2.2, the ONU's clock recovery time constitutes the biggest portion of the total overhead time. To alleviate the impact of having a long recovery time, the authors of [43] designed a fast clock and data recovery circuit (as of GR-ONU-2 and GR-ONU-3) and proposed a just-in-time sleep control mechanism that can enable the ONU to switch faster from the sleep state to the active state.

The authors of [44] proposed two SBA-based MAC protocols to save energy in EPONs. With the first one, namely upstream centric scheme (UCS), the OLT launches the downstream traffic to an ONU whenever the ONU is transmitting in the upstream direction. This forces the OLT to buffer the downstream traffic until there is any allocated upstream slot for the ONU; meanwhile the ONU can have the maximum sleep time depending on the upstream DBA scheme. With the second scheme, namely downstream centric scheme (DCS), the ONU switches into the active mode whenever there is either upstream or downstream scheduled transmission slots, and hence the sleeping can only occur when both the ONU and OLT are silent. While UCS can achieve larger power saving, it may cause higher packet delay if the overlapped downstream and upstream time slots are not scheduled and/or sized efficiently. Conversely by waking up every time a transmission is required, DCS can offer better QoS guarantees than UCS at the expense of higher energy consumption.

Recently, the authors of [45] proposed a dynamic ONU power saving mechanism, whereby the ONU dynamically switches between the burst and continuous modes. With the former, the ONU turns the receiver circuitry off during the power save period, and can be quickly ready for transmission/receiving by recovering the OLT clock using a burst mode receiver. On the contrast, the continuous mode keeps the clock recovery circuit active, which requires only trivial circuit control path modifications. Clearly, burst mode sleeping can achieve better energy efficiency and lower overhead time than that by the continuous mode sleeping at the expense

of more complicated circuitry control (similar to GR-ONU-3).

Finally, the authors of [46] proposed two sleep mode scenarios for ONUs. The study assumes the availability of multi-power-level ONUs where each level or state corresponds to a specific energy consumption level. In the first scenario, the ONU sleeps for more than one DBA cycle. This is achieved by defining a threshold, namely *idle_threshold*, to restrict the maximum time in which the ONU stays idle before going into sleep. In the second scenario, the ONU switches to the sleep mode based on a threshold estimated through the downstream traffic profiles of all ONUs. Without addressing any performance issue, the paper leaves some room for further investigation in terms of the impact on users' QoS perception.

Table 2.4 compares the ONU sleep techniques presented in the art. As observed, most of the schemes are costly, as they require new ONU architectures to operate. They are also either very complex, or able to attain high energy saving at the cost of sacrificing the network performance.

Adaptive Link Rate

Adaptive link rate (ALR) can be achieved due to the ability to select a transmission rate (from a set of available rates) dynamically. With respect to energy efficiency, ALR has been widely employed in wireless networks where most technologies (e.g., WiFi, WiMAX, etc.) have multiple transmission rates. The higher the selected rate, the higher the power consumption is. Nonetheless, lower transmission rates lead to poorer network performance. This technique can be used in GPONs and G-EPONs where multiple rates are available (1 *Gbps*, 2.5 *Gbps*, and 10 *Gbps*). However, it cannot be implemented in EPONs where typically one rate exists. Furthermore, the application of ALR over NG-PON1 and NG-PON2 has not been yet explored. Using ALR in G-EPONs, the authors of [47] proposed a simple scheme to enable the multi-rate ONU to set the optical link rate adaptively based on the monitored traffic load. This allows for the minimization of the ONU active time and hence extends the sleep period so as to save more energy. Again, the proposed scheme

ONU Sleep-based Technique	**Complexity**	**Energy Saving**	**Network Performance**	**Hardware Requirements**
Energy-aware fixed bandwidth allocation [42]	Low	Medium	Poor	Not investigated
Just-in-time sleep control [43]	Medium	Medium	Medium	GR-ONU-2, GR-ONU-3
Upstream centric scheme (UCS) [44]	Low	High	DBA-dependent	GR-ONU-2, GR-ONU-3
Downstream centric scheme (DCS) [44]	Low	Medium	Good	GR-ONU-2, GR-ONU-3
Dynamic ONU power saving [45]	High	High	Good	GR-ONU-2, GR-ONU-3
Energy-aware MAC protocol [46]	High	High	Not investigated	Multi-power-level ONU

Table 2.4: Comparison between the ONU sleep-based techniques proposed in the art.

did not consider any specific QoS requirements that might be affected by such a mechanism.

Shutdown Wavelength(s)

Since NG-PON's OLT is the sole controller of the network and is responsible for much more tasks than sending and receiving data, it is not supposed to contribute to any energy reduction plan. Furthermore, since all the ONUs rely on the OLT's clock to synchronize, putting the OLT into sleep will cause a synchronization problem [24]. In some versions of NG-PONs, namely LR-PONs and WDM-PONs, the OLT can save energy by provisioning the traffic on a subset of wavelengths while shutting down the rest of the wavelengths [48].

2.5 Summary

In this chapter, we present an overview of EPON and WiMAX networks which are the enabling technologies in the fiber-wireless integration. As observed, providing end-to-end QoS protection and bandwidth guarantee in the integration has not been addressed in the related art. These are two crucial themes in the construction of VPNs over the integration.

We also review the mission-critical systems, along with their envisioned multimedia services and their unique network requirements which both require special care and attention.

We finally present a literature survey of the energy saving techniques in NG-PONs, which can either be hardware- or software-based. We conclude that the software-based energy saving techniques are promising solutions for building green NG-PONs, as they can minimize the power consumption at low cost. However, effective mechanisms are required to leverage the advantages of existing and new ONU architectures in order to build an energy efficient NG-PON without breaking the users' service requirements.

Chapter 3

MC-FiWiBAN: An Emergency-Aware Mission-Critical Fiber-Wireless Broadband Access Network

In this chapter we propose MC-FiWiBAN (Fig. 3.1), a new emergency-aware architecture that can help extend the MC multimedia service coverage to rural areas, as well as improve the PSDR user access to the IP-based network core. PSDR and MC services require high security, custom-network control, and fast network access, in addition to a fine degree of QoS assurance and bandwidth guarantees. MC-FiWiBAN enforces these features via the construction of a layer-2 Virtual Private Network (VPN), which has been widely established in wired networks, and is considered a killer application in the modern Internet carriers [52].

3.1 Integration of MC-FiWiBAN and TETRA

Fig. 3.1 shows how MC-FiWiBAN can be easily integrated with the TETRA infrastructure (i.e., TETRA Switching and Management Infrastructure [SwMI]) using

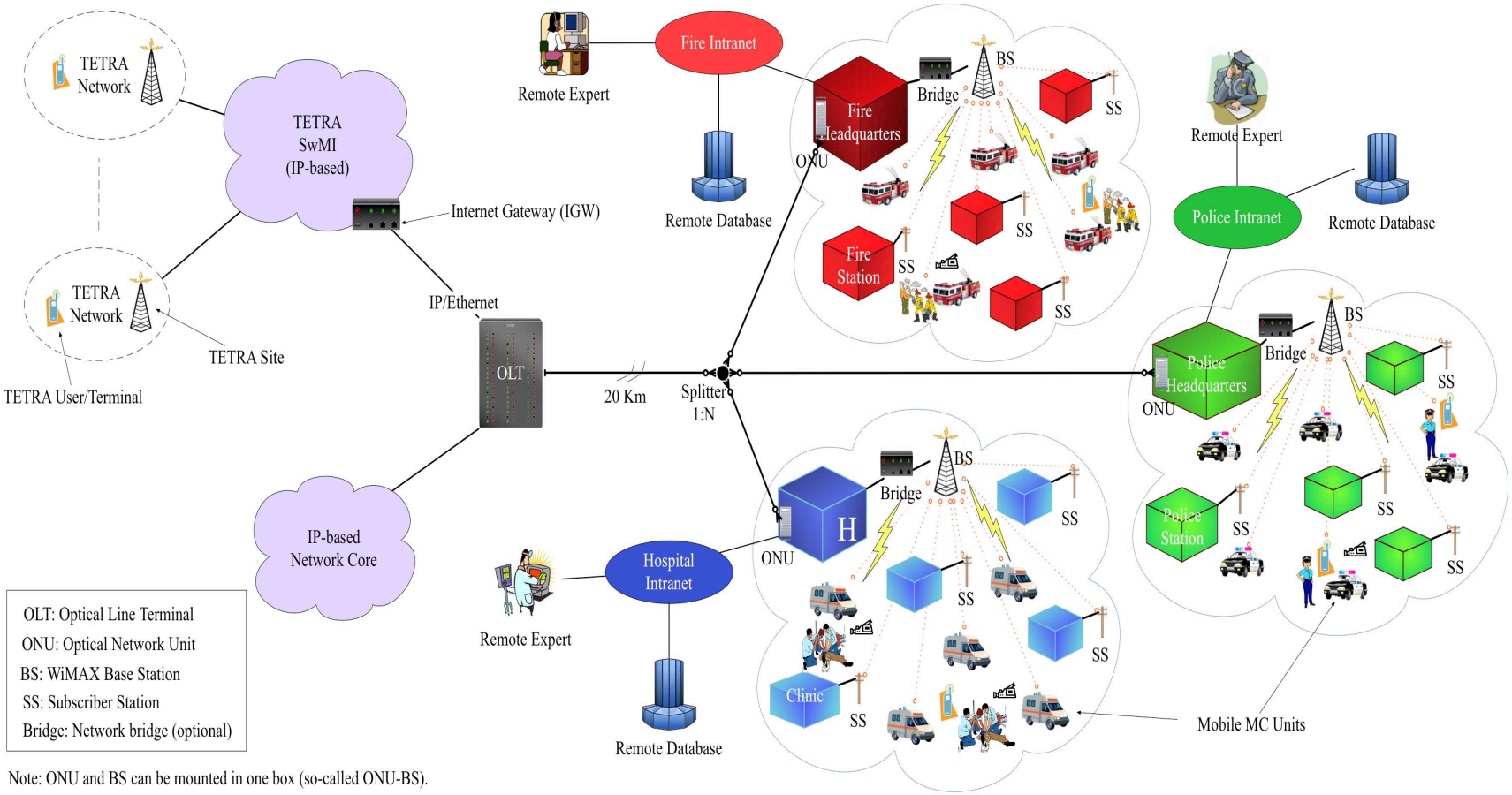

Figure 3.1: MC-FiWiBAN supporting MC VPNs and integrating with TETRA networks. In safety-critical places (e.g., hospitals [H]), a network bridge may be used to connect ONU and BS, such that BS is placed at a small distance away from its designated safety-critical site.

IP/Ethernet as interface between the OLT and an Internet Gateway (IGW) located at the TETRA SwMI. The main function of IGW is to hide from the SwMI the anomalies of MC-FiWiBAN, thereby achieving a seamless integration with almost no SwMI changes [10]. A simpler strategy would be to directly embed the OLT as part of the SwMI infrastructure; yet, a special interconnection agreement will then be required to preserve and/or lease the proper TETRA authorizations to the access network.

A TETRA radio user is envisioned to operate as a dual-mode terminal capable of supporting both TETRA and WiMAX radio/air interfaces in order to provide full interoperability between MC units and systems across these heterogeneous networks. This requires considering the following operational scenarios:

- **Overlapping**: In this scenario, TETRA users may access both networks simultaneously. An Always-Best-Connected (ABC) approach can be used to enable an optimal connection. Furthermore, a "smart" device controller (or a soft switch) can be installed in the TETRA terminal to select a network based on the service type. For example, if a video-streaming application is launched, then an MC-FiWiBAN connection would be primarily selected since it provides a better multimedia support, and so on.

- **Non-overlapping**: Here, PSDR users launch their emergency services using the core network whenever they are located in an area with no TETRA coverage (e.g., rural areas). Being equipped with proper hardware, TETRA users can fully utilize MC-FiWiBAN to conduct their daily MC operations with more functionalities than the direct mobile-to-mobile feature offered by the conventional TETRA standard in remote areas [8].

As described in Chapter 2, the deployment of MC systems compels a set of features to be available in the underlying network. In the following sections, we discern the building blocks of MC-FiWiBAN to embrace these distinctive attributes. With MC-FiWiBAN, we also define a resource management platform which facilitates the allocation of guaranteed resources for the VPNs.

3.2 Layer-2 VPNs over EPON-WiMAX

An MC system provisions a specific bundle of services with different QoS requirements to its users. To support these services over EPON-WiMAX, we propose to construct layer-2 VPNs over the EPON-WiMAX infrastructure such that each VPN corresponds to a specific service requirement bundle issued by a registered MC system. Such VPNs are referred to as *layer-2* VPNs in the sense that they are built upon the layer-2 protocols.

Compared with layer-3 VPNs, layer-2 VPNs can better resolve the complications due to network dynamics and fast wireless changing channel status. In other words, when a layer-3 VPN is installed, a specialized software that forms a control plane (e.g., multi-protocol label switching [MPLS]) has to be in place instead of simply deploying standard IP protocol stacks on top of layer-2. In addition, layer-2 VPNs provide a strong support for premium multimedia services with custom-designed control of layer-3 routing and IP addressing, diverse QoS requirements and security assurance, as well as the features intrinsically exhibited in the MAC layer [52]. These attributes are vital in the course of MC service support over the EPON-WiMAX integration. Alternatively, deploying layer-1 VPNs over the integration cannot be achieved due the physical media heterogeneity of both networks, which requires complex hardware-dependant VPN solutions that can operate over both networks simultaneously [53].

With the initiation of layer-2 VPNs directly upon the integration, users of each registered system can dynamically configure their service requirements and possibly issue call preemption requests through a suite of service access points (SAPs) and interfaces that are manipulatively maintained in the corresponding VPN package. This property is essential to an MC system where stringent bandwidth guarantees and call preemption requests are present [11]. Furthermore, such VPNs enable interoperability between fixed and mobile platforms.

The layer-2 VPN requests that are issued by the users can be handled within the MC organization without the need to involve further overlay and additional VPN

agents [52]. As a result, the *classified* nature of MC operations is preserved; and the constantly changing MC units' locations, especially in mobile tactical scenarios, are easily handled. Meanwhile, survivability of the end-user services can be enhanced by multi-homing[1], which can be easily manipulated in the layer-2 VPNs [52]. The VPN applications can determine if a user should be associated with multiple ONU-BSs through separate air interfaces, so as to enable a fast fault-recovery that is vital to the MC scenario.

3.2.1 Principle of Operation

To enable a unified VPN connection control from the SS to the OLT, and since WiMAX enables a finer bandwidth allocation than EPON, we propose to modify the MAC protocol in EPON to support connection-oriented VPN requests from the ONU-BS to the OLT. This can be implemented by launching IEEE 802.16 MAC PDUs encapsulating Ethernet frames in the optical domain, rather than directly carrying Ethernet frames in upstream and downstream frames/bursts of EPON [4]. As a result, MC-FiWiBAN can support IntServ and be controlled by unified connection-oriented bandwidth management protocols, launching WiMAX PDUs. Consequently, no control frames will be required in the Ethernet frame for the bandwidth allocation and network control in the optical domain.

3.2.2 Network Model

Typically, a VPN consists of three planes 1) control, 2) data, and 3) physical [54]. The control plane handles operations such as connection establishment, routing, and AC. The data plane is concerned with the bandwidth management for VPN services and meeting their SLA-based QoS requirements. The physical plane is basically the underlying network infrastructure (here, EPON-WiMAX). The realization of multi-planed VPNs over EPON-WiMAX is illustrated in Fig. 3.2.

[1]Multi-homing refers to a single host making use of several connections associated with various interconnected networks.

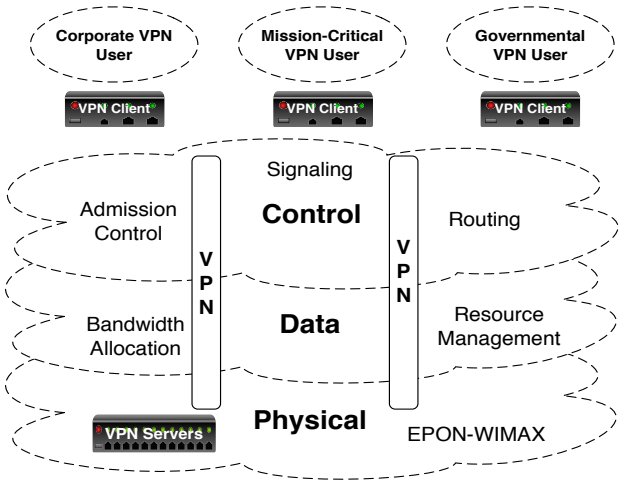

Figure 3.2: Multi-planed VPNs

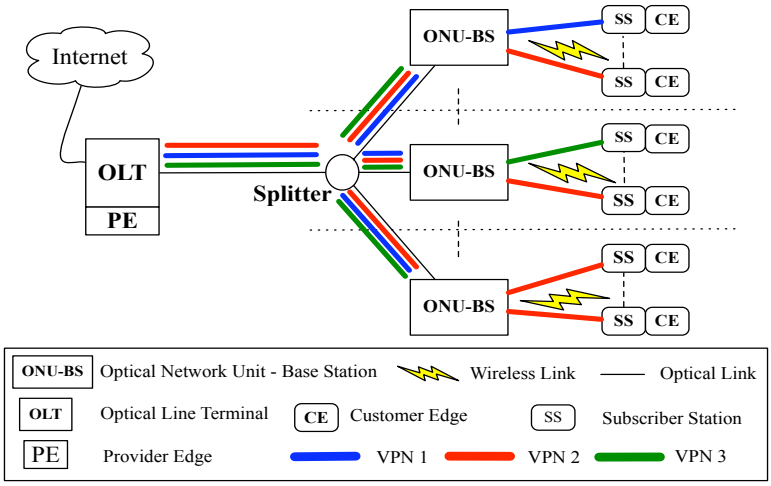

Figure 3.3: Layer-2 VPNs over EPON-WiMAX

With the current heterogenous Internet and access network deployment, it is possible that a connection goes through multiple VPNs supported by different technologies at different network layers, or even any data path without any QoS protection. However, our work emphasizes on the implementation of layer-2 VPNs in terms of per-flow QoS protection, custom-design network control, performance parameter selection, and tunneling between nodes at the network boundary. As illustrated in Fig. 3.3, in the context of EPON-WiMAX networks, the network boundary is formed by the end-users and the OLT. A VPN gateway could be deployed at the OLT so as to interface with other VPNs under some agreements/policies. The

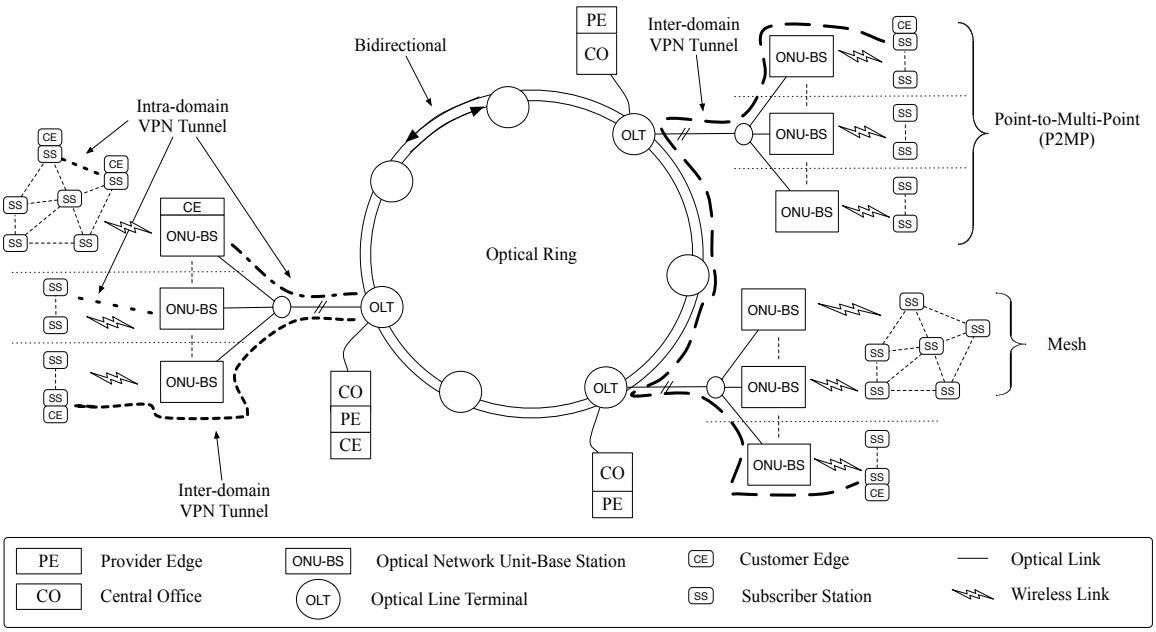

Figure 3.4: VPN tunneling in MC-FiWiBAN

design of the VPN gateway and related issues are nonetheless out of scope of our work.

3.3 VPN Tunneling

As depicted in Fig. 3.4, we classify an MC-FiWiBAN VPN tunnel as either *inter-domain* or *intra-domain*:

- **Intra-domain**: A tunnel is established between customer edges (CE) that belong to the same architectural domain (e.g., between two WiMAX SSs).
- **Inter-domain**: A tunnel is established between CEs that belong to different architectural domains (e.g., between the OLT and an SS).

In addition to being a provider edge (PE), the OLT may act as a CE depending on the VPN tunnel type (e.g., if the OLT co-locates with TETRA SwMI and connects to an MC-FiWiBAN user).

To achieve operability, a VPN tunnel should be established between two MC users such that sufficient resources are allocated in MC-FiWiBAN's uplink/upstream and downlink/downstream channels, and in the optical ring.

3.4 Bandwidth Allocation and Admission Control

As mentioned earlier, due to the broadcast-in-nature of downstream traffic in EPON-WiMAX networks, our work focuses on solutions pertaining to dynamic bandwidth allocation and admission control in the upstream direction.

In the past few years, some related works addressed the upstream resource management problem in EPON-WiMAX (e.g., [32, 34, 36, 37]). Nevertheless, none of the proposed schemes were able to provide bandwidth guarantees or QoS protection for the incoming flows; properties that are required for the support of VPNs. In addition, these schemes did not consider the underlying PHY burst profiling applied on each wireless link, and so the allocation was based on MAC requests only; which makes such an arbitration less effective [55]. Therefore employing any of these mechanisms is not a viable solution in the context of layer-2 VPNs over the integrated network. Conversely, our proposed framework (presented in the next chapter) will address these issues and will provide effective solutions.

3.5 Fault-Tolerance and Error-Recovery

To maintain service continuity, a fast recovery from any possible unexpected failure is required. In MC-FiWiBAN, a VPN tunnel may fail due to the following reasons:

1. A damage in the wireless link between the ONU-BS and the wireless user (an intra-domain VPN error).

2. A fiber cut between the ONU-BS and the splitter (a hybrid inter/intra-domain VPN fault).

3. A fiber cut between the splitter and the OLT (a hybrid inter/intra-domain VPN error).

4. A fiber cut on the metro ring, causing damage to the inter-domain established VPN.

Enabled via multi-homing, a fast fault-recovery can be attained through the following strategies:

- If the wireless channel between the ONU-BS and the SS is deteriorated, the VPN tunnel can be re-routed to another ONU-BS in range using a direct connection (in the case of a P2MP topology), or through a multi-hop route (in the case of a mesh topology and the ONU-BS is not in range).

- If a fiber cut occurs between an ONU-BS and the splitter, or between the OLT and the splitter, the failure can be averted by establishing communication with an alternative ONU-BS of a neighboring EPON-WiMAX network, to reach its network boundary by means of the bidirectional metro ring that is also fault-tolerant by nature [56]. Such a strategy cannot be performed in traditional PONs and/or WiMAX networks [5].

These routing stratagems can be easily accommodated in layer-2 through specialized *routing agents* (located at each network boundary), to maintain service continuity of the VPNs. Nonetheless, other layer-3 FiWi routing protocols (e.g., [57]) may alternatively be employed to serve the same purpose.

3.6 Emergency-Aware QoS Support

As mentioned, the QoS requirements of supported MC service plans are specified in the SLA of each VPN. An MC service plan typically comprises two types of data:

Table 3.1: Envisaged multimedia applications / Service classification and CoS mapping

Service Type	**Application**	**QoS Requirements**			**IEEE 802.16 CoS**
		Data Bit Rate	End-to-End Delay	Jitter	
Emergency Call/Event	Device/Human Trigger	2 - 5 Kbps	$\leq$ 10 ms	N/A	EGS
Audio	Diagnostic (interactive)	4 - 25 Kbps	$\leq$ 1 s	$\leq$ 1 ms	UGS
	Conferencing (real-time)	5 - 70 Kbps	$\leq$ 150 ms	$\leq$ 1 ms	UGS
Video	Video Streaming	1 - 6 Mbps	$\leq$ 10 s	N/A	nrtPS/rtPS
	Conferencing (real-time)	20 Kbps - 1 Mbps	$\leq$ 250 ms	N/A	rtPS
Monitoring Services	Enhanced Telemtry (real-time)	20 - 50 Kbps	$\leq$ 250 ms	N/A	rtPS
	MC Data Transfer	20 - 50 Kbps	$\leq$ 250 ms	N/A	nrtPS
	Bulk Data Transfer	50 Kbps - few Mbps	$\leq$ 10 s	N/A	nrtPS
Multimedia Transfer	Routine Activities	100 Kbps - few Mbps	$\leq$ 10 s	N/A	nrtPS
Best Effort (BE)	E-mail / Web-browsing	Minimum Throughput			BE

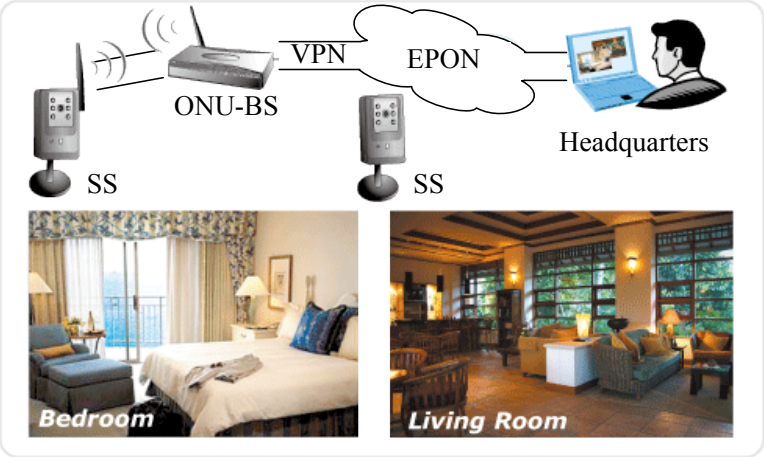

Figure 3.5: An illustration of a surveillance system over MC-FiWiBAN

- The regular periodic traffic (i.e., real-time or store-and-forward) that is transmitted frequently.
- The emergency messages with a highly erratic nature but extremely delay-sensitive.

A particular example of an envisioned regular real-time multimedia application is the live video surveillance system. The deployment of such a system over MC-FiWiBAN, as shown in Fig.3.5, can provide a secure and robust wireless connection that eliminates the wiring/re-wiring overhead caused in conventional surveillance systems.

3.6.1 Emergency Grant Service (EGS)

Table 3.1 shows how the QoS support for regular MC traffic can be achieved via mapping each service to one of the WiMAX CoSs based on its type and QoS requirements. On the other hand, emergency traffic requires QoS protection and immediate transfer; therefore should it not be "mixed" with other types of services. For this reason, we define a new IEEE 802.16 CoS, namely Emergency Grant Service (EGS). EGS has the highest priority over other services and possesses stringent QoS requirements. Moreover, due to its erratic nature and sporadic occurrence (e.g,

once in several weeks/months), EGS traffic is reported to the ONU-BS whenever an emergency event occurs, and is placed in a separate buffering queue.

EGS not only reduces the control overhead caused by reporting the bandwidth needs in each PI, but also eliminates the wastage of bandwidth caused by reserving resources for emergency services in each PI (in case the UGS approach is applied [17]). With a separate buffer, EGS facilitates the implementation of a service preemption mechanism required in emergency situations with congested networks.

3.7 Service Classification and CoS Mapping

The design of a resource management scheme that arbitrates the transmission of MC users over the shared MC-FiWiBAN resources requires an MC service classification at both the end-user/SS and ONU-BS.

3.7.1 At SS

Table 3.1 shows the mapping of the envisaged MC users' applications to the IEEE 802.16 CoSs of each SS. This classification makes MC-FiWiBAN scalable in the sense that the support of more users will then require no changes, especially to the resource allocation schemes; since the VPN-to-MAC mapping, via the pre-defined SAPs, will implicitly take care of satisfying its requirements without compromising the QoS level of existing services.

3.7.2 At ONU-BS

According to the IEEE 802.13ah standard, an ONU is allowed to support and report up to eight queues [26]. As shown in Fig. 3.6, to preserve the standard, we install a total of six queues at the ONU-BS and then perform a simple one-to-one CoS mapping. Consequently, users' incoming flows are initially classified at the SS-side using the packet classifier and mapped to the corresponding CoS queue. In case

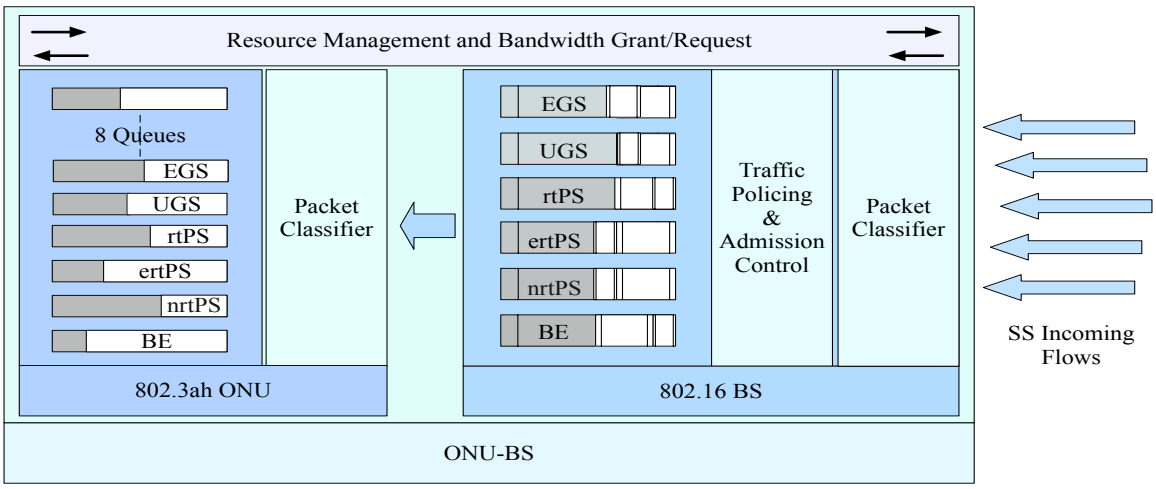

Figure 3.6: Traffic mapping at ONU-BS

the *VOB* architecture is installed, each incoming flow is first classified at the BS-side and then mapped to the corresponding ONU's CoS queue via the intermediate network bridge. Alternatively if a "one-box" ONU-BS is mounted, incoming packets can be directly mapped to one of the six corresponding buffering queues. Before being buffered, flows can be subject to traffic policing and admission control.

3.8 Requesting and Granting

Requesting and *granting* are two fundamental operations standardized in EPON and WiMAX [26, 17], and are used to exchange bandwidth allocation control messages.

3.8.1 In the Wireless Plane

In the wireless plane, to achieve better sensitivity in QoS guarantee, the *polling mode* is employed such that the ONU-BS performs the proper bandwidth allocation and granting in a GPC fashion [17]. Nonetheless, the SS does not need to request bandwidth for UGS traffic since its rate is constant. Therefore the ONU-BS should reserve the corresponding bandwidth for each admitted UGS flow.

3.8.2 In the Optical Plane

In the optical plane, to preserve the REPORT structure, each ONU-BS will report the buffering queue occupancies for real-time flows (i.e., EGS, rtPS, ertPS, and nrtPS queues), and will use the remaining four fields to report up to four BE VPN bandwidth needs. The latter can be implemented by having a *counter* for each VPN to count the number of packets buffered in the BE queue. If an ONU-BS provisions more than four VPNs, multiple REPORT messages may be used to report the rest of VPNs. On the other hand, a GATE message includes a grant for each real-time buffer request and an aggregate grant for all the VPN BE traffic requests. As in the wireless domain, the OLT can also pre-reserve in every cycle the corresponding aggregate bandwidth for admitted UGS flows in the optical domain.

3.9 Traffic Characteristics and QoS Requirements

CBR flows (such as UGS) are non-bursty, and can be simply characterized by their mean data rate ($\overline{\lambda}$) in bits per second (*bps*). They demand strict delay, jitter, and bandwidth guarantee requirements. On the other hand, VBR flows (such as rtPS and nrtPS) are bursty in nature and in addition to the mean data rate, they are characterized by the following TSPEC (Traffic SPECifications) parameters:

- Peak Arrival Data Rate (σ) in bits per second (*bps*).
- Maximum Burst Size (δ) in bits.
- Delay Bound (θ) which is the maximum amount of time (in seconds) allowed to transport a traffic stream/flow measured between the arrival of the flow to the MAC layer and the start of transmission in the network.
- MSDU maximum and minimum sizes (MS_{max} and MS_{min}). For fixed MSDU size streams of size MS, the mean frame size $\overline{MS} = MS = (MS_{max} + MS_{min})/2$.

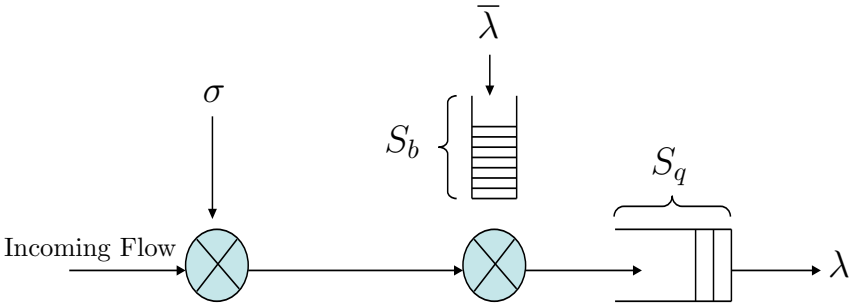

Figure 3.7: Dual-Token Leaky Bucket (DTLB)

While VBR flows demand strict delay and bandwidth guarantee requirements, BE traffic is bursty in nature and imposes no specific QoS requirements. However as we will see in the next chapter, a minimum SLA-based BE throughput is ensured for each provisioned VPN. Thus in MC-FiWiBAN, we focus on achieving statistical bandwidth guaranteed services for each real-time VPN flow, due to the criticality of real-time MC applications and services.

3.10 Statistical Guaranteed Service Rate

To attain a statistical guaranteed bandwidth for each real-time VPN stream, a *guaranteed rate* is computed based on the TSPEC parameters of each flow. For a CBR flow (belonging to CoS c, VPN k denoted V_k, and user i), given a frame error probability $P_{error,i}$ pertaining to user i and which is a function of the channel condition (i.e., the signal-to-noise-rasio, SNR) [58], the bandwidth is statistically guaranteed by defining its guaranteed rate $\lambda_{c,i}^k$ as follows:

$$\lambda_{c,i}^k = \frac{\overline{\lambda}_{c,i}}{1 - P_{error,i}}, \tag{3.1}$$

where $\overline{\lambda}_{c,i}$ is the mean data rate of a flow arriving at user i in CoS c.

For VBR traffic, a dual-token leaky bucket (DTLB) is employed at the entrance of the MAC buffer and is associated with each stream as shown in Fig. 3.7. The

bucket size is calculated as follows:

$$S_b = \delta \times (1 - \overline{\lambda}/\sigma). \tag{3.2}$$

Accordingly, the arrival traffic envelope $A(t)$ of the stream passing through the DTLB during $t \in [0, \infty]$, is computed as follows:

$$A(t) \leq \begin{cases} \sigma t & 0 \leq t \leq \phi \\ S_b + \overline{\lambda} t & t > \phi \end{cases} \tag{3.3a}$$

$$\phi = S_b/(\sigma - \overline{\lambda}). \tag{3.3b}$$

$A(t)$ is then constructed from Eq. (3.3) as shown in Fig. 3.8. With $P_{error,i}$, the

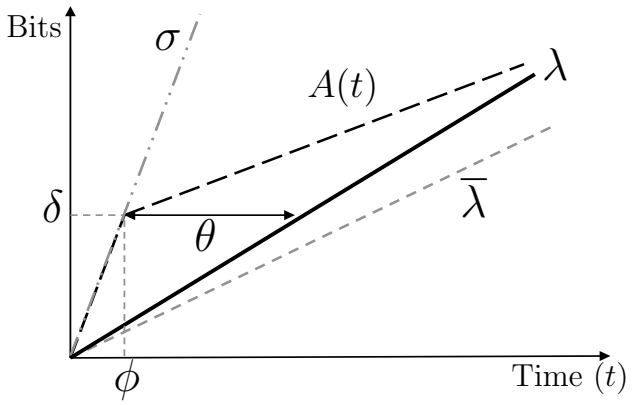

Figure 3.8: Guaranteed rate derivation graph

guaranteed rate for a VBR flow belonging to CoS c, user i, and V_k can be easily derived from Fig. 3.8 using the distance formula [59, 60]:

$$\lambda_{c,i}^k = \frac{\delta_{c,i}}{(\theta_{c,i}^k + (\delta_{c,i}/\sigma_{c,i}))(1 - P_{error,i})}, \tag{3.4}$$

where $\delta_{c,i}$, $\theta_{c,i}^k$, and $\sigma_{c,i}$ are the peak rate, delay bound, and maximum burst size of a flow arriving at user i in CoS c, respectively.

These rates facilitate the design and operation of the bandwidth allocation and admission control schemes, required to establish the VPN tunnels in MC-FiWiBAN.

3.11 Lossless Buffering

As part of ensuring guaranteed throughput for the derived *guaranteed* rates of real-time flows, it is necessary to ensure *lossless buffering* for CoS queues.

Achieving *lossless buffering* means that the packet drop probability for each CoS queue is equal to zero. For CBR flows, lossless buffering can always be achieved by allocating the guaranteed rate as per Eq. (3.1). In contrast, lossless buffering for VBR flows is DTLB-parameters dependent.

Proposition 3.11.1. *To achieve zero packet drop for a VBR flow, the size of the queue S_q must satisfy the following:*

$$\lim_{t\to\infty} \frac{S_q(t)}{t} \triangleq S_q \geq \frac{\theta \times \delta(\sigma - \overline{\lambda})}{\theta(\sigma - \overline{\lambda}) + \delta(1 - \overline{\lambda}/\sigma)}. \tag{3.5}$$

Proof. According to [61], given a DTLB of mean rate $\overline{\lambda}$, peak rate σ, and bucket size S_b, the dynamic queue size at time $t \in [0, \infty]$, $S_q(t)$, should respect the following bound in order to ensure no packet loss for a stream of guaranteed rate λ:

$$S_q(t) \leq \frac{(\sigma - \lambda) \times S_b(t)}{\sigma - \overline{\lambda}},\ t \in [0, \infty]. \tag{3.6}$$

By combining Eqs. (3.2), (3.4), and (3.6) as well as neglecting $P_{error,i}$, with some simplifications, the minimum queue size is computed and Proposition 3.11.1 is proved. □

The value of S_q can be set in the stage of network planning to achieve lossless buffering in the wireless domain. This is essential given that packets transmitted on wireless channels are already prone to loss [58].

3.12 Error Control

Ensuring reliability of PDU transmission is also crucial in achieving guaranteed throughput for admitted services. To achieve so, an infinite persistent Automatic

Repeat reQuest (ARQ)-based error recovery is applied as in [62]. Namely, assuming an independent error process, the probability that x PDUs out of y are successfully received by ONU-BS i, $P_i^{x,y}$, is obtained as follows:

$$P_i^{x,y} = \binom{x}{y}(1 - P_{error,i})^x (P_{error,i})^{x-y}, \quad x \in \{1, 2, ..., y\}. \tag{3.7}$$

3.13 Summary

This chapter presents MC-FiWiBAN, a new emergency-aware FiWi access network that leverages layer-2 VPNs over the EPON-WiMAX integrated network to provide state-of-the-art MC service support. MC-FiWiBAN extends the MC coverage to rural areas and improves the PSDR communications by endorsing the emerging MC multimedia services. By specifying salient network operational features such as requesting and granting, traffic requirements and statistical bandwidth guaranteed rates for real-time services, MC-FiWiBAN offers a resource management platform which facilitates the design of VPN resource allocation schemes.

The key advantages of MC-FiWiBAN can be summarized as follows:

- *Robustness*: By constructing layer-2 VPNs and performing the proper error recovery and resource management strategies, MC-FiWiBAN can be more robust than legacy wired and wireless networks (e.g., traditional PONs, WiMAX, and WiFi) that also possess limited reaching abilities.

- *Centralized Operation and Management*: MC-FiWiBAN not only provides high-speed mobile access in rural areas, but also enables centralized control over the network resources at the OLT using its operation and management unit.

- *VPN Interoperability*: By deploying layer-2 VPNs, MC-FiWiBAN provides an integrated VPN service suite that enables interoperability between fixed and mobile platforms.

- *Scalability*: The installation of WiMAX networks in rural areas enables a seamless support of more users and services, such that no modifications are required to the already installed equipments and layer-2 protocols.

- *Improved TETRA Services*: Due to the increased bit rates of MC-FiWiBAN, TETRA (V+D) services' limitations (such as call setup delays) can be considerably improved. Furthermore, the emerging MC multimedia applications can be supported seamlessly.

Chapter 4

WiMAX-VPON: VPN Resource Management over EPON-WiMAX

With the resource management platform of MC-FiWiBAN, we propose a new VPN resource management framework over the EPON-WiMAX integration, so-called WiMAX-V**P**ON. The proposed framework consists of a new VPN-based QoS provisioning paradigm, two AC schemes, and a DBA mechanism.

The proposed QoS provisioning paradigm enables a robust and fair bandwidth distribution for registered VPNs in the uplink/upstream shared media. The proposed AC schemes are implemented on a three-stage system, which is involved in the collaboration among the SS, ONU-BS, and OLT. Such a decentralized AC design reduces the complexity and "decision time" of the AC scheme, as opposed to installing it at one end (e.g., the OLT). Namely if the latter is applied, the OLT will have to store and process information for every wireless and optical user in the network; whereas with the proposed schemes, ONU-BS and SS collectively handle the wireless domain and leave the optical domain handling to the OLT.

The first AC scheme is a VPN measurement-based AC (VPN-AC) which admits a flow if there is enough bandwidth in both the wireless and optical domains to accommodate its *guaranteed rate*.

While VPN-AC can ensure and protect the QoS for new and existing flows, it might not achieve high network utilization due to the fact that measurement-based AC schemes keep the delay of an admitted flow less than the frame size. Therefore we propose a novel delay-based admission control (DAC) engine which admits a flow if its expected delay is less than the maximum bound that is specified in the VPN SLA. We will show that DAC not only enables inter-VPN statistical multiplexing, but also increases the network utilization by admitting more flows. The expected delay is measured through a new generic approximation model that applies to both WiMAX and EPON networks. Using classical queuing theory, our proposed analytical model is able to provide a fine estimation of the network behavior with different input parameters. Our model also helps in setting a salient network parameter, the OFDM frame length, in order to minimize the wastage of wireless resources.

To complement the proposed AC schemes, we propose a new upstream/uplink VPN-based DBA (VPN-DBA) scheme which provides guaranteed bandwidth for each admitted VPN flow. VPN-DBA differs from previous related work [37, 34, 36, 32] in that it offers robust bandwidth allocation with a MAC–PHY cross layer consideration. Namely rather than relying solely on MAC requests [55], the PHY burst profile of each wireless user is also taken into account.

With WiMAX-V**P**ON, we can achieve per-flow QoS protection and bandwidth guarantee for admitted traffic. From a VPN user perspective, once a VPN tunnel is established, it is definite that the proper resources are "reserved" for this tunnel, and that its bandwidth is allocated by means of the DBA. Our simulation results will show that in the case where no AC is applied, a drastic performance degradation is witnessed for already admitted and newly admitted VPN services.

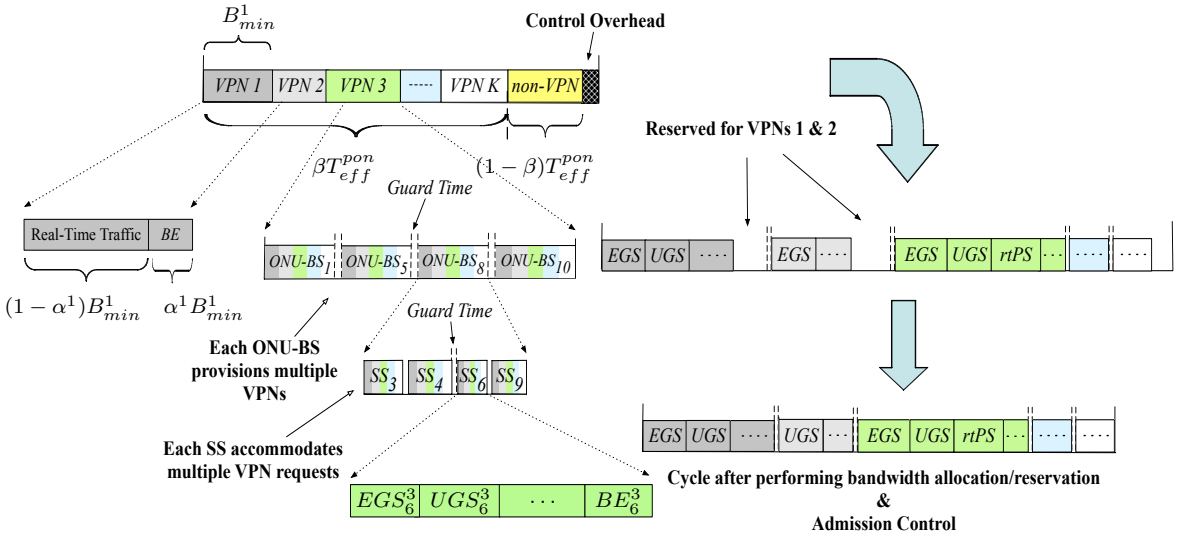

Figure 4.1: Proposed QoS-provisionning paradigm with $K = 4$ VPNs; all supported by ONU-BSs 1, 5, 8, and 10. These ONU-BSs provision V_3 services through SSs 3, 4, 6, and 9. In turn, SS_6 accommodates V_3 requests. EGS^3_6 means EGS bandwidth belongs to SS_6 and V_3.

4.1 QoS-provisioning Paradigm

The proposed VPN-based QoS-provisioning paradigm takes into account the control messaging overheard when distributing the upstream bandwidth among the supported MC systems. Namely, the effective upstream PON cycle T^{pon}_{eff}, which is the upstream optical/fiber cycle length (T^{up}_{fi}) minus the control overhead that is caused by the polling and requesting signaling, is divided into two *sub-cycles*. As illustrated in Fig. 4.1, the first sub-cycle βT^{pon}_{eff} (where $\beta \in [0, 1]$) is shared among all the K VPNs, whereas the second sub-cycle $(1-\beta)T^{pon}_{eff}$ is shared among non-VPN services (to support legacy users as well). Note that T^{pon}_{eff} can either be obtained via simulations by measuring the signaling overhead rate, or analytically (as we will see later).

Let B^k_{min} be the bandwidth reserved for V_k in each PI, and $\mathcal{C}_{pon}$ the transmission speed of PON in Mbps. In addition, let each V_k be given a weight w_k to determine its *agreed-upon* bandwidth share. B^k_{min} (in bytes, thus divide by 8) is then computed

as follows:

$$B^k_{min} = \frac{\beta T^{pon}_{eff} \times \mathcal{C}_{pon} \times w_k}{8}, \quad \text{where} \left(\sum_{k=1}^{K} w_k = 1 \right).$$

An important parameter in the proposed framework is the minimum per-VPN throughput to avoid BE traffic starvation, which can occur in case most admitted flows in the network are EGS and real-time flows (i.e., higher priority traffic). The per-VPN minimum throughput is achieved by reserving a portion $\alpha^k B^k_{min}$ (where $\alpha^k \in [0, 1]$) for BE traffic, while the real-time flows share the remaining $(1-\alpha^k)B^k_{min}$ quota. The value of α^k is assumed to be pre-defined in the SLA, to reflect the minimum BE throughput requirement for V_k.

As noticed, our paradigm is designed to be architecture-independent. Namely, it can operate on top of any of the EPON-WiMAX architectures that were described earlier. In addition, it is designed to allow each SS to access its VPN reserved bandwidth through any ONU-BS, thereby enabling mobile user operation which is vital for the MC scenario.

4.2 System Model

4.2.1 EPON-WiMAX Architecture

Since WiMAX-V**P**ON is designed to be architecture-independant, the decision of selecting any of the described architectures can be left to the network designer's preferences. Such a decision could be made based on the pros and cons of each architecture.

In our framework, we employ the P2MP EPON-WiMAX architecture [4]. However a mesh-based EPON-WiMAX architecture may alternatively be installed to take advantage of the multi-hop routing and relaying capabilities of wireless mesh networks. Nonetheless, routing and the related challenges are far from the scope of this study. More details on how to perform routing in mesh-based FiWi networks can be found in [63].

4.2.2 Wireless Channel Model

The wireless channel is modeled as Rayleigh fading channel [64] that is suitable for flat-fading channels, as well as frequency-selective fading channels encountered with OFDM. The received signal by SS i at time t, $rs_i(t)$ is given as follows:

$$rs_i(t) = g_i(t) \times ts_i(t) + bn_i(t), \tag{4.1}$$

where $ts_i(t)$ is the transmitted signal, and $bn_i(t)$ is the background noise at time t. $g_i(t)$ is the total instantaneous channel gain that jointly considers the multipath effect, shadowing effect, and path loss exponent. For fixed users, the average channel gain g_i can is given as follows [65]:

$$g_i = me_i \sqrt{\frac{\epsilon}{d_i^{(\gamma)}} \times fe_i}, \tag{4.2}$$

where d_i is the distance between SS i and the connected ONU-BS, ϵ is a constant including the transmission and receiving multi-input-multi-output (MIMO) antenna gain [65], and γ is the path loss exponent. fe_i is a random variable denoting the shadow fading effect, and me_i is the multipath fading effect representing the Rayleigh fading channel. The average SNR for SS i is given by:

$$SNR_i = \frac{\mathcal{P}_i}{\mathcal{V}_{bn}}, \tag{4.3}$$

where $\mathcal{V}_{bn}$ is the background noise variance. $\mathcal{P}_i$ is the receiving power and is given by $\mathcal{P}_i = |g_i|^2 \mathcal{P}_t$, where $\mathcal{P}_t$ is the total transmitter power of the ONU-BS. Assuming that $\mathcal{P}_t$ is fixed, $\mathcal{P}_i$ can be allocated by the ONU-BS such that the maximum SNR (SNR_i^{max}) is achieved.

We assume that multiple transmission modes are available, with each mode representing a pair of a specific modulation format and a forward error correcting (FEC) code. Based on the CSI estimated at the receiver, the adaptive modulation and coding (AMC) controller determines the modulation-coding pair/mode, which

Table 4.1: Adaptive Modulation and Coding (AMC) modes

Modulation	BPSK	QPSK		16 QAM		64 QAM	
Transmission Mode (x)	1	2	3	4	5	6	7
Coding Rate (CR)	1/2	1/2	3/4	1/2	3/4	2/3	3/4
Receiver SNR (db)	6.4	9.4	11.2	16.4	18.2	22.7	24.4
bits/symbol ($\mathcal{B}$)	0.5	1	1.5	2	3	4	4.5
Coded bits/subcarrier ($\mathcal{W}_{sc}$)	1	2	2	4	4	6	6

is sent back to the transmitter through a feedback channel for the AMC controller to update the transmission mode.

The target of our study is the VPN setup by taking WiMAX networks as an extension to EPON networks, in order to offer a high-speed wireless access for MC units in the *last mile* [4]. Since EPON is TDMA-based and for simplicity, we employ the OFDM-TDMA air interface for the wireless channel access. OFDM-TDMA is supported by the IEEE 802.16 standard, and is very suitable for fixed wireless users (i.e., using the IEEE 802.16d standard that is widely deployed in both Europe and Asia) [37]. As a result, each VPN user/SS will be allocated all the OFDM subcarriers and a TDD time-slot (or TDD frame physical slots) for uplink transmission.

Given a bit error rate (BER) less than 10^{-6}, Table 4.1 lists the convolutionally coded M-ary rectangular or square QAM modes, adopted from the HIPERLAN/2 or the IEEE 802.11a standards [66] with specific SNR_i^{max} and bits/symbol [67].

Let O_d be the total number of OFDM data subcarriers, and T_{sym} the OFDM symbol duration in seconds. For a transmission mode x, SS i's raw transmission rate $\mathcal{C}_i(x)$ (in bps) is computed as follows:

$$\mathcal{C}_i(x) = \frac{O_d \times \mathcal{W}_{sc}(x) \times CR(x)}{T_{sym}}. \tag{4.4}$$

4.3 VPN-Based Admission Control (VPN-AC)

With the TSPEC specified in MC-FiWiBAN, a measurement-based admission control [60] can be designed as follows:
Given the reserved bandwidth rate for V_k, a new flow f can be admitted if:

$$\lambda_{f,i}^{k} + \sum_{a=1}^{A_k} \lambda_{a,i}^{k} \leq \frac{(1-\alpha^k) B_{min}^{k} \times 8}{\beta T_{eff}^{pon}}, \tag{4.5}$$

where A_k is the number of real-time admitted flows (CBR and/or VBR) of V_k, and $\lambda_{f,i}^{k}$ ($\lambda_{a,i}^{k}$) is the guaranteed rate for flow f (flow a) computed according to either Eq. (3.1) or Eq. (3.4). However, there are other restrictions that need to be taken into consideration in VPN-based EPON-WiMAX networks, rather than simply admitting based on such a rule. Due to the fact that V_k could be simultaneously provisioned at multiple ONU-BSs, the reserved bandwidth for V_k is shared among all the ONU-BSs that provision V_k at a first stage, and meanwhile shared among all the SSs with the same provisioning capability at a second stage. In this case, the AC's decision making needs to further consider the network architecture and SSs' distribution. For this reason, we propose a three-stage AC mechanism, where all of the SS, ONU-BS, and OLT collaboratively perform AC in order to satisfy the conditions defined in Eqs. (3.1) and (3.4). Note that the BE traffic requests are always admitted. In addition, the admitted flows will be further distinguished according to a DBA algorithm (which will be provided in Section 4.5).

4.3.1 At SS

We first denote $\mathbf{M}$ as the set of all ONU-BSs, and $\mathbf{N}$ as the set of all SSs. Let $\mathbf{M}^k$ be the set of ONU-BSs that provision V_k and share the total allocated bandwidth $\alpha^k B_{min}^{k}$ for maintaining the minimum BE throughput. Let also w_j^k be the *weight* of ONU-BS j to determine its portion from V_k's reserved bandwidth. Hence the rate reserved for BE traffic of V_k at each ONU-BS j, denoted $\mathcal{R}_j^{k,be}$ (in bps), can be

expressed by:

$$\mathcal{R}_j^{k,be} = \frac{\alpha^k B_{min}^k w_j^k \times 8}{\beta T_{eff}^{pon}}, \quad \text{where} \left(\sum_{j \in \mathbf{M}^k} w_j^k = 1 \right). \tag{4.6}$$

Similarly, let $\mathbf{N}_j^k$ denote the set of SSs using the services of V_k via ONU-BS j. Let also $w_{i,j}^k$ be the bandwidth *weight* of SS i for V_k's bandwidth provisioned by ONU-BS j, such that $\left(\sum_{i \in \mathbf{N}_j^k} w_{i,j}^k = 1 \right)$. Thus, the reserved BE rate for each user/SS i of V_k at ONU-BS j, denoted $\mathcal{R}_{i,j}^{k,be}$, can be expressed by:

$$\mathcal{R}_{i,j}^{k,be} = \frac{\alpha^k B_{min}^k w_j^k w_{i,j}^k \times 8}{\beta T_{eff}^{pon}}. \tag{4.7}$$

Note that the reserved rate information can be broadcasted by the OLT to all the ONU-BSs and consequently to all the SSs in the EPON-WiMAX *registration* phase (or sent as a unicast message to the newly joined SS) [27].

Upon the arrival of flow f, SS i's admission control unit (ACU) extracts its parameters and admits the flow if it is a BE service. Consequently, flow f shares the reserved BE bandwidth with other admitted BE flows. Conversely if f is a real-time flow, its guaranteed rate is computed and it is admitted to V_k via ONU-BS j if the following condition is satisfied:

$$\lambda_{f,i}^k + \sum_k \left(\sum_a \lambda_{a,i}^k + \mathcal{R}_{i,j}^{k,be} \right) \leq \mathcal{C}_i(x). \tag{4.8}$$

More specifically, a new flow is admitted at the SS-side if its guaranteed rate plus the already admitted traffic (real-time and BE reserved share) is less than or equal to the SS PHY transmission rate. This condition also implies that SS i's PHY rate cannot go lower than $\mathcal{C}_i(x)$; otherwise, the bandwidth will no longer be guaranteed. Thus, our system guarantees the bandwidth for an admitted flow under the condition that its respective SS maintains a minimum PHY rate to obey the admission rule.

Remark 4.3.1. *The value of $\mathcal{C}_i(x)$ can be negotiated in advance between the VPN*

user/SS and the ONU-BS in order to ensure a minimum QoS level for each admitted flow [59]. The negotiation may be based on prior knowledge of the user's channel condition, location, and transmission capability. However determining these parameters is not in the scope of this work.

4.3.2 At ONU-BS

Once a real-time flow is conditionally admitted at the SS level, it is reported to its connected ONU-BS j. The ONU-BS then locally performs rate-based AC according to the bandwidth requirement of the arriving flow along with the overall wireless bandwidth availability. The condition for flow f of V_k from SS i to be admitted at ONU-BS j is defined as follows:

$$\frac{\lambda_{f,i}^{k}}{\mathcal{C}_i(x)} + \sum_{k}\sum_{s\in\mathbf{N}}\sum_{a}\frac{\lambda_{a,s}^{k}}{\mathcal{C}_s(x)} \leq NBR - \sum_{k}\sum_{s\in\mathbf{N}}\frac{\mathcal{R}_{s,j}^{k,be}}{\mathcal{C}_s(x)}, \tag{4.9}$$

where the *nominal bandwidth ratio* is defined as $NBR = (1-C_o)$, and C_o represents the control overhead ratio caused by the signaling required to perform resource allocation, which will be evaluated via simulations. $\frac{\lambda_{f,i}^{k}}{\mathcal{C}_i(x)}$ is the ratio of the channel rate required to transmit flow f in one-second time interval. If sufficient bandwidth is available to accommodate the flow, it will be reported to the OLT for the final stage of AC in the VPN level.

4.3.3 At OLT

After passing the first and second stages, flow f is admitted by the OLT if sufficient bandwidth is available in V_k. The condition of admission is defined as follows:

$$\lambda_{f,i}^{k} + \sum_{s\in\mathbf{N}}\sum_{a}\lambda_{a,s}^{k} \leq \frac{(1-\alpha^{k})B_{min}^{k}\times 8}{\beta T_{eff}^{pon}}. \tag{4.10}$$

A complete flowchart of the proposed VPN-AC scheme is depicted in Fig. 4.2.

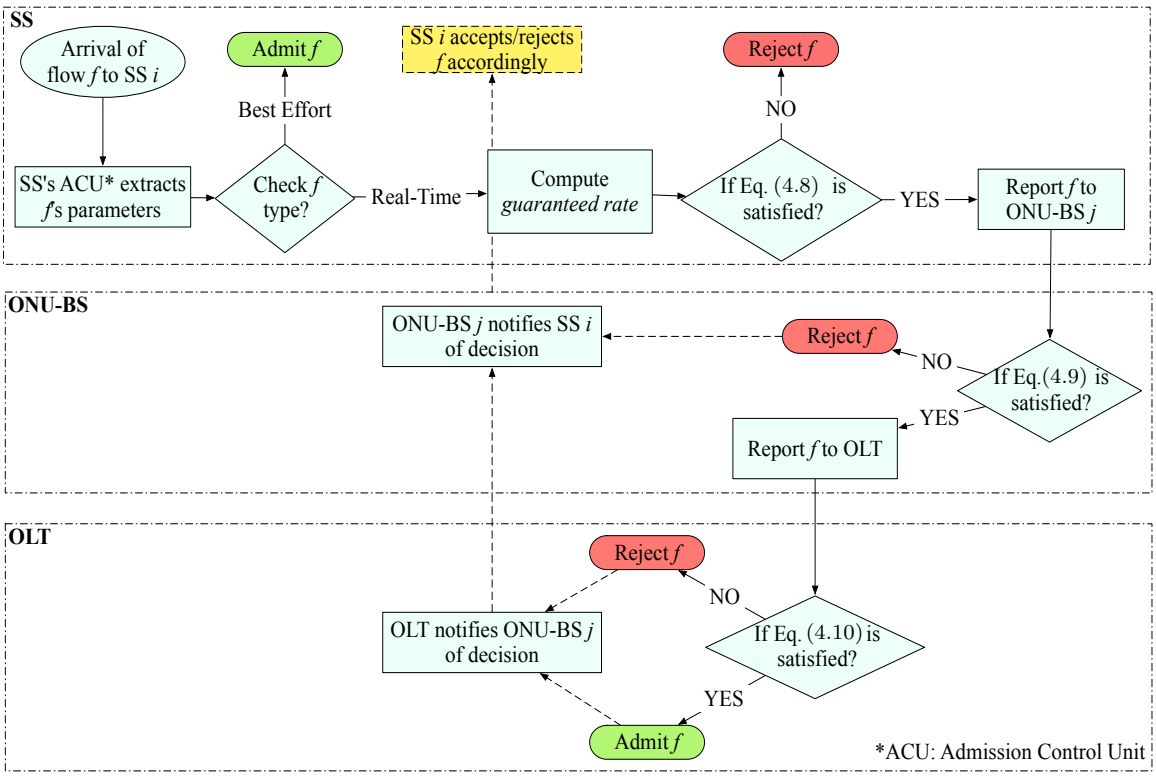

Figure 4.2: VPN-AC flowchart

4.4 Delay-based Admission Control (DAC)

In the SLA, each CoS c of V_k is associated with a maximum E2E delay bound $\mathbb{D}_c^k$. With such information, we design a three-stage delay-based admission control (DAC) engine that admits a flow if with its inclusion the expected E2E delay measurements of all real-time flows are lower than their respective bounds. As shown in the flowchart in Fig. 4.3, The delay computation involves the collaboration of each SS and ONU-BS, as well as the OLT.

4.4.1 At SS

Same as with VPN-AC, the first stage of DAC is performed at the SS where the ACU extracts the parameters for an incoming flow f. Flow f is directly admitted if it is a BE flow, and it shares the reserved BE bandwidth with other admitted BE flows. Conversely if f is a real-time flow, its guaranteed rate is computed and

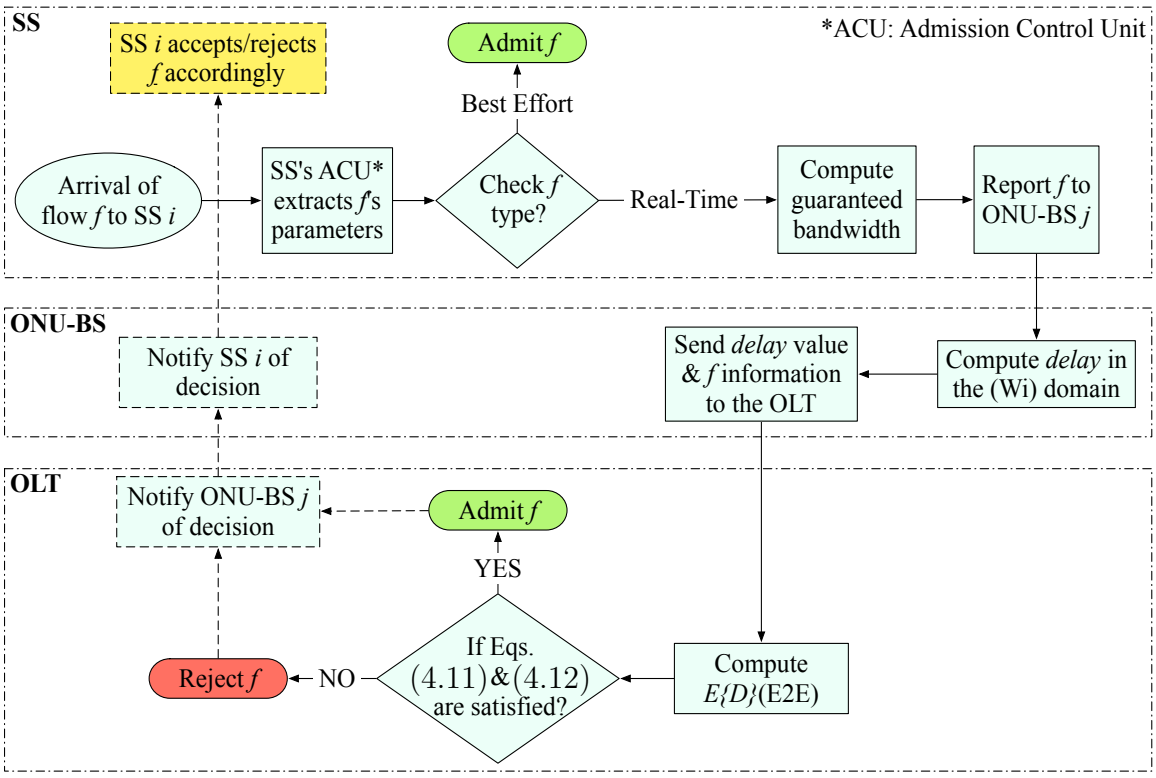

Figure 4.3: DAC flowchart

then reported to the ONU-BS.

4.4.2 At ONU-BS

Upon receiving the flow request from the SS, the ONU-BS computes the expected delay in the wireless domain and forwards it to the OLT along with f's guaranteed rate for the final stage of AC.

4.4.3 At OLT

Since the OLT has all the information about all the connected nodes and users (e.g., number of VPNs and number of ONU-BSs) as well as the SLA-based QoS requirements and the admitted guaranteed rates, it can make the final decision on whether or not to admit the incoming flow by computing the expected E2E flow

delay $E\{D_c^k\}$(E2E). More specifically, the OLT admits a flow if $\forall c = 1, \ldots, n-1$:

$$E\{D_c^k\}(\text{E2E}) \leq \mathbb{D}_c^k, \tag{4.11}$$

$E\{D_c^k\}$(E2E) is computed in the next section. In order to *commit* the minimum per-VPN bandwidth that is computed in Eq. (4.1), bandwidth can be shared among VPNs only if all the VPNs can be accommodated. More specifically, a flow f arriving at SS i in CoS c with guaranteed rate $\lambda_{c,i}^k$ is admitted if the following conditions are satisfied:

$$\sum_c \sum_{s \in \mathbf{N}} \lambda_{c,s}^k = \frac{(1-\alpha^k) B_{min}^k, \times 8}{T_{eff}^{pon}}, \tag{4.12a}$$

and $\exists k' = 1, \ldots, K; k' \neq k$,

$$\lambda_{c,i}^k + \sum_c \sum_{s \in \mathbf{N}} \lambda_{c,s}^{k'} \leq \frac{(1-\alpha^{k'}) B_{min}^{k'} \times 8}{T_{eff}^{pon}}, \tag{4.12b}$$

where $\lambda_{c,s}^{k'}$ is the guaranteed rate of SS $s \in \mathbf{N}$, pertaining to $V_{k'}$. In other words, the flow f will be admitted if there is any room to admit it by any VPN bandwidth.

With such an admission rule, if an admitted flow in $V_{k'}$ does not "leave" the network before the arrival of a new flow of the same class, inter-VPN bandwidth sharing could be enabled between the involved VPNs. With this regards, the upstream bandwidth acts as a pool of resources for all users of different VPNs, thereby achieving inter-VPN statistical multiplexing rather than the fixed bandwidth reservation of VPN-AC. This obviously leads to increased network utilization and thus higher throughput while meeting the QoS requirements of all admitted VPN flows.

Note that with both VPN-AC and DAC, the flows' requests and grants can be embedded as additional fields in the control messages (i.e., BW_Request, UL_MAP, REPORT and GATE). The values of these fields are filled with the proper information whenever a flow request/grant takes place, otherwise they are either left empty or given a negative value.

4.4.4 Analytical Model

In this section, we develop a generic analytical model to measure the expected delay of each admitted VPN flow. We first overview the related work and show how the proposed analytical model is different from the previous art.

In addition to the expected delay required to perform DAC, our model presents other important performance metrics such as average queuing delay and average queue size for each measured CoS. Furthermore, it computes the optimal OFDM frame length that can maximize the network utilization while ensuring the committed bandwidth.

Related Work

To the best of our knowledge, only the work in [68] presented an analytical model to measure the packet delay in EPON-WiMAX. Nonetheless, it only focused on ingress and egress queues at ONU-BSs, with an undefined access mechanism and bandwidth allocation scheme. Therefore, it is necessary to develop a new model that can better serve our framework.

In WiMAX, many previously reported studies have proposed analytical models to measure the packet delay. Notably in [62], the authors proposed an analytical model to measure the performance of polling and non-polling services based on the GPSS allocation scheme. Hence, no per-flow analysis was presented. The authors of [69] proposed an analytical model to measure the performance of unicast polling services with only one packet transmission in each frame. Furthermore, a bandwidth allocation mechanism was absent and the various QoS requirements were not taken into account. Similarly in [70], an analytical model was presented with a hybrid unicast-multicast polling system model. The model only focused on the impact of the number of polls on the overall network performance without a DBA scheme that can achieve multi-class service support.

In EPON, very few works were presented to analytically measure the packet

delay except for [71, 72]. Nonetheless, both studies focused on a single queueing system and did not consider any QoS requirements/measurements under a multi-class and multi-service scenario.

For all these aforementioned reasons, we design a new generic analytical model that applies to both WiMAX and EPON networks, as well as to their integration. Our model clearly differs from the previous work by providing per-flow QoS performance analysis that can facilitate the design of MAC protocols, as well as the optimization of network parameters to offer an efficiently traffic-engineered FiWi network.

Preliminaries

In our model, we refer to a polling node as *server*, and a polled station as *client*. Thus, the OLT is considered a server where polling the ONU-BS (i.e., client) in the optical domain; whereas an ONU-BS acts as a server where polling an SS (i.e., client) in the wireless domain. Therefore client i indicates an SS if the model is applied in the wireless domain, and an ONU-BS if the model is applied in the optical domain. Furthermore where applicable, we use the variable m to denote the number of clients connected to one server in a particular domain (Fi or Wi).

The EPON-WiMAX network consists of multiple clients, with each client having multiple queues, accessing the transmission medium in a TDMA fashion in the optical domain, and in an OFDM-TDMA fashion in the wireless domain. The server allocates bandwidth such that the *guaranteed rate* is ensured; thus the number of packets that are transmitted in each frame/cycle is equal to the guaranteed rate of each service. Therefore, we model each client as a weighted round robin (WRR) scheduler with only one round of scheduling, such that the client transmits all the bandwidth allocated for each CoS in this round. Nonetheless due to the TDMA channel access, each scheduler will be exposed to a "vacation time" before accessing its portion of channel (or time slot). More specifically, this vacation time represents the time where no data packets are being transmitted.

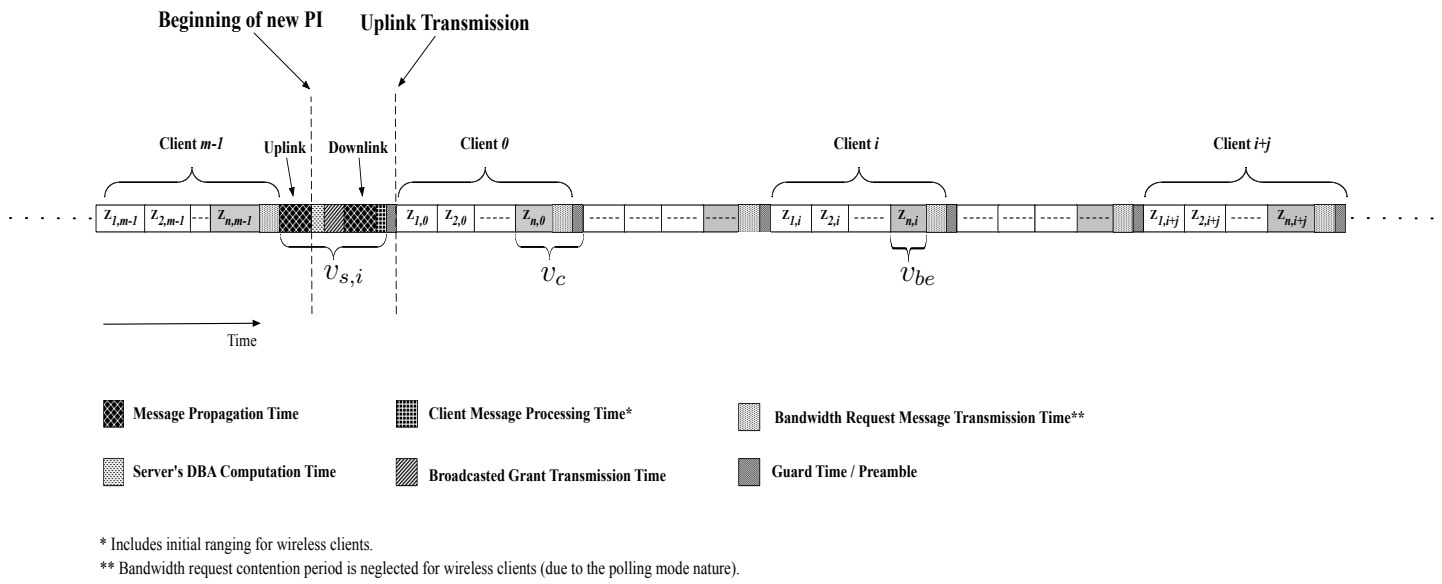

* Includes initial ranging for wireless clients.
** Bandwidth request contention period is neglected for wireless clients (due to the polling mode nature).

Figure 4.4: Illustration of temporal events in each Polling Interval (PI)

In order to facilitate the analysis and with the similarity between polling-based WiMAX and EPON networks, we graphically illustrate in Fig. 4.4 the temporal events that occur in a single PI (wireless or optical). Here, the clients are polled/scheduled sequentially with client 0 as the first polled/scheduled client, henceforth until client $m-1$. The vacation time is divided into three folds: server vacation, best-effort vacation, and client vacation.

- **Server Vacation:** The server vacation, denoted $v_{s,i}$, is the idle period displayed in the system between two consecutive uplink/upstream data transmissions (as seen by client i). That is in each PI, the server waits until all the request messages (i.e., BW_Request messages in WiMAX [17] and REPORT messages in EPON [60]) are received from its connected clients before performing bandwidth allocation. The respective waiting time converges to only the propagation time of the last message sent from client $m-1$, because the transmission time of all request messages is assumed to be of much shorter length than data transmission windows. Hence, all the requests sent from client 0 until client $m-2$ will arrive at the server's side while client $m-1$ is still transmitting data packets in the uplink direction. At the be-

ginning of a new PI, the server spends little time to process the incoming messages and T_{dba} to compute the DBA algorithm. Consequently, the server broadcasts grants (i.e., GATE in EPON and UL_MAP in WiMAX) for each client. Without loss of generality, the analytical model assumes a uniform client-server distance (i.e., equal message propagation time), where the grant message destined to client 0 is transmitted first on the downlink channel.

- **Best-effort Vacation:** The main target of our model is to derive the expected E2E delay for real-time queues (i.e., for $c = 1, \ldots, n-1$), where class ($c = n$) is for BE traffic. However, to measure the performance of real-time VPN streams with the existence of heavy-load BE traffic (i.e., $\alpha^k B^k_{min}$ is fully utilized), we assume that the total BE (of all VPNs) reserved bandwidth portion is represented as a vacation time, denoted v_{be}, for real-time queues of each client. More specifically, we claim the existence of at least one user per V_k, and this user may fully access V_k's reserved BE portion.

- **Client Vacation:** The client vacation, denoted v_c, is the idle period exhibited between any two contiguous transmission time slots. As shown in Fig. 4.4, in addition to the best-effort vacation, v_c consists of the time used for transmitting a request message plus the guard time that separates the transmission of two adjacent clients (e.g., clients 0 and 1) in the uplink/upstream direction.

To make the modeling process tractable, we assume that the guaranteed rates of all clients are Poisson-distributed, and identical and independently distributed (i.i.d.), with per-client i guaranteed rate $\lambda_i = \sum_{c=1}^{n-1} \lambda_{c,i}$. As a result, we model each client as a combination of WRR with one round of scheduling, and multi-service $M/G/1$ queue with vacations [73, 72]. Note that the purpose the model is to capture the long-term estimated average behavior of each admitted flow to perform DAC. While the assumption of Poisson-distributed traffic is valid for unshaped non-bursty traffic, it is a compromise between the precision and tractability of the model by using Poisson distribution to approximate the shaped arrival processes. To support this assumption, we have conducted a simulation study on the traffic

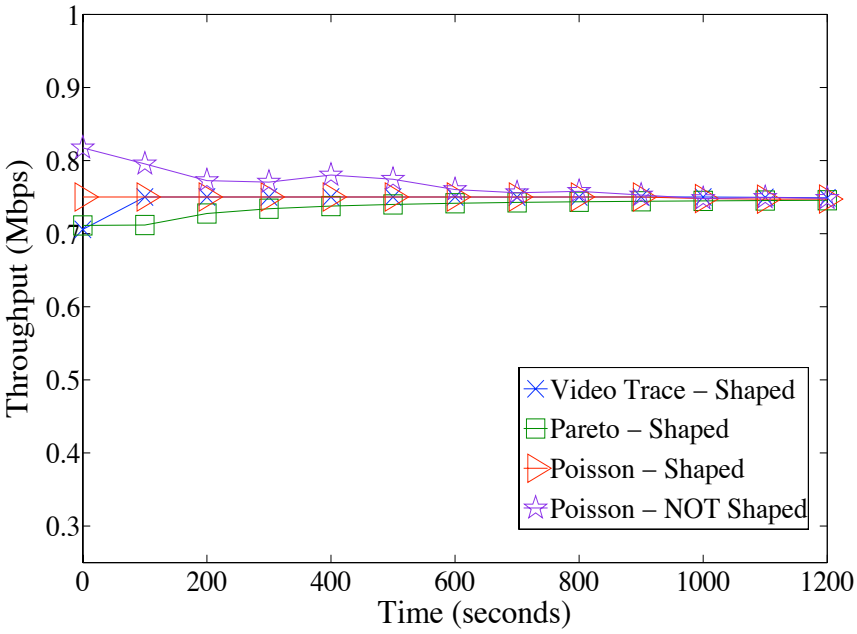

Figure 4.5: Comparison between different traffic profiles

that is being shaped using the DTLB (i.e., $\lambda_{c,i}$). Here, we have applied three incoming traffic profiles 1) a real video trace [1], 2) self-similar Pareto-distributed traffic and 3) Poisson-distributed traffic. As shown in Fig. 4.5, all traffics (of mean rate 750 $Kbps$) after passing through the DTLB, exhibit similar behavior regardless of their incoming traffic profiles. More importantly, the results clearly indicate how the unshaped Poisson-distributed traffic can nicely capture the behavior of the shaped bursty traffic and hence, as we assume, can be used to estimate $\lambda_{c,i}$. Note that it is possible to claim that the shaped traffic can be seen as constant. However, such an assumption is very aggressive as it does not consider any observed traffic fluctuation; whereas the claim of a Poisson-distributed $\lambda_{c,i}$ is regarded as a more conservative and valid assumption. Our numerical results will also verify the statistical adequacy of this approximation. We further apply the following relevant assumptions:

1. The wireless channel quality of each connection remains constant on a per-frame basis.

[1] Available at `http://trace.eas.asu.edu/preencoded/index.html`.

2. Perfect CSI for each SS is available at the ONU-BS receiver. Thus, the SNR reports are correctly received by the ONU-BS through the BW_Requests over an error-free feedback channel.

3. There exist enough OFDM sub-channels to accommodate all admitted users.

4. The buffer size of each queue is computed according to Eq. (3.5), where no packet dropping is possible.

5. All VPNs provision the same types of traffic.

Since all the VPNs are assumed to support the same types of traffic, our analysis will be the same for the all the CoSs. Hence, we omit the usage of k in our notations in the following context. The average arrival rate at class c of a wireless server is the sum of all arrival rates of class c of all wireless clients connecting to the same server. Hence, the total arrival rate λ will then be calculated in the following manner:

$$\lambda = \begin{cases} \sum_{j=0}^{|\mathbf{M}|-1} \sum_{i=0}^{|\mathbf{N}|-1} \sum_{c=1}^{n-1} \lambda_{c,i,j} = |\mathbf{N}||\mathbf{M}| \sum_{c=1}^{n-1} \lambda_c & \text{(Fi)} \\ \\ \sum_{i=0}^{|\mathbf{N}|-1} \sum_{c=1}^{n-1} \lambda_{c,i} = |\mathbf{N}| \sum_{c=1}^{n-1} \lambda_c & \text{(Wi)} \end{cases} \tag{4.13}$$

The first and second moments of the transmission times for a class c and client i packet, can be expressed as $E[X_{c,i}] = \overline{X_{c,i}} = 1/\mu_{c,i}$, and $E[X_{c,i}^2] = \overline{X_{c,i}^2}$, respectively, with $\mu_{c,i}$ denoting the service time. The respective utilization factor is hence given by $\rho_{c,i} = \lambda_{c,i}\overline{X}_{c,i}$. We also assume that a steady state always exists. That is,

$$\rho_i = \rho_{1,i} + \rho_{2,i} + \cdots + \rho_{n-1,i} < 1 \tag{4.14}$$

Note that the steady state is enforced by allowing DAC to reject incoming flows when Eq. (4.14) is violated. In the Fi domain, all clients have equal transmission rates and are assumed to be equally loaded. Conversely in the Wi domain, each

client i may have a different transmission rate $\mathcal{C}_i(x)$ corresponding to an AMC mode x as per Table 4.1, and reflecting the channel condition of the client. Nonetheless as we will see in the next section, VPN-DBA deals with this issue by allocating more "time" (translated to capacity) for users with lower transmission rates, to achieve per-VPN statistical bandwidth guarantees for each CoS. Using Eq. (4.1), we can estimate the best-effort vacation time v_{be} in the following way:

$$v_{be} = \begin{cases} \dfrac{\sum_{k=1}^{K} \alpha^k B_{min}^k}{|\mathbf{M}| \times \mathcal{C}_{pon}} & \text{(Fi)} \\ \\ \dfrac{\sum_{k=1}^{K} \alpha^k B_{min}^k}{|\mathbf{M}| \times |\mathbf{N}| \times \overline{\mathcal{C}}} & \text{(Wi)} \end{cases} \tag{4.15}$$

where $\overline{\mathcal{C}}$ is defined as the average transmission rate in one wireless domain (i.e., at one server) and is computed as follows:

$$\overline{\mathcal{C}} = \frac{1}{|\mathbf{N}|} \sum_{i=0}^{|\mathbf{N}|-1} \mathcal{C}_i(x).$$

The vacation intervals v_c and $v_{s,i}$ are computed based on the domain the client belongs to (i.e., Fi or Wi). The client vacation v_c is uniform in both domains and is given by:

$$\begin{aligned} v_c &= v_{be} + T_{br}^{proc} + T_{br}^{tran} + T_g^a \\ &= \begin{cases} \dfrac{\sum_{k=1}^{K} \alpha^k B_{min}^k}{|\mathbf{M}| \times \mathcal{C}_{pon}} + T_{br}^{proc} + T_{br}^{tran} + T_g^a & \text{(Fi)} \\ \\ \dfrac{\sum_{k=1}^{K} \alpha^k B_{min}^k}{|\mathbf{M}| \times |\mathbf{N}| \times \overline{\mathcal{C}}} + T_{br}^{proc} + T_{br}^{tran} + T_g^a & \text{(Wi)} \end{cases} \end{aligned} \tag{4.16}$$

where T_{br}^{proc}, T_{br}^{tran}, and T_g^a are the bandwidth request processing time, the bandwidth request transmission time, and the guard time in the "active" period, respectively.

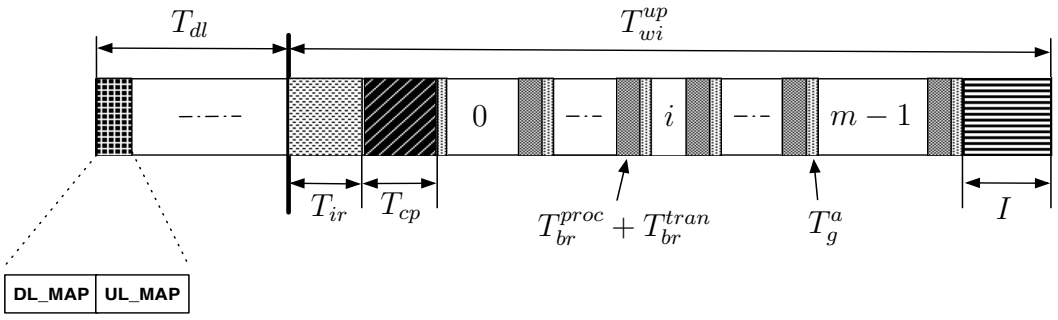

Figure 4.6: TDD WiMAX frame structure

While v_c is uniform, the server vacation $v_{s,i}$ varies due the TDD frame nature in WiMAX (illustrated in Fig. 4.6). Hence, we compute $v_{s,i}$ as follows:

$$v_{s,i} = \begin{cases} T_{br}^{proc} + 2T_i^{prop} + T_{dba} + T_{gr}^{proc} + T_{gr}^{tran} & \text{(Fi)} \\ \\ T_{dl} + T_{ir} + T_{cp} + T_{br}^{proc} + 2T_i^{prop} + T_{dba} + T_{gr}^{proc} + T_{gr}^{tran} + I & \text{(Wi)} \end{cases} \tag{4.17}$$

where T_{dl}, T_{ir}, T_{cp}, T_i^{prop}, T_{gr}^{proc}, and T_{gr}^{tran} are the wireless downlink sub-frame length, the initial ranging time, the contention period, the propagation delay, the grant processing time, and the grant transmission time, respectively. In the wireless domain, OFDM frames have fixed lengths (5, 10, or 20 ms) [17]. Thus in the case where the OFDM uplink sub-frame is not fully utilized, each client will exhibit an additional vacation/idle time I proportional to the frame size (see Fig. 4.6). This time is derived based on the uplink sub-frame utilization U as follows:

$$I = T_{wi}^{up} - (U \times T_{wi}^{up}). \tag{4.18}$$

U is extracted from the traffic transmitted in the uplink channel as follows:

$$U = \frac{T_{ir} + T_{cp} + |\mathbf{N}| \times v_c + C}{T_{wi}^{up}}, \tag{4.19}$$

where C is the average data cycle length and is approximated as follows [74]:

$$C = \sum_{i=0}^{|\mathbf{N}|-1} \sum_{c=1}^{n-1} \frac{\overline{X_{c,i}}}{(1 - \rho_i + \rho_{c,i})}. \tag{4.20}$$

By combining Eqs. (4.18) and (4.20), I will then be given by:

$$I = T_{wi}^{up} - \left(T_{ir} + T_{cp} + |\mathbf{N}| \times v_c + \sum_{i=0}^{|\mathbf{N}|-1} \sum_{c=1}^{n-1} \frac{\overline{X_{c,i}}}{(1 - \rho_i + \rho_{c,i})} \right). \tag{4.21}$$

As noticed, the server vacation $v_{s,i}$ includes only one grant processing and transmission times. This is due to the fact that during the data interval of client 1, the rest of the clients are continuously receiving grant messages on the downlink channel. Hence, the arrival of these clients' grant messages will never be late or entail extra overhead time/delay.

We also define $AI_i(t)$ as the access interval (vacation plus data) for a client i in interval $[0, t)$, and where v_i is the vacation period appearing just before i's data interval. As shown in Fig. 4.4, v_i depends on i's position in each PI and is estimated as follows:

$$v_i = \begin{cases} v_c + v_{s,i} & (i = 0) \\ v_c & (1 \leq i \leq m - 1) \end{cases} \tag{4.22}$$

The polling control overhead in each PI can then be estimated as the sum of all vacations. As a result, T_{eff}^{pon} in Eq. (4.1) will then be computed as follows:

$$\begin{aligned} T_{eff}^{pon} &= T_{fi}^{up} - \sum_i v_i \\ &= T_{fi}^{up} - (|\mathbf{M}| \times v_c + v_{s,0}). \end{aligned} \tag{4.23}$$

End-to-End (E2E) Packet Delay

Each packet ξ may arrive to any client i during the whole PI and can belong to any VPN of class c. In each domain, ξ will be subject to a delay $D_{c,i}$, such that:

$$D_{c,i}(\xi) = W_{c,i}(\xi) + T_i^{prop} + X_{c,i}(\xi), \tag{4.24}$$

where $W_{c,i}(\xi)$ and $X_{c,i}(\xi)$ are ξ's average queuing delay and transmission time, respectively. In the steady state, as $\xi \to \infty$, the expected value of the total delay is given as:

$$E\{D_{c,i}\} = E\{W_{c,i}\} + T_i^{prop} + E\{X_{c,i}\}. \tag{4.25}$$

$E\{X_{c,i}\}$ is given by $1/\mu_{c,i}$ and $T_i^{prop} = d_i/speed$, where d_i is the distance between client i and the server. Therefore in order to compute $E\{D_{c,i}\}$ (also denoted as $\overline{D_{c,i}}$), we need to derive an expression for $E\{W_{c,i}\}$. Once computed, the E2E packet delay will then be equal to the following:

$$\overline{D_{c,i}}(\text{E2E}) = \overline{D_{c,i}}(\text{Fi}) + \overline{D_{c,i}}(\text{Wi}), \tag{4.26}$$

where $\overline{D_{c,i}}(\text{Fi})$ and $\overline{D_{c,i}}(\text{Wi})$ are the average packet delay in the optical and wireless domains respectively.

Queuing Delay Analysis

The queuing delay of ξ arriving at client i is expressed by:

$$W_i(\xi) = R_i(\xi) + N_i(\xi) \times \overline{X}(\xi) + Y_i(\xi), \tag{4.27}$$

where $R_i(\xi)$ denotes the server's residual time seen by packet ξ (i.e., the remaining time until the service time of the packet being processed is complete), $\overline{X}(\xi)$ is the mean service time of packet ξ, $N_i(\xi)$ denotes the total number of backlogged packets at client i, and $Y_i(\xi)$ denotes the gap interval seen by ξ. We note that

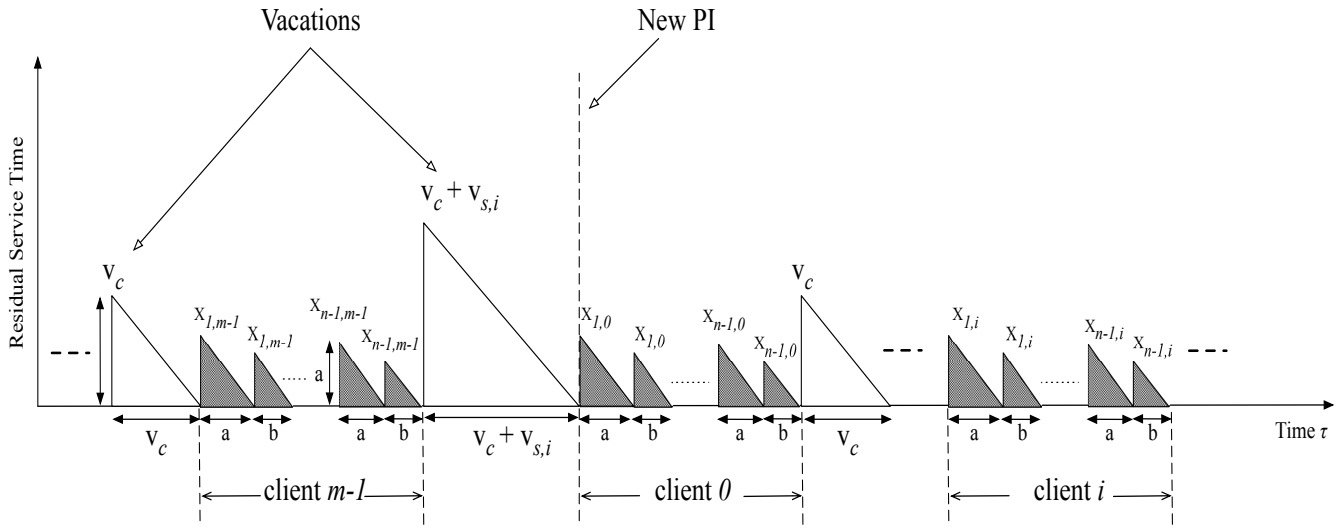

Figure 4.7: Derivation of the mean residual time $\overline{R_i}$ during $[0, t)$

$E\{R_i\} = \lim_{\xi\to\infty} R_i(\xi)$. Similarly, $E\{Y_i\} = \lim_{\xi\to\infty} Y_i(\xi)$, $E\{N_i\} = \lim_{\xi\to\infty} N_i(\xi)$, and $E\{W_i\} = \lim_{\xi\to\infty} W_i(\xi)$.

In the wireless domain, the queuing delay also includes the additional delay θ that is caused by the DTLB shaping (as described in Section 3.10).

We start by computing the queuing delay for classes 1 and 2, and then provide a generalized expression for class c, where $2 < c \leq n-1$. If ξ belongs to class 1, its expected queuing delay will then be equal to the following:

$$E\{W_{1,i}\} = \frac{E\{R_i\}}{\psi_i} + \frac{E\{N_{1,i}\}}{\mu_{c,i}} + E\{Y_i\}, \tag{4.28}$$

where ψ_i is client i's AI proportional to all clients' AIs:

$$\psi_i \triangleq \lim_{t\to\infty} \left(\frac{AI_i(t)}{\sum_{z=0}^{m-1} AI_z(t)} \right). \tag{4.29}$$

In steady state, ξ will see the same average number of packets queued, at both its enqueuing and dequeuing times. The expected number of arriving packets to class

1, at those times, is equivalent to $\lambda_{1,i} \times E\{W_{1,i}\}$. As a result:

$$\begin{aligned} \frac{E\{N_{1,i}\}}{\mu_{1,i}} &= \lambda_{1,i} \times E\{W_{1,i}\} \times \overline{X_{1,i}} \\ &= \rho_{1,i} \times E\{W_{1,i}\}. \end{aligned} \tag{4.30}$$

Hence, the expected queuing delay of the priority queue 1 is then computed as follows:

$$\begin{aligned} E\{W_{1,i}\} &= \frac{(E\{R_i\}/\psi_i) + E\{Y_i\}}{1-\rho_{1,i}} \\ &= \frac{(\overline{R_i}/\psi_i) + \overline{Y_i}}{1-\rho_{1,i}}. \end{aligned} \tag{4.31}$$

According to the aforementioned client i's WRR scheduling mechanism, the expected delay of a packet arriving at the second queue shall wait for all the packets in the higher priority queue and the packets that arrived earlier to the same priority queue, in addition to $\overline{R_i}$ and $\overline{Y_i}$. Thus:

$$\begin{aligned} E\{W_{2,i}\} &= \frac{E\{R_i\}}{\psi_i} + \frac{E\{N_{1,i}\}}{\mu_{1,i}} + \frac{E\{N_{2,i}\}}{\mu_{2,i}} + E\{Y_i\} \\ &= \frac{E\{R_i\}}{\psi_i} + \rho_{1,i}E\{W_{1,i}\} + \rho_{2,i}E\{W_{2,i}\} + E\{Y_i\} \\ &= \frac{(\overline{R_i}/\psi_i)}{1-\rho_{2,i}} + \frac{\rho_{1,i}[(\overline{R_i}/\psi_i) + \overline{Y_i}]}{(1-\rho_{1,i})(1-\rho_{2,i})} + \frac{\overline{Y_i}}{1-\rho_{2,i}} \\ &= \frac{(\overline{R_i}/\psi_i) + \overline{Y_i}}{(1-\rho_{1,i})(1-\rho_{2,i})}. \end{aligned} \tag{4.32}$$

Similarly, a general expression of the expected queuing delay for class c, where $2 < c \leq n-1$, can then be given by:

$$E\{W_{c,i}\} = \frac{(\overline{R_i}/\psi_i) + \overline{Y_i}}{(1-\rho_{1,i})(1-\rho_{2,i})\dots(1-\rho_{c,i})}. \tag{4.33}$$

To find the value of $\overline{R_i}$, we use the concept of the *mean residual service time* [73, 72] with a graphical argument. As shown in Fig. 4.7, $R_i(\tau)$ (the residual time at time τ) exhibits vacation times depending on the position of client i in each PI.

Therefore, the time average of $R_i(\tau)$ in $[0,t]$ is:

$$\frac{1}{t}\int_0^t R_i(\tau)d\tau = \frac{1}{t}\left(\sum_{x_{c,i}\in S_{c,i}(t)}\frac{1}{2}x_{c,i}^2 + \sum_{y_i\in L_i(t)}\frac{1}{2}y_i^2\right), \tag{4.34}$$

where $L_i(t)$ is the number of vacations appeared in $AI_i(t)$, and $S_{c,i}$ denotes the number of CoS c serviced packets, both during $[0,t]$. By assuming equally loaded clients, the number of vacations in $AI_i(t)$ can be evaluated as just $L(t)/m$, with $L(t) = \sum_i L_i(t)$ (the total number of vacations occurred during $[0,t]$). This is due to the fact that the vacations in $AI_i(t)$ repeat once in every m consecutive vacations. Hence, we can rewrite Eq. (4.34) as follows:

$$\begin{aligned}\overline{R_i} &= \frac{1}{t}\left[\Big(\sum_{c=1}^{n-1}\sum_{a=1}^{S_{c,i}(t)}\frac{1}{2}x_a^2\Big) + \Big(\frac{1}{m}L(t)\times\frac{1}{2}v_i^2\Big)\right]\\ &= \frac{1}{2}\left[\Big(\sum_{c=1}^{n-1}\frac{S_{c,i}(t)}{t}\Big)\overline{X_i^2} + \frac{1}{m}\Big(\frac{L(t)}{t}\times v_i^2\Big)\right],\end{aligned}$$

where v_i is computed from Eq. (4.22), and $\overline{X_i^2}$ denotes the second moment of client i's service time averaged over all classes. More specifically,

$$\overline{X_i^2} = \frac{\lambda_{1,i}}{\sum_{c=1}^{n-1}\lambda_{c,i}}\overline{X_{1,i}^2} + \cdots + \frac{\lambda_{n-1,i}}{\sum_{c=1}^{n-1}\lambda_{c,i}}\overline{X_{n-1,i}^2}.$$

We note that:

$$\lim_{t\to\infty}\sum_{c=1}^{n-1}\frac{S_{c,i}(t)}{t} = \sum_{c=1}^{n-1}\lambda_{c,i}.$$

Furthermore, we have:

$$\lim_{t\to\infty}L(t) = \frac{t(1-\rho_i)}{\overline{v}},$$

where $\overline{v} = (mv_c + v_{s,i})/m$, is the average duration of one vacation period. When

$t \rightarrow \infty$, the mean residual time will then be given as:

$$\begin{aligned} \overline{R_i} &= \frac{1}{2}\left[\Big(\sum_{c=1}^{n-1}\lambda_{c,i}\Big)\overline{X_i^2} + \frac{v_i^2(1-\rho_i)}{m\overline{v}}\right] \\ &= \frac{1}{2}\left[\Big(\sum_{c=1}^{n-1}\lambda_{c,i}\overline{X_{c,i}^2}\Big) + \frac{v_i^2(1-\rho_i)}{mv_c + v_{s,i}}\right]. \end{aligned} \tag{4.35}$$

The value of ψ_i in Eq. (4.29) is basically equivalent to the computation of the probability that packet ξ arrives during $AI_i(t)$ when $t \rightarrow \infty$, denoted as $\pi_i^{\xi}(t)$. By assuming equal data interval lengths for all clients, at steady state ξ can belong to client i with probability $1/m$. As a result ξ will arrive during client i's data interval with probability ρ_i/m, and to its vacation interval with probability $(1-\rho_i)v_i/\sum_{z=0}^{m-1} v_z$. Consequently, ψ_i is computed as follows:

$$\begin{aligned} \psi_i = \lim_{t\rightarrow\infty}\pi_i^{\xi}(t) &= \frac{\rho_i}{m} + (1-\rho_i)\frac{v_i}{\sum_{z=0}^{m-1} v_z} \\ &= \begin{cases} \dfrac{\rho_i}{m} + (1-\rho_i)\dfrac{v_c + v_{s,i}}{mv_c + v_{s,i}} & (i=0) \\ \\ \dfrac{\rho_i}{m} + (1-\rho_i)\dfrac{v_c}{mv_c + v_{s,i}} & (1 \le i < m) \end{cases} \end{aligned} \tag{4.36}$$

To determine Y_i, we first denote:

$$\gamma_{i,z} = E\{Y_i(\xi)|\pi_{i,z}^{\xi}\},$$

where,

$$\pi_{i,z}^{\xi}(t) \;=\; P\Big\{\text{packet } \xi \text{ arrives during } AI_i(t) \text{ and belongs to client } (i+z)\%m\Big\}.$$

$P\{.\}$ denotes the probability of the operand. As noticed, the computation of $\gamma_{i,z}$ is dependent on the location of $(i+z)\%m$ (see Fig. 4.4). In other words, if $0 \le (i+z)\%m \le i$, this means that ξ will be requested in the next PI and transmitted in the one after. This is due to the fact that a packet cannot be transmitted in

a PI by a client unless it is first reported to the server in the pervious PI. Hence, ξ will have to wait for a full PI before transmission, as well as the remaining PI before being requested. As a result, the total amount of gaps intervals exhibited in such scenario is equal to $zv_c + v_{s,i}$ (for the current PI) plus $mv_c + v_{s,i}$ (the average vacation time in one PI). Similarly, if $i+1 \leq (i+z)\%m \leq m-1$, then ξ will be reported in the current PI, and transmitted in the one after. Consequently, the total vacation time exhibited in this scenario will be equal to zv_c (for the current PI) plus $mv_c + v_{s,i}$. Note that in case ξ arrives during AI_0, then the total exhibited vacation time will also fall under this category (i.e., $i+1 \leq (i+z)\%m \leq m-1$). Accordingly, we can evaluate $\gamma_{i,z}$ as follows:

$$\gamma_{i,z} = \begin{cases} (z+m)v_c + 2v_{s,i} & (0 \leq (i+z)\%m \leq i) \\ (z+m)v_c + v_{s,i} & (i+1 \leq (i+z)\%m \leq m-1) \end{cases}$$

Since each client has a total mean rate of λ/m, hence each arriving packet ξ can belong to any client with probability $1/m$. This implies that the conditional probability that ξ arrives at client $(i+z)\%m$ during $AI_i(t)$ is also $1/m$. Thus with $\pi_i^{\xi} = \lim_{t\to\infty} \pi_i^{\xi}(t)$ (defined in Eq. 4.36), $E\{Y_i(\xi)|\pi_i^{\xi}\}$ is computed as follows:

$$E\{Y_i(\xi)|\pi_i^{\xi}\} = \frac{1}{m} \begin{cases} \sum_{z=0}^{m-1}[(z+m)v_c + v_{s,i}] & (i=0) \\ \sum_{z=0}^{m-i-1}[(z+m)v_c + v_{s,i}] + \sum_{z=m-i}^{m-1}[(z+m)v_c + 2v_{s,i}] & (1 \leq i \leq m-1) \end{cases} \tag{4.37}$$

As a result, with some simplifications, we obtain the value of $\overline{Y_i}$ as follows:

$$\overline{Y_i} = \frac{1}{2} \begin{cases} (3m-1)v_c + 2v_{s,i} & (i=0) \\ (3m-1)v_c + 2(1+\frac{i}{m})v_{s,i} & (1 \leq i \leq m-1) \end{cases} \tag{4.38}$$

Finally, by gathering the values of $\overline{R_i}$, ψ_i, and $\overline{Y_i}$ from Eqs. (4.35), (4.36), and

(4.38) respectively, we can obtain the expected queuing delay $E\{W_{c,i}\}$ for each class $c : 1 \leq c \leq n-1$. Using $\overline{W_{c,i}}$ in both domains, we also get $\overline{D_{c,i}}$(Fi) and $\overline{D_{c,i}}$(Wi).

Per-class Average Queue Size

Using Little's theorem [73], the average queue size of CoS c and client i, denoted $E\{Q_{c,i}\}$, is given by:

$$E\{Q_{c,i}\} = \overline{Q_{c,i}} = \lambda_{c,i}\overline{W_{c,i}}. \tag{4.39}$$

Optimal Frame Length

It has long been a challenging problem in wireless networks to determine the frame length that can achieve the best compromise between high loss/retransmission rate due to lengthy frames and larger overhead in case the frame length is set small. The issue is addressed as follows.

Proposition 4.4.1. *Given a number of homogenous wireless users $|\mathbf{N}|$, and CoS traffic parameters $\lambda_{c,i}$ and $\overline{X_{c,i}}$, to achieve the best utilization of uplink sub-frame while ensuring guaranteed QoS, the OFDM frame length T_{wi}^{f} should be set as follows:*

$$T_{wi}^{f} = T_{dl} + T_{ir} + T_{cp} + |\mathbf{N}| \times v_c + \left(\sum_{i=1}^{|\mathbf{N}|-1} \sum_{c=1}^{n-1} \frac{\overline{X_{c,i}}}{(1 - \rho_i + \rho_{c,i})} \right). \tag{4.40}$$

Proof. An optimal frame length means that the idle time is kept the minimal. With the assumption that all users are homogenous and by solving Eq. (4.21) for $I = 0$, T_{wi}^{up} will then be computed as follows:

$$T_{wi}^{up} = T_{ir} + T_{cp} + |\mathbf{N}| \times v_c + \left(\sum_{i=1}^{|\mathbf{N}|-1} \sum_{c=1}^{n-1} \frac{\overline{X_{c,i}}}{(1 - \rho_i + \rho_{c,i})} \right). \tag{4.41}$$

By replacing Eq. (4.41) in $T_f^{wi} = T_{wi}^{up} + T_{dl}$ (see Fig 4.6), we end our proof. □

From the computed value of T_{up}^{f}, we can select the closest OFDM frame length to either 5, 10, or 20 ms; thereby minimizing the idle frame length and maximizing the network utilization while achieving a guaranteed service for each user.

4.4.5 Further Analysis

Case of sending grants *"On-The-Fly"*

If the server schedules a client "on-the-fly" (i.e., directly upon receiving the request message from a client), the propagation time plus grant transmission time overheads will be eliminated. Hence, $v_{s,i} = 0$. As a result, ψ_i, $\overline{Y_i}$, and $\overline{R_i}$ will then be updated as follows, respectively:

$$\psi_i = \frac{1}{m}, \tag{4.42}$$

$$\overline{Y_i} = \frac{1}{2}(3m-1)v_c, \tag{4.43}$$

$$\overline{R_i} = \frac{1}{2}\left[\Big(\sum_{c=1}^{n-1}\lambda_{c,i}\overline{X_{c,i}^2}\Big) + \frac{v_c}{m}\Big(1-\rho_i\Big)\right], \quad i = 0,\ldots,m-1. \tag{4.44}$$

4.5 VPN-based Dynamic Bandwidth Allocation (VPN-DBA)

As a complement to the AC schemes in the course of a per-flow QoS guarantee, we provide a VPN-based dynamic bandwidth allocation (VPN-DBA) scheme that is installed at both the OLT and ONU-BSs, in order to arbitrate the transmission of ONU-BSs over the upstream optical channel, and to arbitrate the transmission of SSs over the uplink wireless channel, respectively. Moreover at the ONU-BS, VPN-DBA takes into consideration different channel conditions of each SS reported through the CSI, where the allocated time share is adaptive to the fluctuating channel condition in order to achieve the desired bandwidth guarantee.

4.5.1 At ONU-BS

To determine the time share for a flow, each ONU-BS j first calculates the aggregated rates of the admitted real-time flows (denoted as Λ_j), and the total reserved VPN BE rates (denoted as $\mathcal{R}_j^{be}$) using the following equation:

$$\mathcal{R}_j^{be} = \sum_k \mathcal{R}_j^{k,be} \times \Gamma_k, \tag{4.45}$$

where,

$$\Gamma_k = \begin{cases} 1 & \text{if } \exists\ SS\ i, \text{ such that } SS\ i \text{ has } V_k \text{ requests} \\ 0 & \text{otherwise} \end{cases} \tag{4.46}$$

To protect real-time (RT) traffic from being shared with BE traffic, we divide each cycle/frame into $K+1$ sub-cycles, where sub-cycle 1 is for RT flows, while the rest K sub-cycles are for all VPNs' BE traffic. The size of each sub-cycle should be determined in each PI so as to adapt to the bandwidth request fluctuation of each flow. Thus, T_{wi}^{rt} (i.e., the sub-cycle of all real-time flows in the wireless domain) and $T_{wi}^{k,be}$ (i.e., the sub-cycle assigned to V_k's BE traffic in the wireless domain) are computed as follows, respectively:

$$T_{wi}^{rt} = \frac{\Lambda_j \times T_{wi}^{up}}{\Lambda_j + \mathcal{R}_j^{be}}, \tag{4.47a}$$

$$T_{wi}^{k,be} = \frac{\mathcal{R}_j^{k,be} \times T_{wi}^{up}}{\Lambda_j + \mathcal{R}_j^{be}}, \tag{4.47b}$$

where T_{wi}^{up} is the wireless uplink sub-frame length, and $\mathcal{R}_j^{k,be}$ is the reserved rate for V_k's BE traffic as defined in Section 4.3.1.

In addition,VPN-DBA differentiates the SSs with admitted RT (and possibly BE) flows from those with only BE admitted flows. For an RT SS i, the time share in the real-time sub-cycle T_i^{rt} is expressed by:

$$T_i^{rt} = \frac{(1/\mathcal{C}_i(x)) \times T_{wi}^{rt}}{(1/(\sum_z \mathcal{C}_z(x)))}, \tag{4.48}$$

where $\sum_z \mathcal{C}_z(x)$ is the sum of transmission rates for all real-time SSs. The inverse of the transmission rate is used because an SS with lower transmission rate requires more time share to transmit an admitted flow rate.

Similarly, the time share allocated to SS i for V_k's BE sub-cycle, $T_i^{k,be}$, is expressed as follows:

$$T_i^{k,be} = \frac{(1/\mathcal{C}_i(x)) \times T_{wi}^{k,be}}{(1/(\sum_z \mathcal{C}_z(x)))}. \tag{4.49}$$

Next and based on the admitted flow rate and reported frame size, our scheme estimates the amount of bandwidth required to satisfy each admitted flow in each frame. Thus, the estimated guaranteed bandwidth $B_{f,i}^g$ for real-time flow f launched by SS i in each polling interval is determined as:

$$B_{f,i}^g = \frac{\lambda_{f,i}^k \times \mathcal{C}_i(x) \times T_i^{rt}}{\Lambda_j \times 8}. \tag{4.50}$$

To explore the bandwidth usage of each frame and avoid any possible resource waste, the number of packets per polling cycle estimated for flow f, denoted as $np_{f,i}$, is first obtained:

$$np_{f,i} = \left\lceil \frac{B_{f,i}^g}{\overline{MS}_f} \right\rceil, \tag{4.51}$$

where $\overline{MS}_f$ is flow f's average MAC service data unit size as defined in Section 3.9. Thus, the allocated bandwidth for flow f in the next cycle/frame, denoted as $B_{f,i}^{alloc}$, is then given by:

$$B_{f,i}^{alloc} = \min\left(np_{f,i} \times \overline{MS}_f, r_{f,i}\right), \tag{4.52}$$

where $r_{f,i}$ is the requested bandwidth for real-time flow f (i.e., the buffering queue occupancy). As mentioned, UGS traffic needs not to be requested. Hence, the ONU-BS may periodically grant it the desired bandwidth.

With OFDM, one physical symbol may carry different bits of MAC layer data according to channel condition that in turn affects the modulation scheme employed. Therefore, each ONU-BS has to convert the allocated bandwidth into number of symbols accordingly. The number of OFDM symbols required for flow f by SS i,

denoted as $F_{f,i}$, is computed as follows [37]:

$$F_{f,i} = \frac{B_{f,i}^{alloc} \times 8}{\mathcal{B}(x)}, \tag{4.53}$$

where $\mathcal{B}(x)$ is given in Table 4.1. For BE traffic, the allocated bandwidth $B_{be,i}^{alloc}$ (in bytes) is determined in the same approach as follows:

$$B_{be,i}^{alloc} = \min\left(\frac{\mathcal{C}_i(x) \times T_i^{k,be}}{8}, r_{be,i}\right), \tag{4.54}$$

where $r_{be,i}$ is the requested bandwidth for BE traffic in every PI.

4.5.2 At OLT

The OLT receives REPORT messages from ONU-BS j specifying the length of its real-time CoS queue c, (i.e., $r_{c,j}$) and a BE VPN counter of V_k (i.e., $r_{be,j}^k$). Moreover, we have the total BE traffic rate computed as follows:

$$\mathcal{R}_{be} = \sum_k \sum_j \mathcal{R}_j^{k,be}, \tag{4.55}$$

where $\sum_j R_j^{k,be}$ is the total reserved BE bandwidth for V_k.

Similar to VPN-DBA at the ONU-BS, the OLT divides each transmission cycle into two sub-cycles (real-time and BE) respectively, and each BE sub-cycle is further subdivided into K sub-cycles. Consequently, the optical/fiber upstream RT and BE sub-cycles T_{fi}^{rt} and a V_k sub-cycle $T_{fi}^{k,be}$ are computed as follows, respectively:

$$T_{fi}^{rt} = \frac{\beta T_{eff}^{pon} \sum_j \Lambda_j}{\sum_j \Lambda_j + \mathcal{R}_{be}}, \tag{4.56a}$$

$$T_{fi}^{k,be} = \frac{\beta T_{eff}^{pon} \sum_j \mathcal{R}_j^{k,be}}{\sum_j \Lambda_j + \mathcal{R}_{be}}. \tag{4.56b}$$

In the optical plane all ONU-BSs transmit at the same speed, thus with a real-

time sub-cycle T_{fi}^{rt}, the time share for each ONU-BS j in the real-time sub-cycle T_j^{rt} is fairly assigned as follows:

$$T_j^{rt} = \frac{T_{fi}^{rt} \times \mathcal{C}_{pon}}{|\mathbf{M}| \times 8}. \tag{4.57}$$

Finally, the OLT calculates the allocated bandwidth for CoS c of ONU-BS j, $B_{c,j}^{alloc}$ in the same manner as the computation done by the ONU-BS. The same logic also applies for the BE computation.

Note that for a non-VPN flow, the computations are done with $(1-\beta)T_{eff}^{pon}$ instead of βT_{eff}^{pon}.

Remark 4.5.1. *While VPN-DBA ensures that the committed guaranteed rate for each admitted flow is allocated, its "reservation" process might cause more flows to be dropped (as we will see in the results), and hence the network may exhibit lower throughput than the maximum possible one. Therefore an advanced DBA may be designed jointly with either VPN-AC or DAC to achieve higher network throughput.*

4.6 Performance Evaluation

To evaluate the effectiveness of the proposed AC and DBA algorithms, we have developed a simulator using OMNET++ [75]. The simulation parameters are shown in Table 4.2. Here, the case of $\beta = 1$ implies that "non-VPN" traffic is NOT considered, and therefore the available bandwidth is divided among $K = 4$ VPNs. Without loss of generality, we assume that all the VPNs, ONU-BSs, and SSs have equal weights, respectively. Namely, $w_k = 1/K \ \forall k$, $w_{i,j}^k = 1/N_j^k$, and $w_j^k = 1/M_k$ $\forall i, j, k$. As a result, each VPN is reserved a total of 249.5 *Mbps*, out of which, 24.95 *Mbps* are reserved for BE traffic (since $\alpha^k = 0.1, \forall k$).

To test the resilience of our proposed algorithms in handling fluctuating channel conditions, the following two simulation scenarios are investigated.

Table 4.2: Simulation parameters

General	T_{dba}	$neglected$
	Processing time (T_{gr}^{proc} and T_{br}^{proc})	10^{-3} μs
EPON	Number of ONU-BSs ($\|\mathbf{M}\|$)	16
	Channel Speed ($\mathcal{C}_{pon}$)	1 $Gbps$
	Distance from OLT to ONU-BS (d_j)	25 km
	T_{fi}^{up}	2 ms
	T_g^a	1 μs
	ONU-BS Queue Size	10 $Mbytes$
WiMAX	Channel Bandwidth	20 MHz
	O_d	1440
	T_{sym}	0.1 ms
	T_{ir}	0.1 ms
	T_{wi}^f	$5, 10, 20$ ms
	T_{dl}	1 ms
	T_g^a	12.5 %
	Distance from SS to ONU-BS (d_i)	5 km
	SS Queue Size	10 $Mbytes$
	$\forall i, P_{error,i}$	10^{-6}
VPN	Number of VPNs (K)	4
	β	1
	$\forall k, \alpha^k$	0.1
	$\forall k, \mathbb{D}_{c=1}^k$ (UGS)	100 ms
	$\forall k, \mathbb{D}_{c=2}^k$ (rtPS)	150 ms
	$\forall k, \mathbb{D}_{c=3}^k$ (nrtPS)	250 ms
	SS V_k	$random(1, 4)$

- *Scenario A*: The highest transmission rate is employed for every SS i of each ONU-BS (i.e., $\mathcal{C}_i(x) = \mathcal{C}_i(7), \forall i \in \mathbf{N}$).

- *Scenario B*: Here, various channel conditions are considered for different SSs. The transmission mode of each SS is randomly generated ($x = random(1, 7)$).

We realize that scenario A (which is applied in most of the related work in the literature [37, 34, 36, 32]) is not realistic in presence of the powerful AMC function provided by the IEEE 802.16 standard. Nonetheless, the result of scenario A is explored and positioned to serve as a benchmark for scenario B, and is expected to provide some insights in case other types of wireless air interfaces are employed, such as IEEE 802.11.

Each incoming VPN user/SS has four flows (UGS, rtPS, nrtPS, and BE). Every UGS flow is generated with a mean/guaranteed rate of 64 $Kbps$ and a packet size equal to 70 *bytes* [64]. We generate rtPS traffic at a guaranteed rate of 5 $Mbps$ (which is the average bit rate of a DVD-quality video) and a packet size of 800 *bytes* [59]. Similarly, nrtPS traffic is generated at a guaranteed rate of 500 $Kbps$ and a packet size of 600 *bytes* [64]. BE traffic is highly bursty, and we use self-similar traffic (Pareto distribution with a Hurst parameter $H = 0.8$) for modeling it [27]. Each BE flow is generated at a mean rate of 2 $Mbps$ with packet sizes uniformly distributed between 64 and 1518 *bytes* [27, 38].

The number of VPN users used in the figures increments by $|\mathbf{M}|$ with time and reflects the arrival (or request for joining) of a new SS in time (with its CoS flows) to each ONU-BS simultaneously. Hence, every time a new SS wants to join the network, it will be subject to the AC scheme and consequently included in the VPN-DBA computation.

A confidence interval of 90 % is considered for a averaging the exhibited results.

4.6.1 VPN-AC Performance Evaluation

We first start by running scenario A to extract the nominal bandwidth ratio (NBR) that is needed to apply the VPN-AC rules (Eq. 4.9). NBR is computed as follows:

$$NBR = \frac{Total\ Throughput}{Transmission\ Rate} = \frac{59.0976\ Mbps}{64.8\ Mbps} = 0.912 \tag{4.58}$$

For a more conservative AC, we set $NBR = 0.9$.

To study the performance of real-time traffic under VPN-AC, we measure the instantaneous average packet delays of a selected SS's real-time flows. Figs. 4.8, 4.9, and 4.10 show these measurements with VPN-AC (plus VPN-DBA) and without AC (i.e., NO-AC) under both scenarios. Note that with VPN-DBA, there is no intra-ONU/intra-SS scheduling required since the OLT/ONU-BS allocates bandwidth per-CoS, for every ONU-BS/SS. On the other hand with NO-AC, we employ the SP scheduler which, as described in Section 2.2.3, satisfies higher priority queues first [37].

Clearly using the SP scheduler, UGS traffic shows the optimal performance where its average packet delay remains under $2 - 10\ ms$ even when the number of SSs continuously increases, regardless of the OFDM frame length. This is a direct result of the SP policy which always selects packets from a queue with a higher priority. As for VPN-DBA, it makes sure to satisfy the QoS requirements in terms of delay and throughput by reserving every real-time traffic with appropriate bandwidth in every cycle. Since a UGS flow is admitted only if its guaranteed bandwidth is assured in every cycle, we can see that VPN-DBA maintains a UGS average packet delay of $5 - 20\ ms$ under scenario A. However, the delay variation is affected by the OFDM frame length, especially in scenario B, where the delay might reach $\approx 90\ ms$ with a $20\ ms$ frame size. This is due to the fact that in this scenario, the bandwidth is allocated to each SS with respect to its transmission rate, and hence the cycle might saturate because some SSs have requested for more OFDM symbols than others to support the admitted flow rate. Nonetheless, VPN-

DBA still maintains a UGS packet latency less than the maximum required one (i.e., $\leq 100\ ms$).

As for rtPS and nrtPS traffics, Figs. 4.9 and 4.10 demonstrate that VPN-AC maintains their delay performance to meet the specified target QoS requirements of the stream (i.e., $\leq 150\ ms$) while the delay witnesses an exponential increase with NO-AC, especially after system saturation. This behavior highlights the need for the application of AC in WiMAX-V**P**ON, because when the system reaches saturation and all the arriving streams are admitted, the performance is no longer maintained. More specifically, no bandwidth is guaranteed for each type of traffic, and the QoS requirements can no longer be met not only for new flows but also for the existing ones. On the other hand, the deployment of AC allows for a bandwidth guaranteed service with protected and guaranteed QoS that will meet the VPN SLA and maintain it.

We further evaluate the proposed VPN-AC framework by measuring the throughput of one flow from each CoS of a tagged SS. It is demonstrated in Fig. 4.11 that the selected UGS flow exhibits similar performance behavior to that with NO-AC, whereas the selected rtPS and nrtPS flows show different behaviors. Here, rtPS and nrtPS flows (see Figs. 4.12 and 4.13) with VPN-AC maintain their guaranteed 5 $Mbps$ and 500 $Kbps$ throughputs respectively throughout the simulation, even after the system saturation. On the other hand when NO-AC is applied, these flows do not show a stable throughput behavior and when the system reaches saturation, the throughput starts degrading. This is due to the fact that when more real-time flows are admitted and no AC is applied, the bandwidth that was guaranteed for the already admitted flows (before saturation) is now shared among more flows. Hence, the bandwidth is no longer guaranteed for the already admitted flows as well as for the newly admitted ones. This again proves the effectiveness of our AC framework in stabilizing and guaranteeing the throughput for all admitted flows by rejecting the flows that will break this theme. In real and practical settings, this will deny malicious users from monopolizing the bandwidth provided, and at

the same time, it will protect the bandwidth assigned for other well-behaved users, and will maintain the QoS requirements for each VPN service as specified in the SLA. Furthermore, our framework proves that no matter what channel condition each user possesses, it can still provide its flows with the guaranteed bandwidth (given that the transmission rate does not go below the total admitted data rate), which are well demonstrated by the results under scenario B. This is achieved by allocating more OFDM frames to transmit the same flow rate, as described earlier.

We now study the performance of BE traffic in both scenarios under different OFDM frame lengths. Since BE has no QoS requirement in terms of delay [64], we show the total BE throughput in Fig. 4.14, which is highly affected by the OFDM frame length. For example, with 5 ms frame length under scenario A, V_3 yields a total throughput of 10 $Mbps$ knowing that its reserved one is 24.95 $Mbps$. The total throughput increases to reach $\approx$ 25.5 $Mbps$ when the frame length is increased to 20 ms. This is due to the fact that with a smaller frame size, the VPN BE sub-cycle's portion of one SS might be smaller than the head-of-line (HOL) packet in its BE queue. As a result, not only those packets cannot be transmitted, but they could be successively blocked from being transmitted, and therefore the throughput is suppressed. On the other hand with a larger frame length, each VPN BE sub-cycle will be large enough to accommodate most packet sizes for all SSs, and hence the throughput can reach as high as $\approx$ 24.95 $Mbps$ (i.e., the reserved one). Nonetheless, using an OFDM frame length of 10 ms also meets the expected throughput under both scenarios and produces a throughput equivalent to the reserved one. This shows that WiMAX-V**P**ON can achieve the desired/expected performance for all types of traffic, if the network parameters are set properly.

As mentioned before, our proposed VPN-DBA divides each transmission cycle into multiple sub-cycles in order to protect real-time traffic from being shared with BE traffic. To highlight this advantage, we plot in Fig. 4.15 the overall average E2E packet delay for all CoS, with multiple BE traffic VPN portions (i.e., with multiple α values). As noticed, real-time traffic (i.e., UGS, rtPS and nrtPS) maintains

an overall average delay $\leq 10\ ms$ regardless of the assigned BE portion for each VPN. On the other hand, BE traffic witnesses a delay decrease as its reserved portion increases, which is under our expectations. This shows how VPN-DBA can efficiently preserve the QoS requirements for real-time flows while satisfying BE traffic with the "agreed-upon in the SLA" throughput.

Finally, Table 4.3 summarizes the statistics collected from our simulations about a particular VPN (here, V_4). These results show that 100% and 52% of the generated V_4 UGS traffic is admitted, while its overall QoS and bandwidth requirements are guaranteed, under scenarios A and B respectively. Approximately 64% and 24% of its rtPS flows are also admitted under both scenarios; and approximately 82% and 38% of its nrtPS flows are admitted as well; whereas all BE flows are admitted. The difference of admission rates between scenarios A and B is caused by VPN-AC (i.e., Eq. 4.9), where the overall wireless system capacity is proportional to each SS's transmission rate. Thus, the admission rule becomes more conservative if more SSs have lower transmission rates. The table also shows that the monitored/measured throughput for each CoS traffic meets the expected/calculated one. This again demonstrates the effectiveness of our proposed framework in providing the expected performance under various channel conditions. Note that with no AC, all flows are admitted; however, their QoS requirements are not guaranteed (except for UGS traffic). Note also that these collected results are traffic model-dependent. In other words, more flows can be admitted or rejected, depending on all of the required guaranteed throughput for real-time and BE traffic, the generated flows mean rates, and the number of flows/SSs generated.

With EGS Support

We have extended WiMAX-V**P**ON to support EGS services and requests. More specifically in the extended version of WiMAX-V**P**ON, VPN-AC admits all EGS and BE flows while the other types of flows are treated in the same way as described earlier. For VPN-DBA, if the uplink channel is overloaded and an emergency event

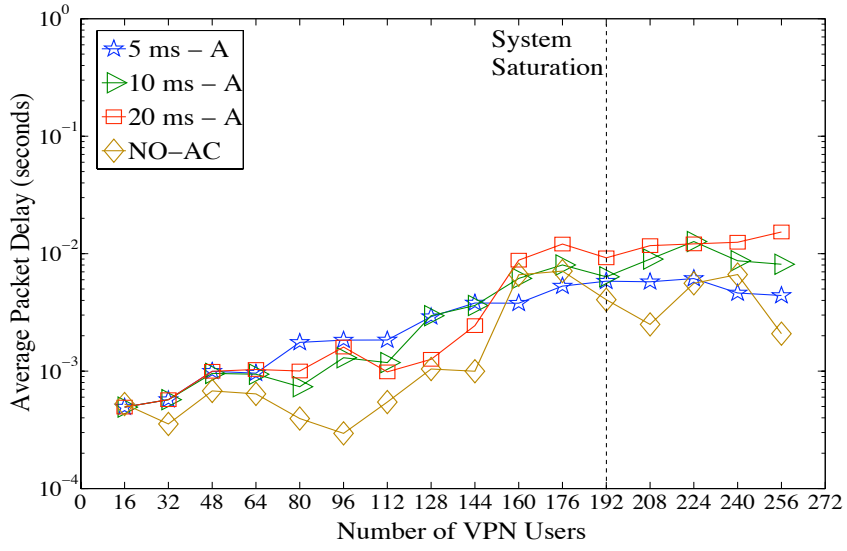

(a) Scenario A

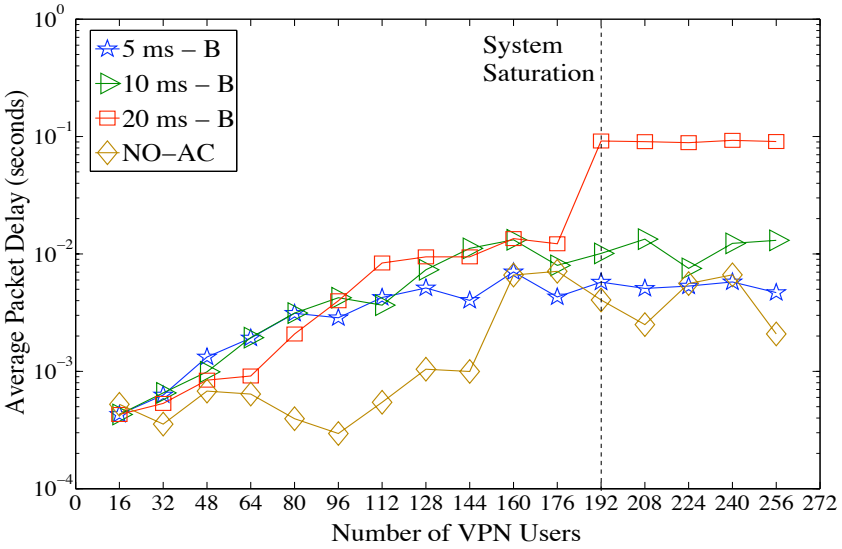

(b) Scenario B

Figure 4.8: UGS flow average E2E packet delay under VPN-AC and with NO-AC, with $T^f_{wi} = 5, 10$, and 20 ms, under scenarios A and B.

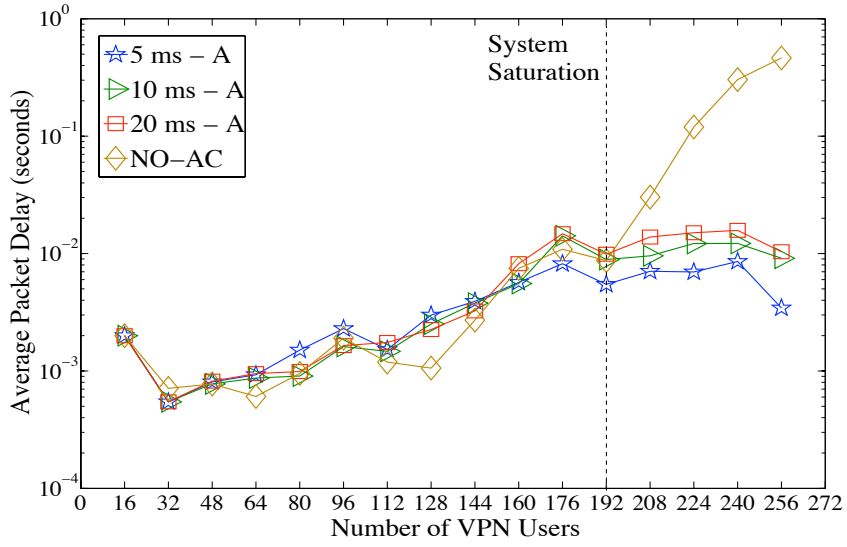

(a) Scenario A

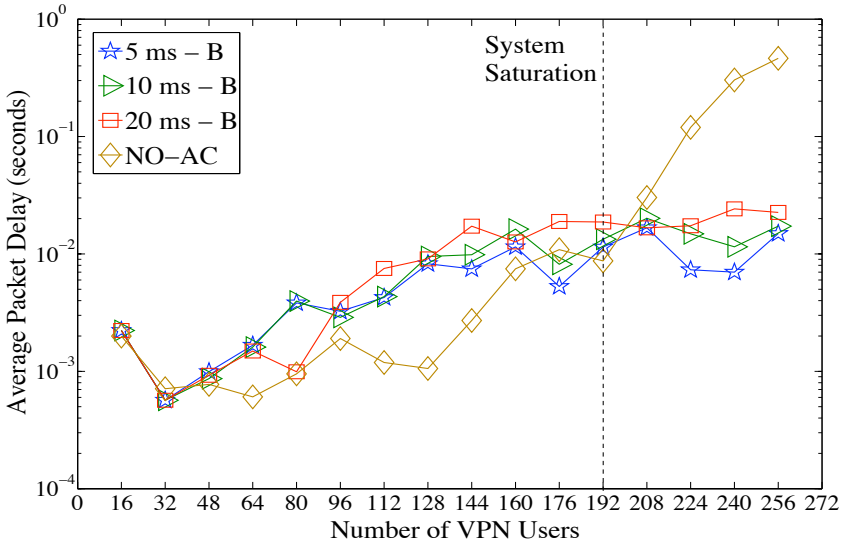

(b) Scenario B

Figure 4.9: rtPS flow average E2E packet delay under VPN-AC and with NO-AC, with $T^f_{wi} = 5, 10$, and 20 ms, under scenarios A and B.

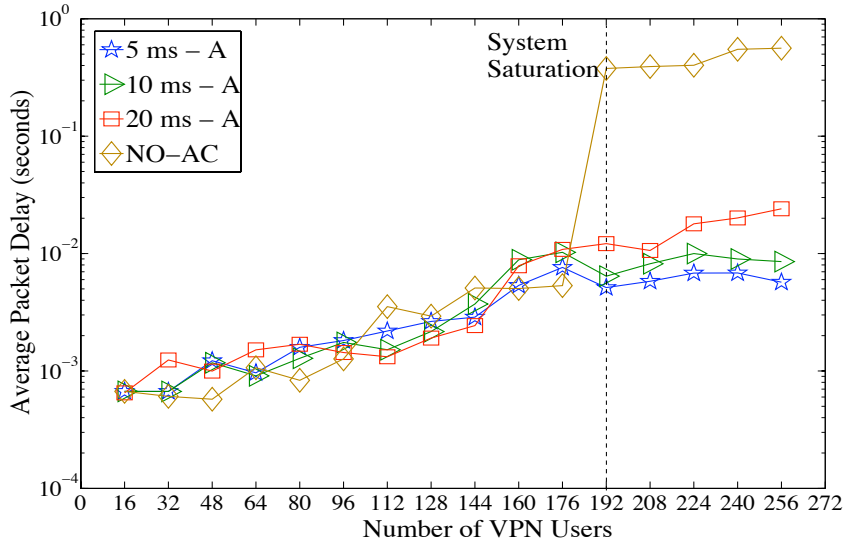

(a) Scenario A

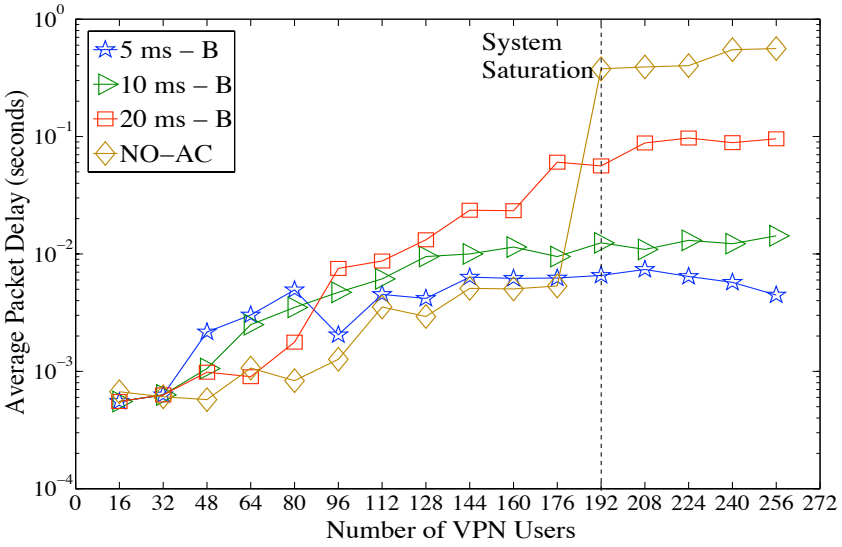

(b) Scenario B

Figure 4.10: nrtPS flow average E2E packet delay under VPN-AC and with NO-AC, with $T^f_{wi} = 5, 10$, and 20 ms, under scenarios A and B.

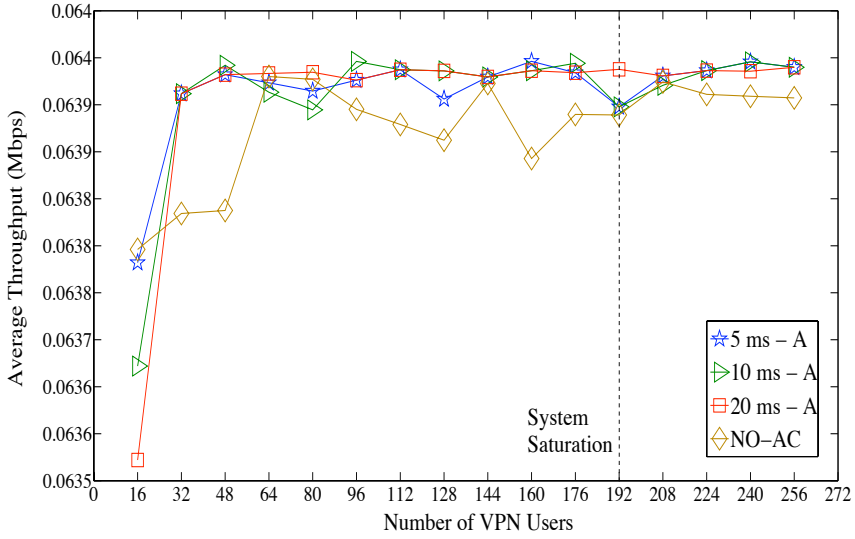

(a) Scenario A

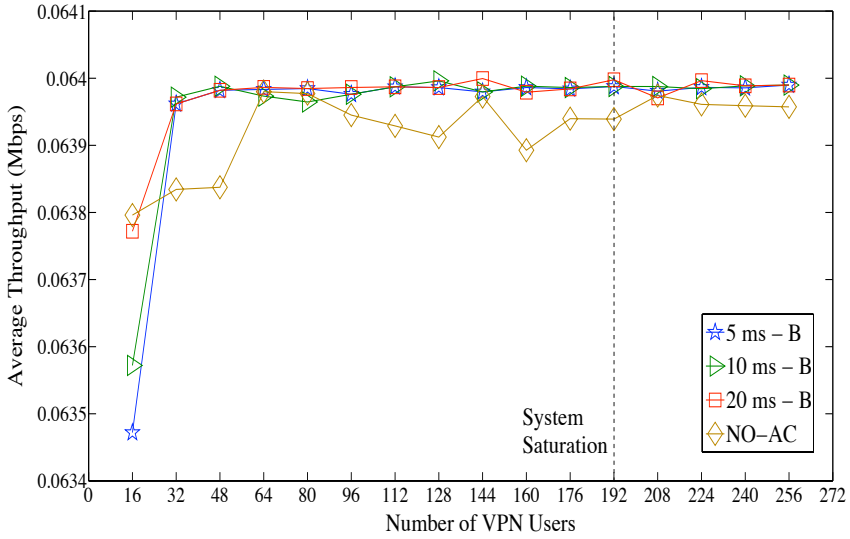

(b) Scenario B

Figure 4.11: UGS Flow E2E throughput under VPN-AC and with NO-AC, with $T_{wi}^{f} = 5, 10$, and 20 ms, under scenarios A and B.

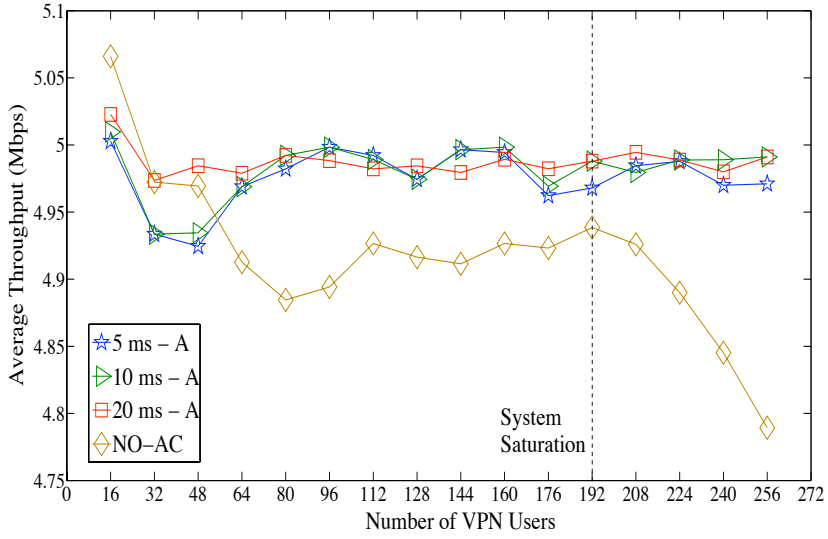

(a) Scenario A

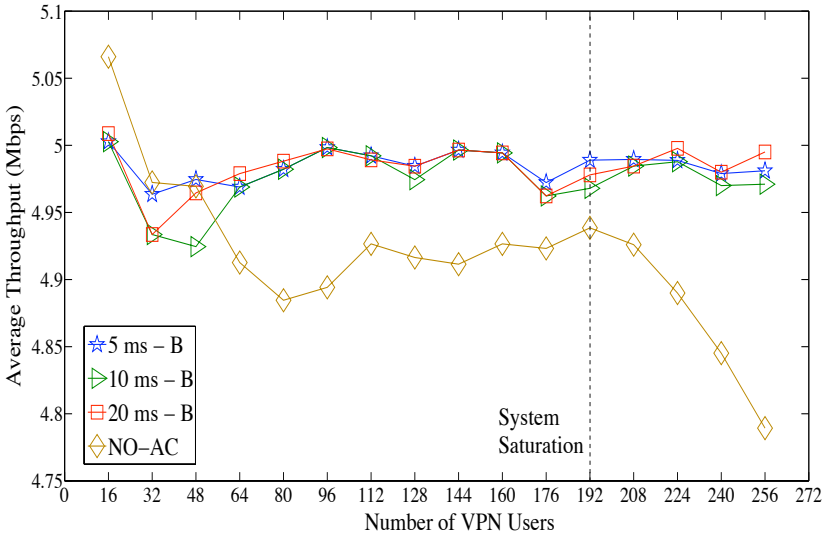

(b) Scenario B

Figure 4.12: rtPS flow E2E throughput under VPN-AC and with NO-AC, with $T_{wi}^{f} = 5, 10$, and 20 ms, under scenarios A and B.

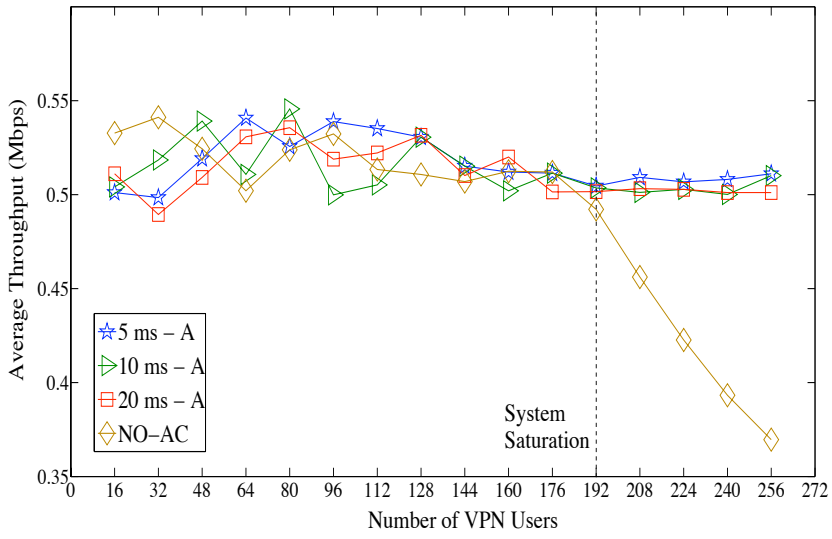

(a) Scenario A

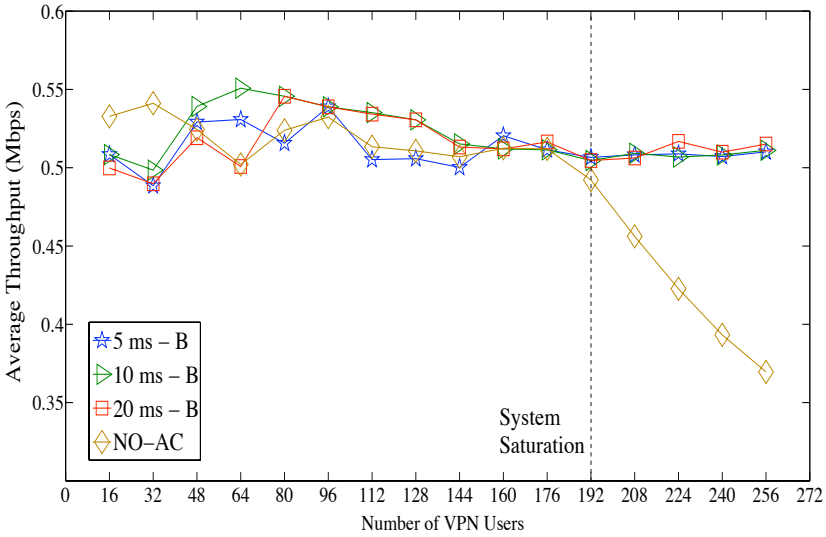

(b) Scenario B

Figure 4.13: nrtPS flow E2E throughput under VPN-AC and with NO-AC, with $T^f_{wi} = 5, 10$, and 20 ms, under scenarios A and B.

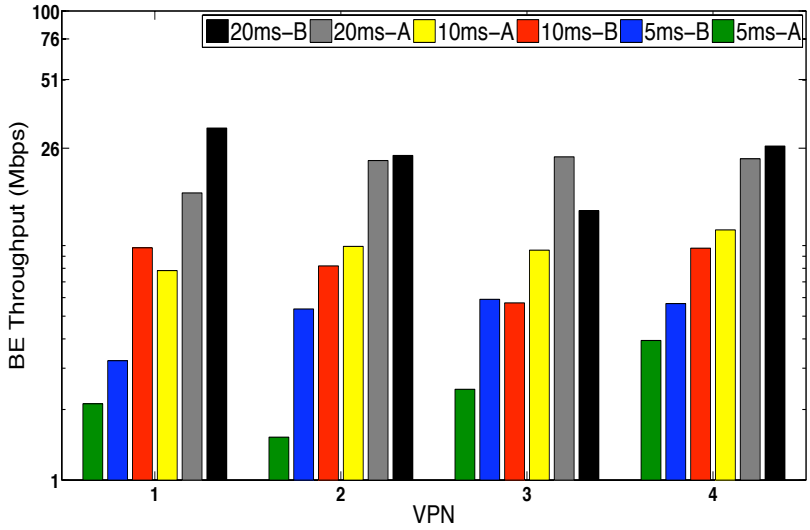

Figure 4.14: Per-VPN BE E2E throughput, with $T_{wi}^{f} = 5, 10$, and 20 ms, under scenarios A and B.

Table 4.3: V_4 traffic statistics

VPN	4					
CoS	**UGS**		**rtPS**		**nrtPS**	
Scenario	**A**	**B**	**A**	**B**	**A**	**B**
Number of Generated Flows	59	50	59	50	59	50
Number of Admitted Flows	59	26	38	12	48	19
Number of Rejected Flows	0	24	21	38	11	31
Admission Rate (%)	100%	52%	$\approx$ 64%	24%	$\approx$ 82%	38%
Expected Throughput (Mbps)	3.776	1.664	190	60	24	9.5
Monitored Throughput (Mbps)	3.76376	1.66151	189.815	58.6636	23.7408	9.51106

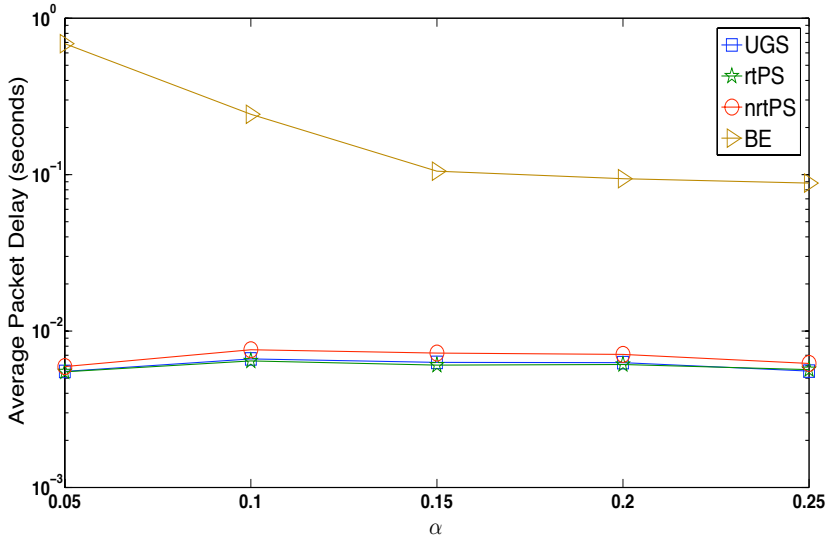

Figure 4.15: Average E2E packet delay versus α

occurs, a call preemption mechanism is designed to "borrow enough" bandwidth from the BE quota to serve the incoming EGS flow(s). The borrowed bandwidth is then reallocated back to BE traffic once all emergency flows are served and satisfied.

To stress test our framework, we assume that each SS has five flows (i.e., EGS, UGS, rtPS, nrtPS, and BE). We inject each EGS flow at a rate of 5 $Kbps$ and the rest of traffic types are generated as before. The extended framework is evaluated versus the MC QoS requirements listed in Table 3.1. We also consider the simulation scenarios A and B.

Fig. (4.16) and Fig. (4.17) show the end-to-end average packet delay for EGS and real-times flows of a tagged SS, and the total per-VPN BE traffic throughput, respectively. As noticed, although able to meet the QoS requirements for some services (e.g., UGS and nrtPS), typical resource management schemes (with no AC) are unable to maintain the QoS requirements for all MC VPN services, especially after system saturation.

On the other hand, the application of WiMAX-V**P**ON (with AC) is able to maintain the QoS requirements for all types of services (in terms of delay and

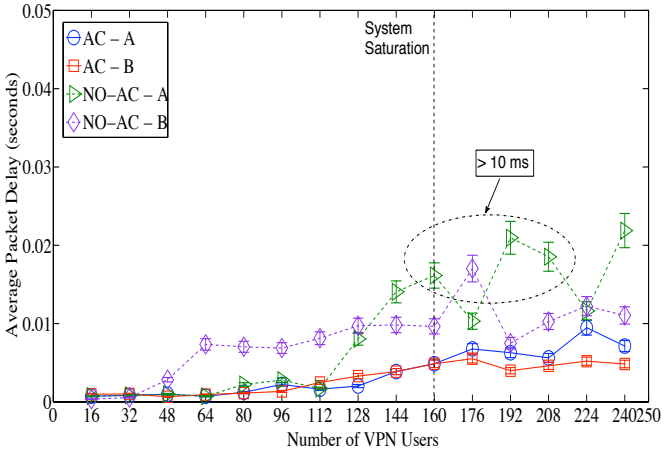

(a) EGS Flow

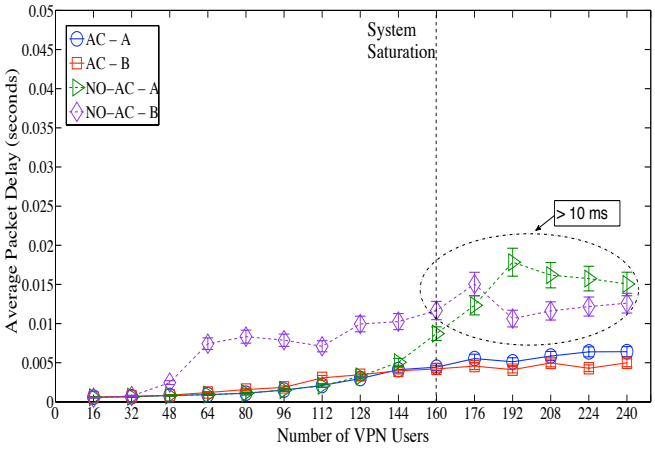

(b) UGS Flow

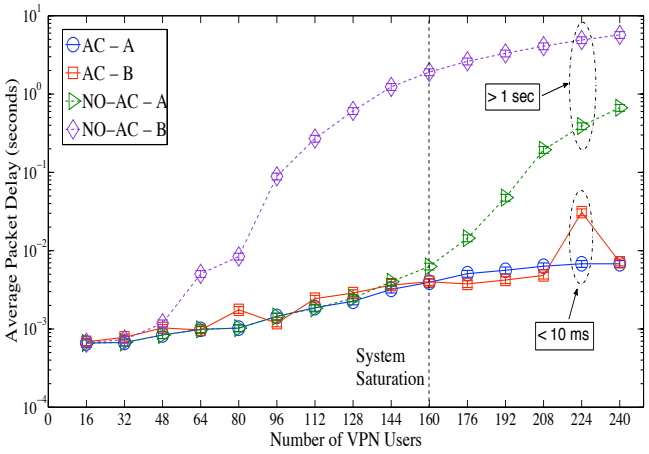

(c) rtPS Flow

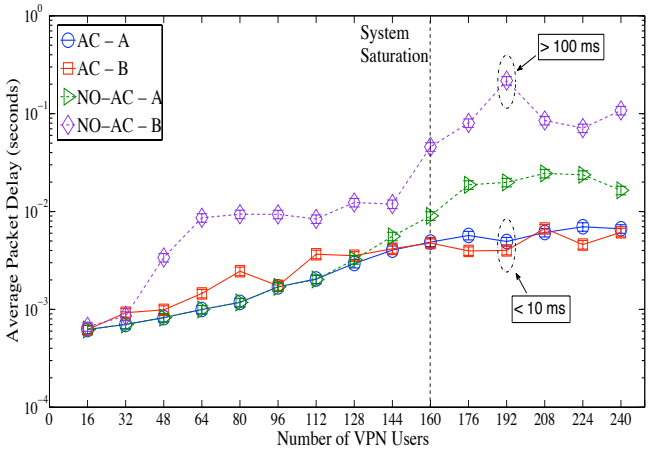

(d) nrtPS Flow

Figure 4.16: One-way E2E (from SS to OLT) average packet delay with and without our AC framework (90 % Confidence Interval), under scenarios A and B.

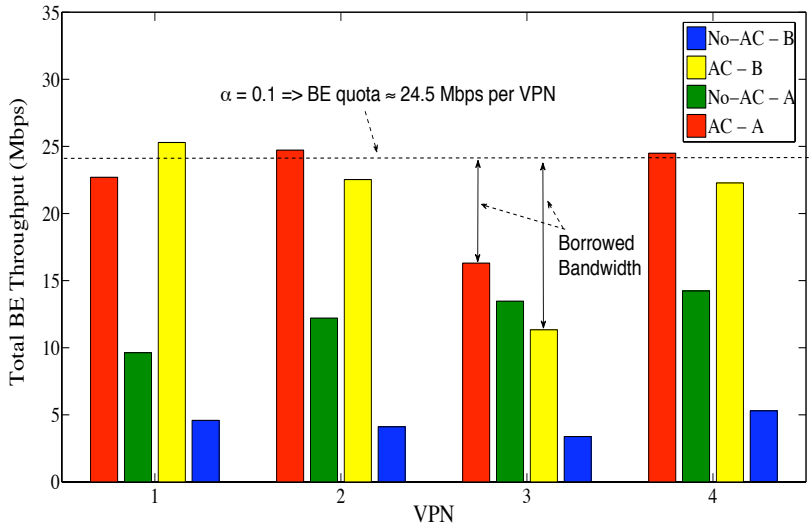

Figure 4.17: Total per-VPN BE throughput, under scenarios A and B.

throughput). This proves the effectiveness of our framework in maintaining network stability, as well as ensuring and protecting the QoS level for all types of traffic. Fig. (4.17) also shows how the "bandwidth borrowing" mechanism may affect the overall BE throughput. However in our simulations, flows never leave the network; therefore by giving up some of its bandwidth quota, the total V_3 BE traffic witnesses a permanent throughput degradation.

4.6.2 DAC Performance Evaluation

In this section, we validate the effectiveness of the proposed analytical model versus the simulated proposed framework. We also show how DAC increases the network utilization.

We first plot in Fig. 4.18 the relation between the utilization factor in the optical domain (i.e., at the OLT) and the utilization factor in the wireless domain (i.e., at one ONU-BS). Since all SSs and ONU-BSs are assumed to be equally loaded, the load on one ONU-BS can be generalized to all ONU-BSs and hence can give the load in the optical domain. As a result, as an alternative to a 3D graph, this relation will simplify the representation of the subsequent figures to make them

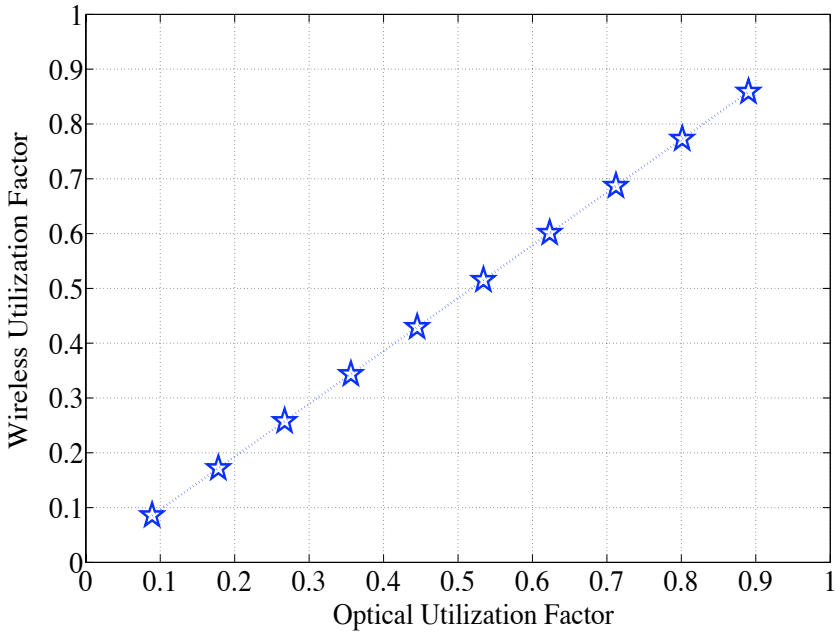

Figure 4.18: Relationship between wireless and optical utilization factors

easily readable. In those figures, the results are drawn versus the optical utilization factor. The 90% confidence interval of the simulation results are shown in the figures. The first 10% of the simulation time are considered as the transient period, and are thus discarded.

Fig. 4.19 depicts the E2E average packet delay, obtained by theoretical and simulation experiments, for 3 CoSs of tagged clients $i = 0$ and $i = m - 1$. Note that in our simulations and unlike the assumption made in the analytical model, BE traffic load builds up gradually with time. This fact results in a very slight increase of the E2E packet delay in the analytical part versus the simulation one, at moderately lower network loads ($0.1 \rightarrow 0.4$). Nonetheless, both results in general match with a fine degree at all loads and a very small difference of 2 ms (especially at high loads), even when the BE reserved portion is fully utilized. Moreover, although our simulation model has been implemented without the assumptions made in the analytical model (e.g., guaranteed rate is Poisson-distributed), the results show that these assumptions are statistically requisite.

Fig. 4.20 shows the average queue size of each CoS in the optical domain, where

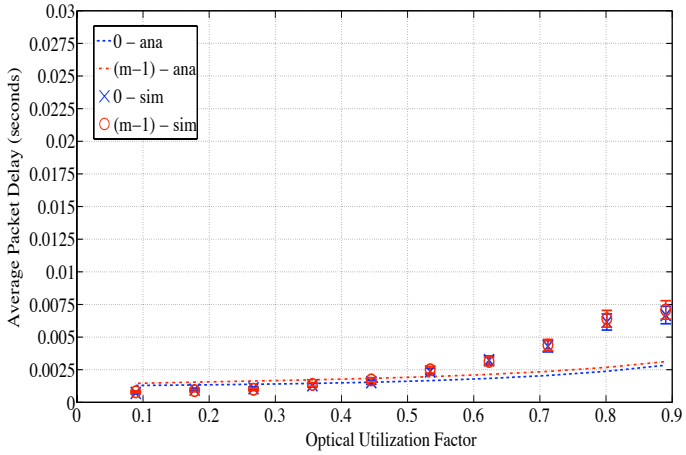

(a) $c = 1$: UGS

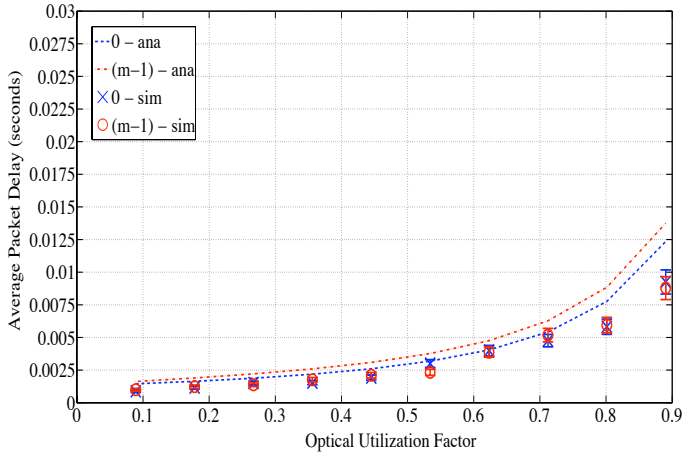

(b) $c = 2$: rtPS

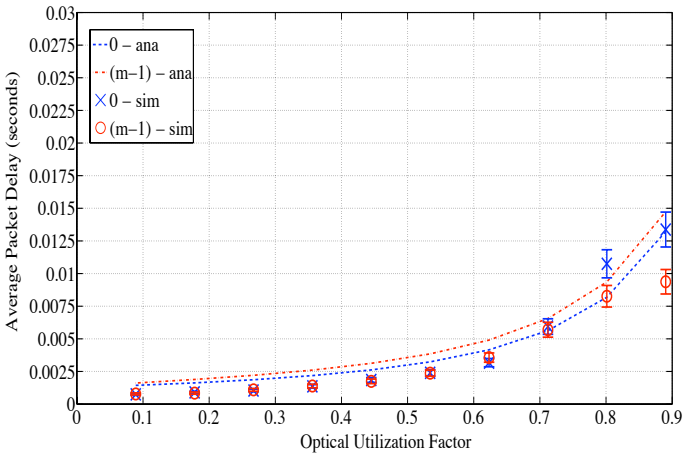

(c) $c = 3$: nrtPS

Figure 4.19: Average E2E packet delay: $\overline{D_c}$(E2E), for clients 0 and $m - 1$.

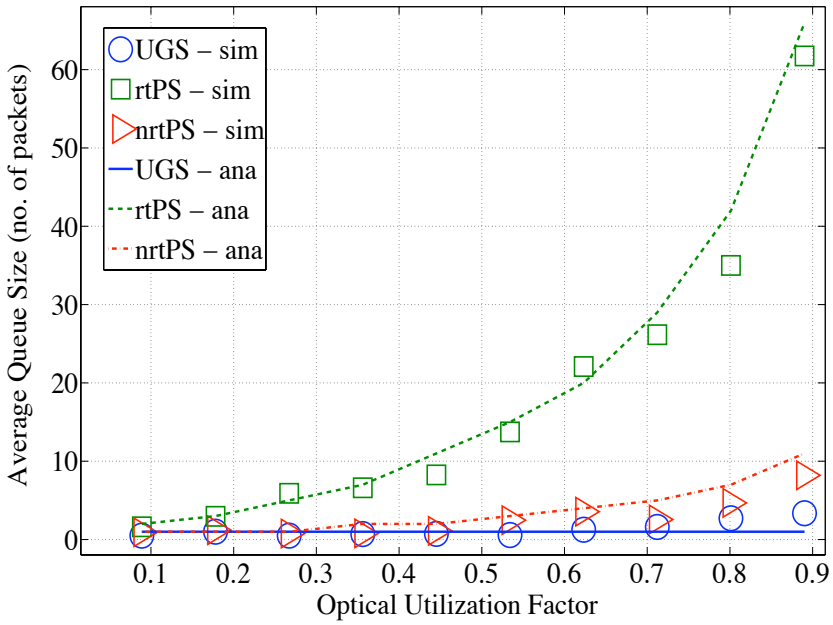

Figure 4.20: Average queue size in the (Fi) domain

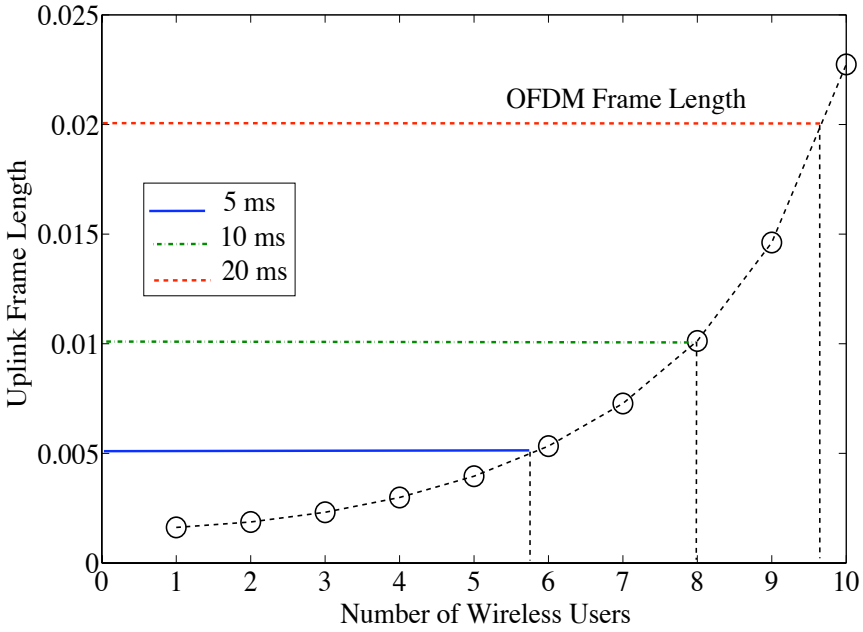

Figure 4.21: Optimal wireless frame length

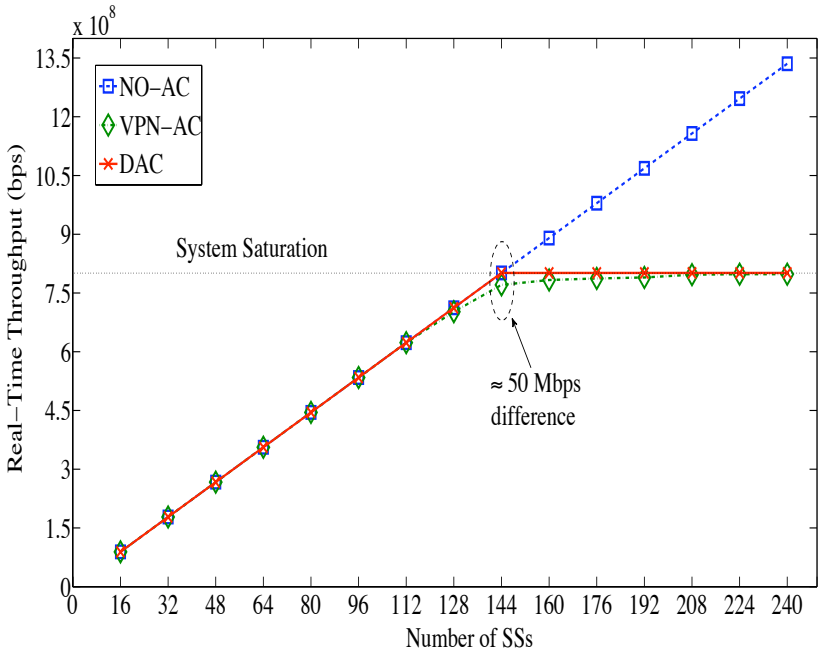

Figure 4.22: Admitted real-time traffic throughput

each optical client (at the same time a wireless server) acts as a multiplexer of all traffic arriving from the wireless clients connected to it. As shown, both the analytical and simulation results show a fine match of almost 95% for all classes; which again shows the effectiveness of our analysis. Note that we do not plot the wireless client's average queue size because a similar behavior was observed. We also do not plot the throughput behavior as it is the same as the one observed under VPN-AC.

To study the selection of the OFDM frame length under the proposed framework, we show in Fig. 4.21 the frame length versus the number of wireless users. As noticed, for an OFDM frame length of 5 ms, the maximum number of users that can be accommodated while achieving a *guaranteed rate* service, is almost 6. Similarly, 8 users can be best accommodated for a 10 ms OFDM frame length; and almost 10 users for a 20 ms frame length. With these values, we could configure our network such that the resource wastage is minimized while guaranteeing the bandwidth for each admitted flow/user.

Finally, to show the advantage of our proposed DAC scheme over other AC

mechanisms that also achieve guaranteed bandwidth, we plot in Fig. 4.22 the admitted real-time traffic throughput under DAC and VPN-AC, and with the application of no admission control (i.e., NO-AC). As elaborated in the figure, enabling inter-VPN statistical multiplexing allows DAC to admit more real-time flows in the network, which in turn increases the resource utilization and throughput. We note here that since our analysis assumes a steady-state network, all incoming flows are rejected once the network saturation is reached (same as with VPN-AC).

4.7 Summary

This chapter presents a new framework for establishing layer-2 VPNs over the EPON-WiMAX integration. The new framework, namely WiMAX-V**P**ON, provides per-VPN service QoS protection and assurance via new DBA and AC schemes, which are critical issues in the course of fixed-mobile convergence.

WiMAX-V**P**ON implements two new three-stage AC mechanisms, and a DBA scheme to achieve end-to-end bandwidth guarantee. The AC and DBA schemes are designed for the scenario where the users of a VPN may connect to any ONU-BS, but are not allowed to utilize more bandwidth than their predefined bandwidth share in the upstream channel. Such a feature is critical to build-up layer-2 VPNs over EPON-WiMAX integration. The first AC scheme, so-called VPN-AC, is a measurement-based mechanism which admits a flow if enough bandwidth is available to accommodate its guaranteed rate. Although it is shown that VPN-AC is robust and effective, it may offer low network utilization in case the wireless users possess heterogeneous channel conditions. The second AC scheme, namely DAC, is able to increase the network utilization and enable inter-VPN statistical multiplexing by admitting the incoming flows based on their maximum delay requirements. Extensive simulations demonstrate that the lack of efficient AC and DBA mechanisms could not preserve the QoS requirements of various types of flows. On the other hand, WiMAX-V**P**ON shows much improved performance in terms of

maintaining the QoS requirements of the existing flows while providing an overall per-VPN acceptable minimal throughput for BE traffic even when the network load approaches to saturation. We conclude that the proposed framework is a promising candidate for the operation of future FiWi backhaul-access networks.

Chapter 5

Energy Efficiency in Next-Generation Passive Optical Networks

In this chapter we propose a new green bandwidth allocation (GBA) framework that leverages the sleep mode feature of the ONU to possibly achieve maximum energy saving in NG-PONs. The salient feature of GBA is that the QoS requirements of all types of services are taken as a constraint when the sleep time is computed for every ONU. Further, due to its novel design in terms of batch-mode transmissions, more energy can be saved with the same amount of sleep time. Our results show that GBA can minimize the ONU energy consumption by almost 90% without impairing the QoS demands of all types of traffic. We also show that the saving is not much affected by the increased traffic loads as generally expected.

5.1 Green Bandwidth Allocation

The proposed GBA framework is featured with the following techniques:

1. Hybrid cyclic/deep sleep enabled at ONUs.

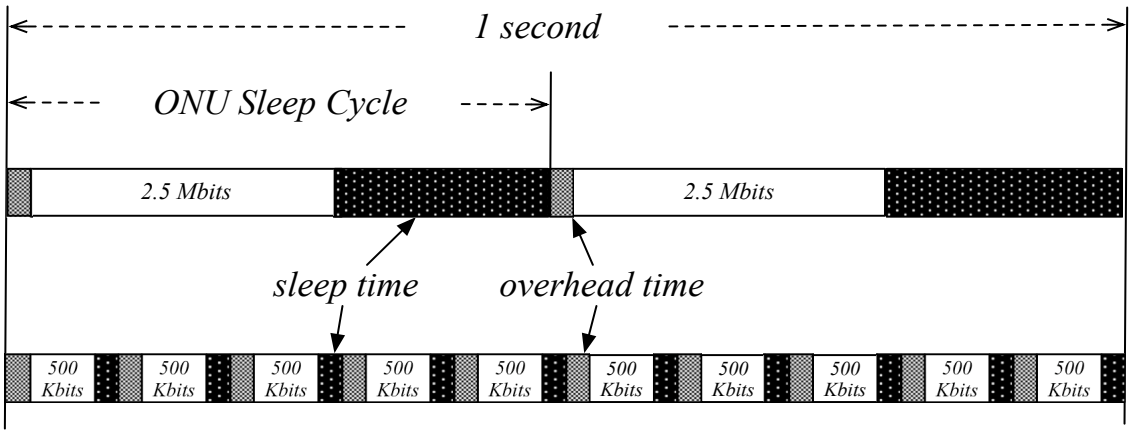

Figure 5.1: Transferring 5 $Mbps$ traffic using batch-mode (upper diagram) and legacy-mode (lower diagram) transmissions.

2. Batch-mode transmission at OLT and ONUs.

3. UCS-based bandwidth allocation.

Thus, the ONU goes into the sleep mode for a certain amount of time before waking up to send/receive a batch of buffered upstream/downstream traffic. The main purpose of this strategy is to extend the ONU sleep time as much as possible so as to reduce the total overhead time that accumulates due the frequent switching of the ONU between the active and sleep modes. Fig. 5.1 illustrates the difference between the batch-mode transmission of the proposed GBA (upper diagram) and the legacy transmission strategy (lower diagram). Although the total active time is the same for data transmission (i.e., 5 $Mbits$), the proposed GBA can yield a much longer ONU sleep period in total due to much shorter overhead time, thereby saving more power. Specifically, using the legacy transmission scheme results in a total overhead of $10 \times 5.125 = 51.25\ ms$ under the GR-ONU-1/C architecture. On the other hand with the proposed batch-mode transmission, the total overhead is reduced to $2 \times 5.125 = 10.25\ ms$. The remaining challenge would be to determine the ONU sleep time, which should be long enough to possibly save maximum energy, yet short enough to maintain the QoS requirements of all types of traffic, especially for delay-sensitive applications. The expression of the sleep time is dependent on the employed DBA scheme as well as the sleep signaling protocol between the OLT

and ONUs. We suggest using a UCS-based DBA scheme because as discussed in Chapter 2, it can ensure maximum saved energy at the ONUs. With these techniques, the proposed framework implements a hybrid deep/cyclic sleep mode at the ONUs.

The rest of the section describes the GBA functions in the OLT and ONUs, respectively. Discussions will be provided on how the maximum sleep time is determined and how the proposed framework can comply with the currently available NG-PON standards, as well as how it can operate over WDM-based PONs.

5.1.1 GBA at OLT

With GBA, the ONU sleeping is initiated by the OLT, where the general procedure's steps are provided as follows:

S1: Wait until all the request messages[1] from all ONUs are received on every shared channel. These can either be multiple requests per channel in the case of TDM-based PONs (e.g., EPON/GPON), or a single request per channel in the case of WDM-based PONs (e.g., WDM-PON and LR-PON).

S2: Given a per-class maximum delay requirement and a scheduling service discipline (e.g., fixed, gated, limited, etc.), compute the expected/approximated sleep time for every ONU j (denoted T_j^s).

S3: Schedule the buffered downstream data for the ONUs to be transmitted during the allocated upstream transmission window.

S4: Send grant messages with embedded sleep time values to all the ONUs.

Hence, the time spent by the OLT to serve ONU j, $v_{s,j}$ is given by:

$$v_{s,j} = T_{br}^{proc} + 2T_j^{prop} + T_{gba} + j \times T_{gr}^{proc} + (j-1)T_g^{gr} + T_{gr}^{tran}, \tag{5.1}$$

[1]In addition to the buffering queues occupancies, the ONU request messages contain information about the admitted flows' rates and profiles.

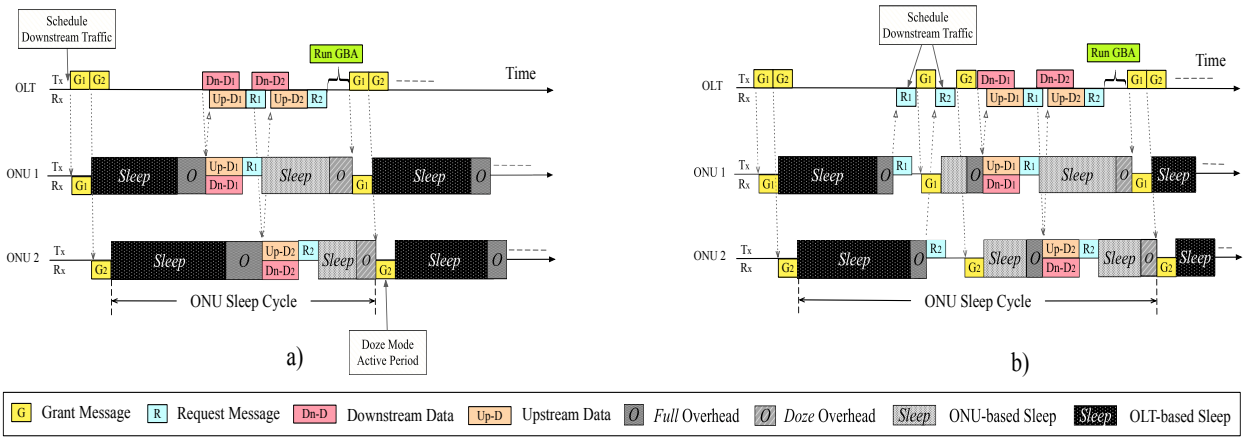

Figure 5.2: Green bandwidth allocation with a) Direct ONU Transmission and b) Request After Sleep.

where T_{gba} is the GBA computation time and T_{br}^{proc}, T_{j}^{prop}, T_{gr}^{proc}, T_{g}^{gr} and T_{gr}^{tran} are as defined in the previous Chapter. In other words, $v_{s,j}$ is the time spent by the OLT directly after the last polled ONU sends its request message to the OLT, and until ONU j receives its designated grant message.

5.1.2 GBA at ONU

Upon receiving the grant message, the ONU immediately goes into the sleep mode and sets its timer accordingly. In the ONU active period and as illustrated in Fig. 5.2, the following two scenarios could be applied:

a) **Direct ONU Transmission:** In this scenario, upon waking up, the ONU starts sending/receiving the buffered data directly. As shown in Fig. 5.2, the total overhead exhibited in every ONU sleep cycle will be low without any wasted idle time. However in TDM-based PONs, the OLT will be required to sort/synchronize the sleep time periods of all ONUs to avoid any possible collision in case two or more ONUs try to access the same channel simultaneously.

b) **Request After Sleep**: Here, upon waking up, the ONU has to issue a request in the upstream direction and wait for the OLT grant. Compared with

the first scenario where the request-grant procedure right after the sleeping is eliminated, this scenario does not require high precision of OLT synchronization among the ONUs. Such a request-grant procedure certainly causes additional delay as shown in figure, and should be included in the computation of the sleep time, thereby making it more complex and possibly less energy efficient.

With either scenario, after sending the request message to the OLT, each ONU will remain idle until receiving a grant message from the OLT. In TDM-based PONs, this idle time might be lengthy in case other ONUs have large amounts of data to be transmitted and/or received. Hence, the ONU can meanwhile switch to the sleep mode in order to save energy. As a result, the OLT will be required to specify in the grant message two sleep times:

1. **ONU-based sleep ($T_j^{s,2}$)**: which represents the time that the ONU spends in the sleep mode directly after sending a request message and until receiving a grant message (i.e., while other ONUs are transmitting).

2. **OLT-based sleep ($T_j^{s,1}$)**: which represents the time that the ONU spends in the sleep mode directly upon receiving the grant message, such that:

$$T_j^{s,1} = T_j^s - T_j^{s,2}. \tag{5.2}$$

The case of a "short" sleep time might be problematic for slow recovery ONUs (e.g., GR-ONU-1). To resolve this issue, the OLT can allow the ONU to switch into the sleep mode (in either OLT-based or ONU-based mode) only if the respective sleep time is greater than its overhead time. Furthermore, since the ONU goes directly into the OLT-based sleep mode once it receives a grant message, it can spend the time receiving the grant message in the doze mode (or alternatively sleep-aware mode[2]). Consequently, after the OLT-based sleep period, ONU j will spend the

[2]The sleep-aware mode keeps the ONU primarily active for the purpose of collecting potential wake-up messages from the OLT [51].

overhead period, denoted $T_j^{o,1}$, to switch from the cyclic/deep sleep mode to the active mode, and the overhead period, denoted $T_j^{o,2}$, to switch from the cyclic sleep mode to the doze mode (which consumes low power as indicated in Table 2.2). With all these methods, GBA can achieve the maximum possible energy reduction.

5.1.3 GBA Compliance with MPCP and PLOAM

EPON's MPCP defines three timeout mechanisms for the interconnection between OLT and ONUs:

1. *mpcp_timeout*: which forces the ONU to send a REPORT message at least once every second in order to maintain registration.

2. *gate_timeout*: which forces the OLT to generate a (possibly empty) GATE message for a particular ONU at least once every 50 ms.

3. *report_timeout*: which specifies a 50 ms timeout between two consecutive REPORT messages of the same ONU.

Similarly, GPON's Physical Layer Operations and Maintenance (PLOAM) defines a timeout period of 100 ms after which, an ONU will fully deactivate [23].

To comply with MPCP and PLOAM, an ONU should wake up by 50 ms. Alternately, MPCP and PLOAM can be amended to enable a dynamic timeout setting so as to allow the sleep time to exceed 50 ms or possibly 1 *second*, and thus maximizing energy saving in NG-PON.

5.1.4 GBA for WDM-based NG-PONs

The operation of GBA over WDM-based NG-PONs (i.e., WDM-PONs and LR-PONs) is straightforward and requires no amendment. Namely instead of having the OLT wait for all the requests of all ONUs, it can send the sleep time grant

(specifying only the OLT-based sleep time value) for every ONU directly upon receiving the request message[3]. In addition, no sleep time scheduling/synchronization is required under the Direct ONU Transmission scenario. For hybrid TDM/WDM-PONs where a subset of ONUs share the same wavelength in a TDM fashion (as in EPON/GPON), GBA operates in the same manner on every shared channel as described earlier.

5.2 Power Model

Let E_{olt} and E_j denote the energy consumed by the OLT and ONU j, respectively. Hence the total energy consumed by a single NG-PON system, E_{pon} can be formulated as follows:

$$E_{pon} = E_{olt} + \sum_{j \in \mathbf{M}} E_j. \tag{5.3}$$

In current NG-PON systems, as mentioned in Section 2.4.2, it is argued that the OLT cannot go into the sleep mode and its power consumption is fixed to 20 W [76]. This is due to the fact that the OLT plays the role of distributor, arbitrator, and aggregator of the network and is responsible for controlling and initiating the energy saving mechanism at the ONUs [44]. In addition, putting the OLT into sleep might cause a synchronization problem for the ONUs. It is also argued that the statistical multiplexing nature of the upstream channel and the bursty traffic from ONUs forbids us to turn off the OLT's receiver as it will threaten the QoS of the network [51]. Nevertheless, these arguments were presented given that the ONUs are allowed to sleep within one DBA cycle, and without considering the fact that all ONUs may be sleeping simultaneously.

With GBA, the OLT can go into the sleep mode when all ONUs are in the sleep mode, which is well known for the OLT at the beginning of every GBA cycle. This can significantly reduce the power consumption of an NG-PON system and achieve high energy efficiency. However, new OLT architectures and sleep

[3]In WDM-PONs, every ONU is connected to the OLT through a separate wavelength channel.

control mechanisms will be required to avoid the aforementioned synchronization problem (e.g., by keeping the OLT clock functional, etc.), which is subject to further investigations and is outside the scope of this work. Hence in our model, we do not consider the possibility of putting the OLT into the sleep mode. The energy saving is achieved by putting the ONU into the sleep mode.

The total energy consumed by a sleep-enabled ONU is given by:

$$E_j = E_j^a + E_j^s + E_j^o. \tag{5.4}$$

where E_j^a, E_j^s, and E_j^o denote the energy consumed by ONU j in the active state, the sleep state, and the overhead period, respectively. In the active state, the energy consumed by ONU j is estimated as follows:

$$E_j^a = P_j^a \times \Big[(T_j^{tran} \cup T_j^{recv}) + T_j^{idle}\Big], \tag{5.5}$$

where P_j^a, T_j^{tran}, T_j^{recv}, and T_j^{idle} are the power consumption in the active state, the data transmission period, the data receiving period, and the idle period, respectively. The union of T_j^{tran} and T_j^{recv} is taken because an ONU may receive and transmit traffic simultaneously (e.g., the UCS protocol).

The total energy consumed by ONU j during the sleep state is given by:

$$E_j^s = P_j^s \times T_j^s, \tag{5.6}$$

where P_j^s and T_j^s are the power consumed in the sleep state, and the ONU sleep time, respectively.

5.2.1 Overhead Time

The overhead time spent by the ONU to transition from the sleep state to the active state consists of a period T_j^{laser} denoting the time to have the transceiver ready, the clock synchronization period T_j^{sync}, and the clock recovery period T_j^{rec} .

Hence, the overhead time is formulated as follows [4]:

$$T_j^o = \max\left(T_j^{rec} + T_j^{sync}\ ,\ T_j^{laser}\right) \tag{5.7}$$

T_j^o occurs every time the ONU wakes up to send or receive data. If the downstream and upstream transmissions do not overlap, the overhead is displayed twice in every sleep cycle; otherwise an additional T_j^{laser} is consumed to turn the receiver and/or transmitter on. Therefore, overlapping the downstream and upstream transmissions can save maximum energy, on the expense of making the required QoS performance for downstream and upstream traffic harder to achieve.

Assuming that turning the laser diode of the transceiver on also consumes P_j^a, the total overhead energy consumed by ONU j is given by[5]:

$$E_j^o = P_j^a \times T_j^o. \tag{5.8}$$

5.2.2 ONU Sleep Mode Condition

Theorem 5.2.1. *In TDM-based PONs, ONU j can go into the sleep mode only if the following condition is satisfied:*

$$T_j^s \geq \sum_{z\in\mathbf{M},z\neq j} T_z^a + |\mathbf{M}| \times T_g^a + v_{s,j} - T_j^o, \quad \forall j \in \mathbf{M}. \tag{5.9}$$

Specifically, the sleep time (plus the overhead time) of an ONU should be greater than or equal to the transmission time of all other ONUs (which are separated with a guard time), plus the OLT serving time.

Proof. A necessary condition for ONU j to switch into the sleep mode in TDM-

[4]The laser on time can be found in [76].

[5]Normally, the energy consumed when turning on a device is higher than when it is functioning at normal operation.

based PONs, is that it is idle [44], which gives us the following:

$$T_j^s \geq T_j^{idle} - T_j^o, \tag{5.10}$$

where T_j^{idle} is the ONU idle time which is equivalent to the time while other ONUs are transmitting and receiving data, plus the time spent by the OLT to serve ONU j. Thus, T_j^{idle} can be formulated as follows:

$$T_j^{idle} = \sum_{z \in \mathbf{M}, z \neq j} T_z^a + |\mathbf{M}| \times T_g^a + v_{s,j}. \tag{5.11}$$

Replacing (5.11) in (5.10) ends our proof. □

Remark 5.2.1. *Breaking the condition in Eq. (5.9) means that the ONU cannot be idle and hence the NG-PON system is not stable. We thus assume that this condition always holds and the system is stable.*

5.3 Maximum ONU Sleep Time

Taking the maximum ONU sleep time without violating the user's QoS requirements is the core theme of GBA. This should be jointly determined by the idle statuses of the ONUs (or whether or not they have traffic to transmit), and by their expected traffic patterns. Computing the sleep time for each ONU in advance without relying on conventional polling mechanisms can effectively reduce the control messaging overhead needed to learn about every ONU's status.

This section introduces the proposed analytical model for the Direct ONU Transmission scenario, to measure the expected delay for each CoS c of ONU j. To the best of our knowledge, this is the first closed-form sleep time model for multi-class NG-PONs using M/G/1 queue with vacations. Consequently, based on the maximum expected delay for every CoS, we optimize the energy saving without impairing the desired QoS for each service class.

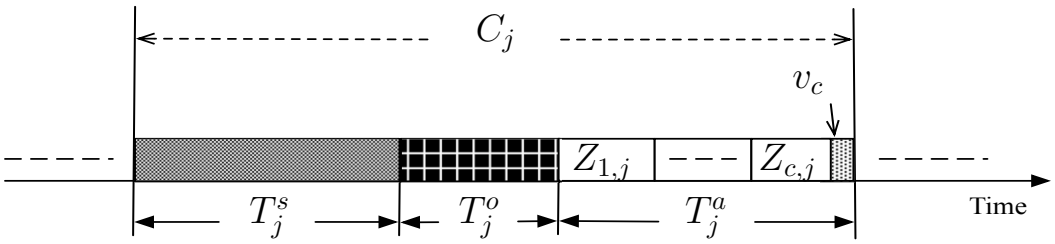

Figure 5.3: Illustration of ONU sleep cycle

To facilitate the analysis, we illustrate in Fig. 5.3 the ONU sleep cycle denoted as C_j, which consists of the sleep and overhead vacation times, and the ONU active period denoted as T_j^a. In the active period, the ONU spends a period $Z_{c,j}$ (c = $1, \ldots, n$) for each served queue, and then spends a "vacation" period v_c for control messages. Assuming that the upstream data arrivals of all classes are Poisson-ditributed with arrival rate $\lambda_{c,j}$, we model each ONU as an M/G/1 with vacations. Note that because the sleep time of one ONU is at least the time when other ONUs are transmitting or receiving traffic (in the case of a TDM-based NG-PON), the whole system can be represented by only one ONU server and multiple vacation periods (same as in WDM-PONs). The first and second moments of the packet transmission times belonging to class c and ONU j can be expressed as $E\{X_{c,j}\} = \overline{X_{c,j}} = 1/\mu_{c,j}$, and $E\{X_{c,j}^2\} = \overline{X_{c,j}^2}$, respectively, with $\mu_{c,j}$ denoting the service rate of a CoS c packet belonging to ONU j, and μ_j as the total service rate. The utilization factor per class c and ONU j is $\rho_{c,j} = \lambda_{c,j}\overline{X}_{c,j}$. We also denote $\overline{V_j}$ and $\overline{V_j^2}$ as the first and second moment of ONU j's vacation time, respectively. We assume that a steady state always exists. That is,

$$\rho_j = \rho_{1,j} + \rho_{2,j} + \cdots + \rho_{n,j} < 1. \tag{5.12}$$

Furthermore due to the UCS mechanism, to ensure controlled downstream traffic delay, the following condition must be satisfied:

$$\frac{\lambda_j^{ds}}{\sum_{c=1}^{n} \lambda_{c,j}} < 1, \tag{5.13}$$

where λ_j^{ds} is the downstream traffic arrival rate. The vacation time for ONU j, denoted as v_j, is then given by:

$$v_j = v_c + T_j^s + T_j^o. \tag{5.14}$$

5.3.1 Expected Packet Delay

Each incoming packet ξ may arrive at any ONU j during C_j and can belong to any class $c = 1, \ldots, n$. Packet ξ will be subject to a total delay $D_{c,j}$, given as follows:

$$D_{c,j}(\xi) = W_{c,j}(\xi) + T_j^{prop} + X_{c,j}(\xi), \tag{5.15}$$

where $W_{c,j}(\xi)$ and $X_{c,j}(\xi)$ are ξ's average queuing delay and transmission time, respectively. In the steady state, as $\xi \to \infty$, the expected value of the total delay is given as:

$$\begin{aligned} E\{D_{c,j}\} &= E\{W_{c,j}\} + T_j^{prop} + E\{X_{c,j}\} \\ &= E\{W_{c,j}\} + \frac{d_j}{\mathcal{C}_{pon}} + \frac{1}{\mu_{c,j}}, \end{aligned} \tag{5.16}$$

where d_j is the distance between the OLT and ONU j. Thus in order to compute $E\{D_{c,j}\}$, we need to derive an expression for $E\{W_{c,j}\}$.

5.3.2 Queuing Delay Analysis

The queuing delay of ξ arriving at ONU j is expressed by:

$$W_j(\xi) = R_j(\xi) + N_j(\xi) \times \overline{X}(\xi) + Y_j(\xi) \tag{5.17}$$

where $\overline{X}(\xi)$ is the mean service time of packet ξ. We note that $E\{R_j\} = \lim_{\xi\to\infty} R_j(\xi)$. Similarly, $E\{Y_j\} = \lim_{\xi\to\infty} Y_j(\xi)$, $E\{N_j\} = \lim_{\xi\to\infty} N_j(\xi)$, and $E\{W_j\} = \lim_{\xi\to\infty} W_j(\xi)$.

A packet ξ belonging to class $1 \leq c \leq n$, will exhibit an expected queuing delay

equal to the following:

$$E\{W_{c,j}\} = E\{R_{c,j}\} + \frac{E\{N_j\}}{\mu_j} + E\{Y_j\}. \tag{5.18}$$

Hence in order to get the value of $E\{W_{c,j}\}$, we need to find $E\{N_j\}$, $E\{R_{c,j}\}$, and $E\{Y_j\}$. The values of these variables depend on the type of service employed by the DBA. Namely, many DBA schemes have been proposed in the literature. Most famously, IPACT with *gated service* has been well studied and analyzed [27] . We therefore proceed with the analysis given that a gated service is employed.

5.3.3 Analysis with Gated Service

In the steady state, packet ξ of CoS c will see the same average number of packets queued, at both its enqueuing and dequeuing times. Using Little's theorem [73], the expected number of arriving packets to all CoSs while ξ is waiting, can be expressed by $\sum_{z=1}^{n} \lambda_{z,j} \times E\{W_{c,j}\}$. As a result:

$$\begin{aligned} \frac{E\{N_j\}}{\mu_j} &= \sum_{z=1}^{n} \lambda_{z,j} \overline{X_{z,j}} \times E\{W_{c,j}\} \\ &= \rho_j \times E\{W_{c,j}\}. \end{aligned} \tag{5.19}$$

Hence, the expected queuing delay of the priority queue c is computed as follows:

$$E\{W_{c,j}\} = \frac{E\{R_{c,j}\} + E\{Y_j\}}{1 - \rho_j}. \tag{5.20}$$

Lemma 5.3.1. *The residual time seen by a packet arriving at ONU j in CoS c is given as follows:*

$$E\{R_{c,j}\} = \frac{1}{2}\Big(\frac{\lambda_{c,j}}{\sum_{z=1}^{n} \lambda_{z,j}} \overline{X_{c,j}^2}\Big) + \frac{\overline{V_j^2}\Big(1 - \rho_j\Big)}{2\overline{V_j}}. \tag{5.21}$$

Proof. To find the value of $E\{R_{c,j}\}$, we use the concept of the *mean residual service time* with graphical argument [73]. The residual time at time τ, $R_{c,j}(\tau)$, exhibits

vacation times depending on the position of class c in C_j. Therefore, the time average of $R_{c,j}(\tau)$ in $[0,t]$ is:

$$\begin{aligned} E\{R_{c,j}\} &= \frac{1}{t}\int_0^t R_{c,j}(\tau)d\tau \\ &= \frac{1}{t}\left(\sum_{x_{c,j}\in S_{c,j}(t)}\frac{1}{2}x_{c,j}^2 + \sum_{y_j\in L_j(t)}\frac{1}{2}y_j^2\right), \end{aligned} \tag{5.22}$$

where $L_j(t)$ is the number of vacations seen in C_j, and $S_{c,j}(t)$ denotes the number of CoS c serviced packets. $x_{c,j}$ denotes a class c serviced packet and y_j denotes the single vacation time seen by ONU j, all during $[0,t]$. We then rewrite Eq. (5.22) as follows:

$$\begin{aligned} E\{R_{c,j}\} &= \frac{1}{t}\left[\Big(\sum_{a=1}^{S_{c,j}(t)}\frac{1}{2}x_a^2\Big) + \Big(\sum_{b=1}^{L_j(t)}\times\frac{1}{2}y_b^2\Big)\right] \\ &= \frac{1}{2}\left[\Big(\frac{S_{c,j}(t)}{t}\overline{X_{c,j}^2}\Big) + \Big(\frac{L_j(t)}{t}\times\overline{V_j^2}\Big)\right]. \end{aligned} \tag{5.23}$$

We note that:

$$\lim_{t\to\infty}\frac{S_{c,j}(t)}{t}\overline{X_{c,j}^2} \longrightarrow E\{Z_{c,j}\}.$$

Furthermore, as $t\to\infty$, the fraction of time spent serving packets from all queues approaches ρ_j, and thus the fraction of time occupied with vacations is $(1-\rho_j)$. Assuming time averages can be replaced by ensemble averages, we get:

$$\lim_{t\to\infty}\frac{t(1-\rho_j)}{L_j(t)} \longrightarrow \overline{V_j}.$$

To get $E\{Z_{c,j}\}$, we use the *conservation law* of [77] which states that the total amount of work in a cyclic gated system (which can best describe our model) does not depend on the order of service. Hence, a packet arriving to any CoS will witness the same work load in the system. Therefore, the amount of work for CoS c queue, $E\{Z_{c,j}\}$ is given as:

$$E\{Z_{c,j}\} = \frac{\lambda_{c,j}}{\sum_{z=1}^{n}\lambda_{z,j}}\overline{X_{c,j}^2}. \tag{5.24}$$

Replacing all the approximations in Eq (5.23) ends our proof. □

Lemma 5.3.2. *The expected interval time $E\{Y_j\}$ that the system waits for in every ONU sleep cycle is given as follows:*

$$E\{Y_j\} = (1-\rho_j)(T_j^o + T_j^s + v_c). \tag{5.25}$$

Proof. In a gated system, $E\{Y_j\}$ is the total vacation time appearing in one server cycle, times the probability of the server being idle [73]. In our system, the total vacation time appearing in C_j is v_j, and the probability of the system being idle is given by $(1-\rho_j)$. □

Theorem 5.3.1. *The expected queuing delay in a NG-PON system for a CoS c packet of ONU j, under a gated service, is:*

$$E\{W_{c,j}\} = \frac{\lambda_{c,j}\overline{X_{c,j}^2}}{2(1-\rho_j)\sum_{z=1}^{n}\lambda_{z,j}} + \frac{3v_j}{2}. \tag{5.26}$$

Proof. By combining $E\{R_{c,j}\}$ from Eq. (5.21), and $E\{Y_j\}$ from Eq. (5.25), we obtain the expected queuing delay $E\{W_{c,j}\}$ for CoS $c : 1 \leq c \leq n$ as follows:

$$E\{W_{c,j}\} = \frac{\lambda_{c,j}\overline{X_{c,j}^2}/\sum_{z=1}^{n}\lambda_{z,j} + (1-\rho_j)v_j}{2(1-\rho_j)} + \frac{\overline{V_j^2}}{2\overline{V_j}}. \tag{5.27}$$

We have $\overline{V_j^2} = (\overline{V_j})^2 = v_j^2$. Hence, by substituting these values in Eq. (5.27), we get $E\{W_{c,j}\}$ in Eq. (5.26). □

5.3.4 Expression of Sleep Time

Theorem 5.3.2. *Given the QoS delay requirement $\mathbb{D}_{c,j}$, ONU j can sleep for a period $T_{c,j}^s$, given as follows:*

$$T_{c,j}^s = \frac{2}{3}\Big(\mathbb{D}_{c,j} - \frac{d_j}{\mathcal{C}_{pon}} - \overline{X_{c,j}}\Big) - \frac{\lambda_{c,j}\overline{X_{c,j}^2}}{3(1-\rho_j)\sum_{z=1}^{n}\lambda_{z,j}} - T_j^o - v_c. \tag{5.28}$$

Proof. By substituting the value of $E\{W_{c,j}\}$ from Eq. (5.16) in Eq. (5.26), and by extracting T_j^s from v_j as well as inverting the equation, we get $T_{c,j}^s$. □

Finally, T_j^s is set as the minimum value as follows:

$$T_j^s = \min\left(T_{1,j}^s, \ldots, T_{n,j}^s\right). \tag{5.29}$$

Remark 5.3.1. *Due its design flexibility, GBA can utilize any other selected sleep time value (e.g., from [46]), but may require further DBA considerations. Also note that while our analysis is based on the upstream packet delay requirement, a similar analysis may be performed to measure the sleep time based on the expected downstream packet latency and its respective requirement (if any). The OLT will then set the ONU sleep time to be the minimum between the upstream-based and downstream-based values.*

5.3.5 ONU "Wake Up Call"

By replacing the value of T_j^s in Eq. (5.26), we can get the maximum $E\{W_{c,j}\}$. Then using Little's theorem [73], we compute the expected average queue size of class c and ONU j, $E\{Q_{c,j}\}$, as follows:

$$E\{Q_{c,j}\} = \lambda_{c,j} E\{W_{c,j}\}. \tag{5.30}$$

Consequently, as an alternative to setting a timer which yields additional overhead due to clock synchronization, each ONU may hold a "counter" for each CoS queue, denoted $count_{c,j}$, to measure the number of buffered packets in each queue. When $count_{c,j} = E\{Q_{c,j}\}$, the ONU switches to the active state.

5.3.6 Model Validation and Observations

To validate the correctness of the proposed model, we have simulated an EPON system using OMNET++ [75]. EPON's speed $\mathcal{C}_{pon}$ is set to $1Gb/s$. We simulate

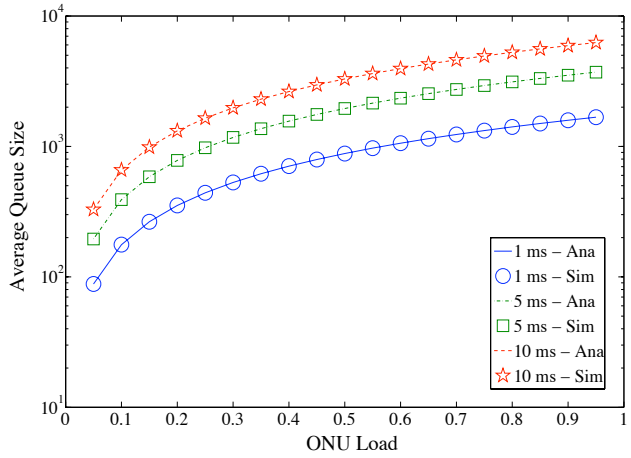

(a) $c = 1$: CBR

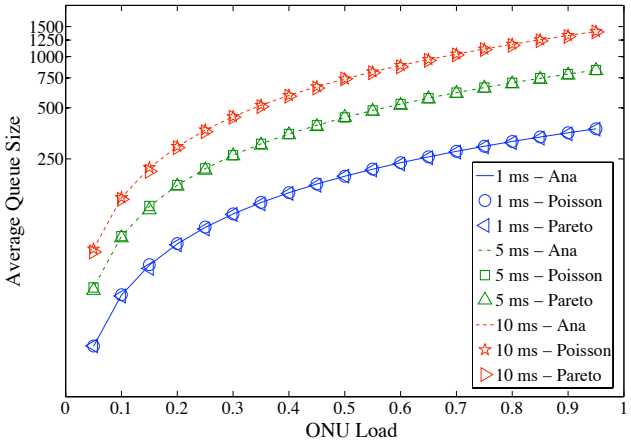

(b) $c = 2$: VBR

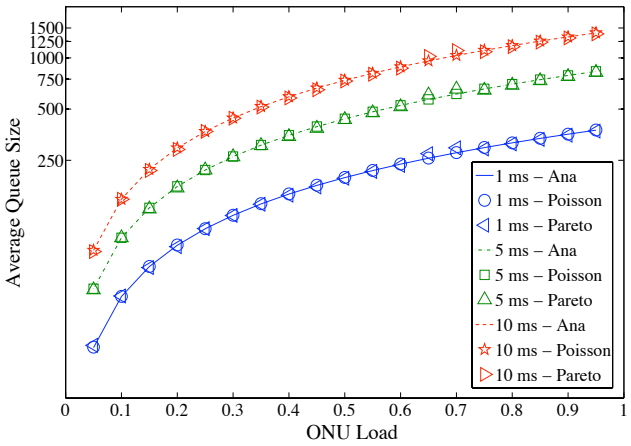

(c) $c = 3$: BE

Figure 5.4: Average queue size for GR-ONU-1/A, with $T_j^s = 1, 5$ and 10 ms.

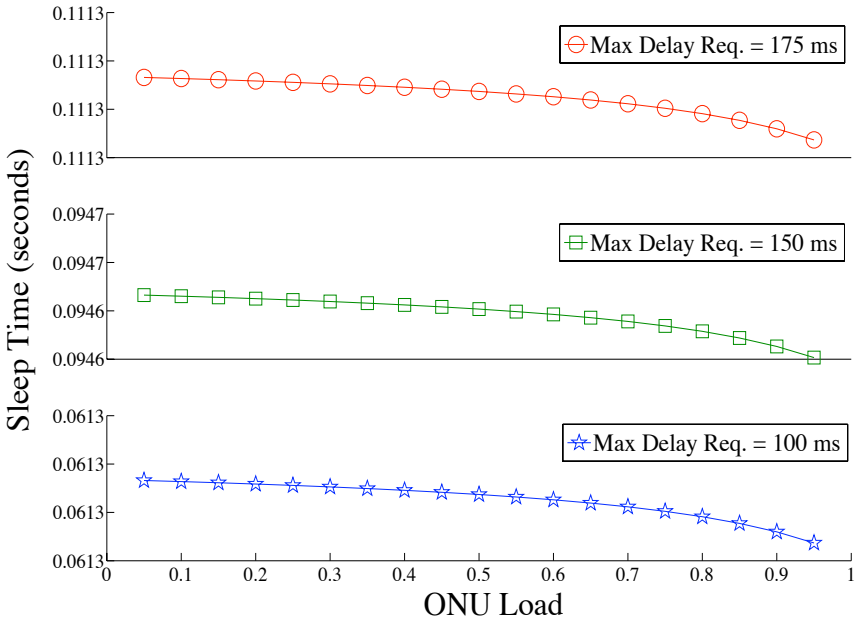

(a) T_i^s with GR-ONU-1/C

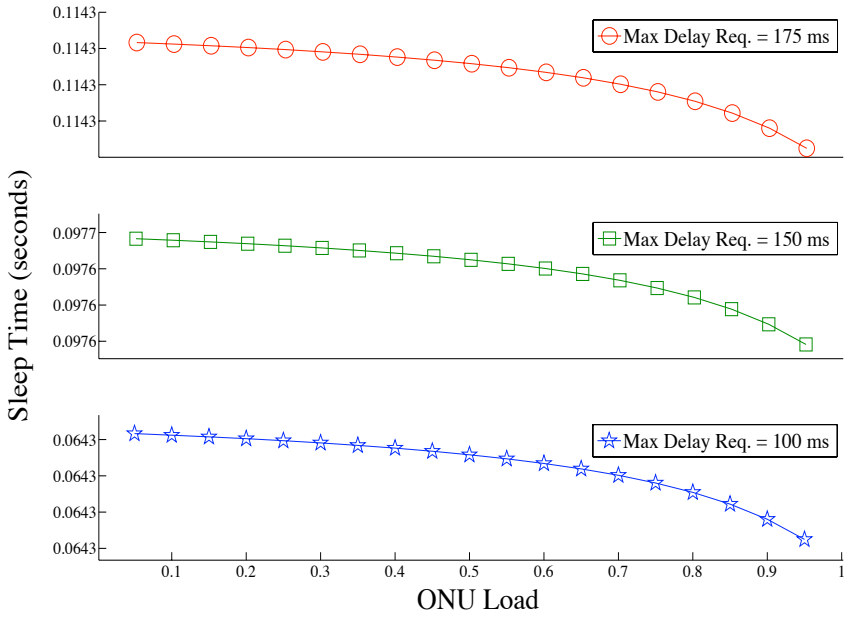

(b) T_i^s with GR-ONU-1/A

Figure 5.5: Sleep time with Max. delay requirement $\mathbb{D}_{c,j} = 100$, 150 and 175 ms.

with a single ONU because 1) the derived model cannot be simulated without sorting the sleep time of the ONUs, and 2) as mentioned earlier, the model assumes that a single ONU can represent the whole system, since its sleep time includes the time when other ONUs are transmitting. For WDM-PONs, the simulation model applies as is. The traffic profile for the ONU is divided as follows: 20% of the total generated traffic is considered for CBR traffic, and 80% is divided equally between VBR and BE traffics [39, 38]. CBR flows have fixed size packets equal to 70 bytes, whereas VBR and BE flows have packet payload sizes that vary from 64 to 1518 bytes with the distribution based on [39] as follows: 64 bytes (47%), 300 bytes (5%), 594 bytes (15%), 1300 byte (5%), and 1518 bytes (28%). Because VBR and BE traffics are bursty by nature, we simulate them as both Poisson and Pareto-distributed, whereas the CBR traffic is simulated as Poisson[6]. The 95% confidence interval of the simulation results gives a very small variation, and is thus not shown.

We first plot in Fig. 5.4 the average queue size of each CoS (mainly used to switch the ONU back to the active mode) under GR-ONU-1/A. The figure shows that while Poisson-modeled traffics perfectly match with the analytical model, only a small deviation of approximately $10 \sim 15\%$ at higher loads (e.g., $\rho_j = 0.6, 0.7$) is observed for Pareto-modeled traffics from the analytical results, especially with longer sleep times. Therefore, we can claim that our model can be effectively used to compute the ONU sleep time without major adjustments.

We then plot in Fig. 5.5 the sleep time T_j^s versus the maximum delay requirement $\mathbb{D}_{c,j} = 100, 150$, and 175 ms, with GR-ONU-1/C and GR-ONU-1/A. Results show that for a 100 ms delay requirement, GR-ONU-1/C can sleep for 61.3 ms, and for a 150 ms delay requirement (which is the typical voice/video maximum delay requirement [78]), it can sleep for 94.7 ms, and finally for a 175 ms delay requirement, the ONU can sleep for 111.3 ms. On the other hand, GR-ONU-1/A can sleep for 64.3 ms with a 100 ms delay requirement, for 97.6 ms with a 150 ms delay requirement, and for 114.3 ms with a 175 ms delay requirement. These numbers highlight the advantages of batch-mode transmission which can keep the ONU

[6]Note that CBR traffic has long been modeled as Poisson in Diff-Serv PONs [38, 60].

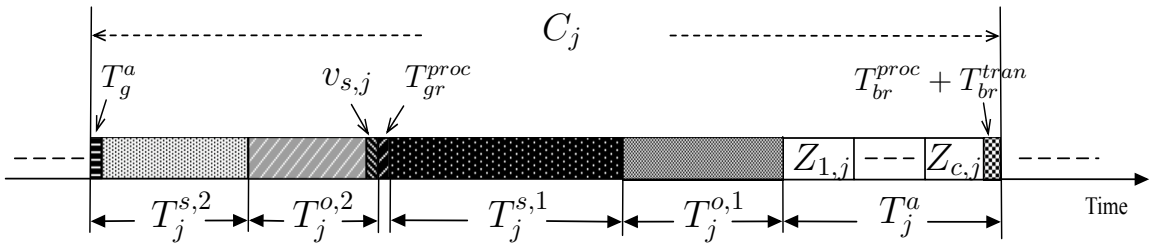

Figure 5.6: Illustration of ONU *sleep cycle* after dividing the sleep time into two.

in the sleep mode for a long time so as to minimize the wasted overhead frequency, and thus save maximum possible energy while maintaining the delay requirements for all types of traffic.

Remark 5.3.2. *It is observed in Fig. 5.5 that the sleep time barely varies as the load increases (in fact the variation is in fractions of milliseconds, therefore is not noticed). This is due to the fact that the value of T_j^s is DBA-dependant (in our case we employ the gated service). For more details on the delay variation under the gated service in PONs, we refer the reader to [71, 72, 79]. There, unlike in our model, multiple ONUs contribute to the vacation time, which causes a higher packet delay as the load increases, yet with the order of few milliseconds. Hence other advanced DBAs or intra-ONU scheduling schemes may be employed and analyzed to compute the maximum sleep time for each ONU, and which will result in different delay and sleep time behaviors.*

5.4 Sleep Time Sizing

With a Direct ONU Transmission-based GBA mechanism, every ONU is required to transmit/receive traffic immediately after $T_j^{s,1}$ is expired; hence for TDM-based PONs, a collision might occur. The OLT's GBA is therefore required to schedule and size the OLT-based sleep time of every ONU such that the collision is avoided. Furthermore, it should ensure that the total assigned sleep time T_j^s is fully granted in order to achieve the required energy saving.

5.4.1 Problem Formulation

To formulate the problem, we first define the transmission start time and end time of every ONU as follows (see Fig. 5.6):

$$t_j^{st} = t_j^0 + T_j^{s,1} + T_j^{o,1}, \tag{5.31}$$

$$t_j^{end} = t_j^0 + T_j^{s,1} + T_j^{o,1} + T_j^a, \tag{5.32}$$

where t_j^0 denotes the time instant when the grant message is received and processed at the ONU, and is calculated as follows:

$$t_j^0 = t_0 + T_{gba} + T_j^{prop} + T_{gr}^{tran} + (j-1)T_g^{gr} + (j+1)T_{gr}^{proc}, \tag{5.33}$$

with t_0 denoting the time instant when the OLT processes all the received ONUs' requests.

For equally distant ONUs, given the negligible grant guard time ($T_g^{gr} = 1\ \mu s$) and grant processing time ($T_{gr}^{proc} = 10^{-3}\ \mu s$), the instant time t_j^0 is almost the same for all ONUs (i.e., $t_1^0 \approx t_2^0 \approx \cdots \approx t_{|\mathbf{M}|}^0$). Note that the OLT is required to maintain the same polling order in every GBA cycle in order to accurately calculate $v_{s,j}$ and t_j^0.

Assuming that a collision takes place with the current start and end times of all ONUs, each ONU j will be required to shift its sleep time with a portion h_j until the collision is eliminated. However, this should be done while ensuring that the computed sleep time $T_j^{s,1}$ gets its maximum value. As a result, we formulate the sleep time sizing problem as follows:

$$\text{Find: } \max\left(T_j^{s,1} - h_j\right), \quad \forall j \in \mathbf{M}, \tag{5.34}$$

which is equivalent to:

$$\text{Find: } \min\left(\sum_{j\in\mathbf{M}} h_j\right), \tag{5.35}$$

subject to:

$$t_z^{st} - h_z \geq t_j^{end} - h_j + T_g^a \quad \forall j, z \in \mathbf{M}, \quad z > j. \tag{5.36}$$

$$h_j \leq T_j^{s,1} + T_j^{o,1} \quad \forall j \in \mathbf{M}. \tag{5.37}$$

Constraint (5.36) requires the transmission start time of an ONU to be larger than or equal to the transmission end time of any other ONU of lower index plus a guard time. Constraint (5.37) means that the shifted time cannot be greater than the sleep time (plus the overhead time) of the ONU.

5.4.2 Sort-And-Shift (SAS) Scheme

To solve the active time collision problem, we propose a new sleep time sizing scheme, so-called Sort-And-Shift (SAS), which is initiated at the OLT to determine the start time t_j^{st} of each ONU in every GBA cycle. With SAS, the ONUs are sorted according to the length of the maximum allowable sleep time, and t_j^{st} is determined sequentially such that no collision between any ONU's transmission occurs (or to enforce Constraint 5.36). In this case, Constraint (5.36) can be rewritten as follows:

$$h_j \geq h_z + T_g^a + t_j^{st} - t_z^{st} + T_j^a. \tag{5.38}$$

The solution to the problem is optimal by setting the shift time of the ONU with the longest sleep time (or the "last" ONU after the sorting), $h_{|\mathbf{M}|} = 0$. The steps of the SAS mechanism are shown in Fig. 5.7 and the detailed pseudo-code is given in Algorithm 1. The shifted time is included in the ONU-based sleep time in order to ensure that the ONU is fully granted its assigned sleep time. The ONU-based sleep time is computed as follows:

$$T_j^{s,2} = \begin{cases} t_{|\mathbf{M}|}^{end} + v_{s,j} + T_g^a - t_j^{end} - T_j^{o,2} & \text{if} \left(t_{|\mathbf{M}|}^{end} + v_{s,j} + T_g^a - t_j^{end} > T_j^{o,2} \right) \\ 0 & \text{otherwise} \end{cases} \tag{5.39}$$

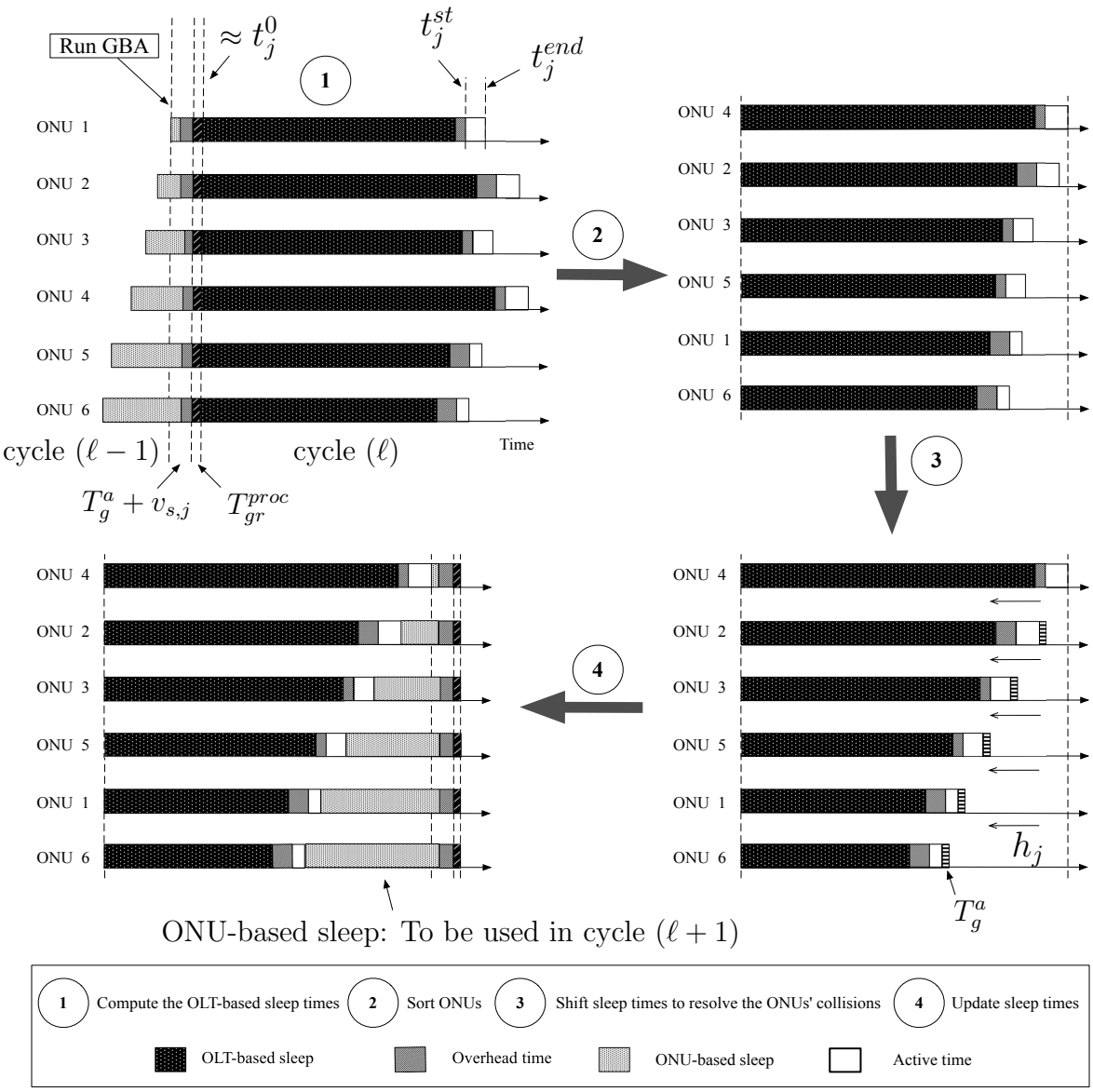

Figure 5.7: Illustration of the proposed Sort-And-Shift (SAS) sleep time sizing mechanism.

Algorithm 1 Sort-And-Shift (SAS) mechanism

for $i = 1 \rightarrow |\mathbf{M}|$ **do**
  Given $T^{s,2}_{j,\ell-1}$ from cycle $(\ell - 1)$,
  compute $T^{s,1}_{j,\ell}$ for cycle (ℓ) according to Eq. (5.2).
end for
/* Initialize and sort the set of ONU start-times $\mathbf{X}$ */
$\mathbf{X} \leftarrow \{t^{st}_1, t^{st}_2, \ldots, t^{st}_{|\mathbf{M}|}\}$;
Sort $\mathbf{X}$ s.t., $t^{st}_j < t^{st}_z$, $\forall j, z \in \mathbf{M}$
/* Set the shift time at the last index to zero */
$h_{|\mathbf{M}|} \leftarrow 0$;
/* Compute the ONU shift time according to Eq. (5.38) */
for $j = |\mathbf{M}| - 1 \rightarrow 1$ **do**
  $h_j \leftarrow h_{j+1} + t^{st}_j - t^{st}_{j+1} + T^a_j + T^a_g$;
end for
/* Update all values if overlapping occurs */
for $j = |\mathbf{M}| - 1 \rightarrow 1$ **do**
  if $h_j > 0$ **then**
    $T^{s,2}_j \leftarrow T^{s,2}_j - h_j$;
    $t^{st}_j \leftarrow t^{st}_j - h_j$;
    $t^{end}_j \leftarrow t^{end}_j - h_j$;
  end if
end for
/* Compute the ONU-based sleep time */
for $j = 1 \rightarrow |\mathbf{M}|$ **do**
  Compute $T^{s,2}_{j,\ell}$ according to Eq. (5.39).
end for

Theorem 5.4.1. *The obtained solution by SAS is optimal.*

Proof. The obtained solution is optimal if it satisfies constraints (5.36) and (5.37) and ensures $T^{s,1}_j + T^{s,2}_j = T^s_j$.

Constraint (5.36) is always satisfied by computing h_j according to Eq. (5.38). For constraint (5.37), the ONU is assumed to be able to go into sleep mode. Thus, Eq. (5.9) is always true, and we re-write it as follows:

$$T^{s,1}_j + T^{s,2}_j + T^{o,1}_j + T^{o,2}_j - h_j \geq \sum_{z \in \mathbf{M}, z \neq j} T^a_z + |\mathbf{M}| \times T^a_g - h_j + v_{s,j}. \tag{5.40}$$

We note that:

$$h_j \leq T_g^a \left(\sum_{z \in \mathbf{M}, z > j} T_z^a \right). \tag{5.41}$$

The worst-case scenario occurs when the shifted time of ONU j is equivalent to the sum of all other ONUs' data intervals (e.g., the worst case scenario for ONU 6 in Fig. 5.7). Assuming such a scenario for ONU j, we then get:

$$h_j = \sum_{z \in \mathbf{M}, z \neq j} T_z^a + (|\mathbf{M}| - 1) \times T_g^a,$$

which reduces Eq. (5.40) to:

$$T_j^{s,1} + T_j^{s,2} + T_j^{o,1} + T_j^{o,2} - h_j \geq v_{s,j} + T_g^a.$$

From Eq. (5.2), we can have two cases:

1. $T_j^{s,2} + T_j^{o,2} \geq v_{s,j} + T_g^a$.
2. $T_j^{s,2} = T_j^{o,2} = 0$.

For the first case, we can write $T_j^{s,2} + T_j^{o,2} = v_{s,j} + T_g^a$, as the minimum value (e.g., the case of ONU 4 in Fig. 5.7), and hence we get:

$$T_j^{s,1} + T_j^{o,1} \geq h_j.$$

For the second case, we get:

$$\begin{aligned} T_j^{s,1} + T_j^{o,1} &\geq h_j + v_{s,j} + T_g^a \\ &> h_j. \end{aligned}$$

Finally, SAS ensures $T_j^{s,1} + T_j^{s,2} = T_j^s$ by allocating the shifted time in the ONU-based sleep time as per Eq. (5.39). Hence, the solution is optimal. □

5.4.3 Updated Vacation Time

With SAS, the sleep time is divided into two. Hence, we can re-write the vacation time of ONU j in Eq. (5.14) as follows:

$$v_j = T_j^{s,1} + T_j^{o,1} + T_j^{s,2} + T_j^{o,2} + v_c. \tag{5.42}$$

The model assumes that $T_j^{s,1} + T_j^{o,1} \geq v_{s,j} + T_g^a$, which might not be always true, especially at high loads with asymmetric ONU loads. In such a case, the OLT might sort the ONUs differently in each cycle, resulting in having the ONU-based sleep time of some ONUs in multiple cycles equal to zero as per Eq. (5.39). Therefore v_j needs to be updated as follows:

$$v_j = T_j^{s,1} + T_j^{o,1} + v_c + \max\left(T_j^{s,2} + T_j^{o,2}, v_{s,j} + T_g^a\right). \tag{5.43}$$

As illustrated in Fig. 5.8, by embedding SAS in the proposed GBA framework, we

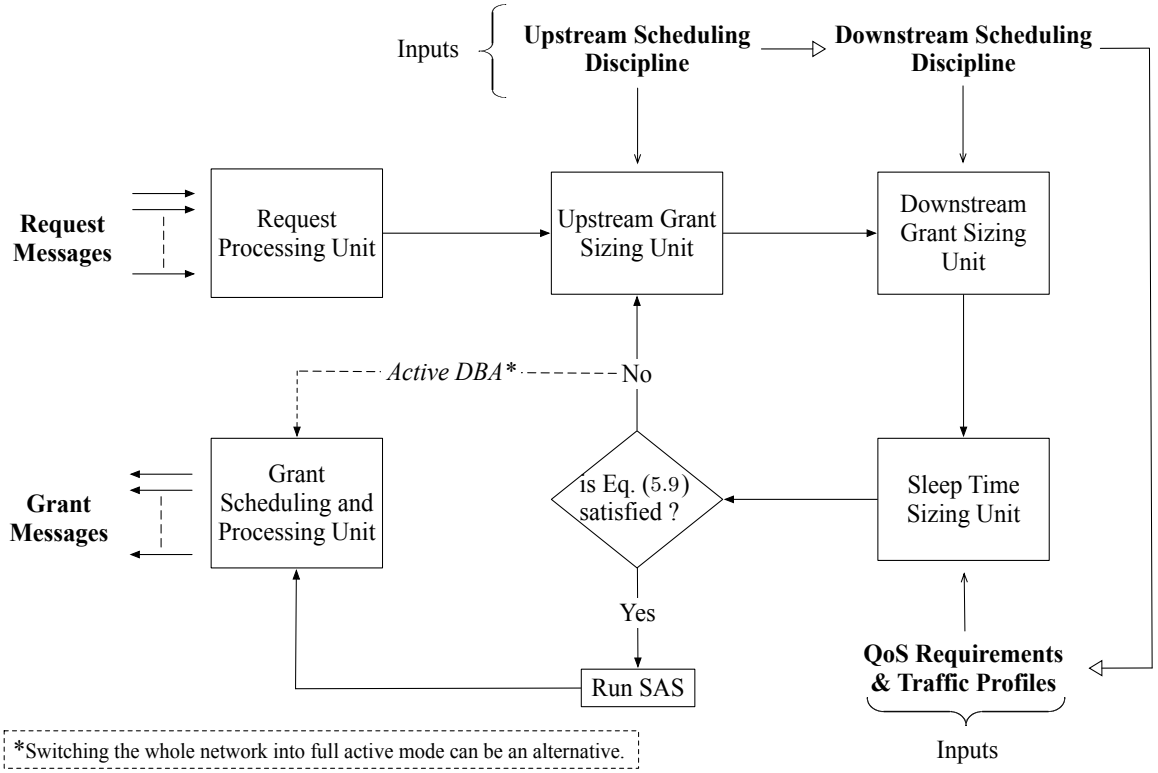

Figure 5.8: Green resource management flowchart at the OLT.

Table 5.1: Simulation parameters

Number of ONUs ($\|\mathbf{M}\|$)	16
Channel speed ($\mathcal{C}_{pon}$)	1 $Gbps$
Distance from OLT to ONU (d_j)	25 km
Guard time (T_g^a and T_g^{gr})	1 μs
Processing time (T_{gr}^{proc} and T_{br}^{proc})	10^{-3} μs
GBA computation time (T_{gba})	*neglected*

can achieve a complete *green* resource management framework for NG-PONs. With the framework, the OLT can decide which downstream and upstream scheduling disciplines to employ by checking if the ONU sleep mode condition in Eq. (5.9) is maintained. Alternatively if the condition in Eq. (5.9) is not satisfied, the OLT may decide to switch the system into "full active" mode and abolish the energy saving plan by employing a legacy DBA.

5.5 Simulation Results

To validate the effectiveness of the proposed solution, we have simulated an EPON system using OMNET++ [75]. The simulations parameters are shown in Table 5.1. To stress test our solutions, we consider four simulation scenarios as detailed in Table 5.2. The traffic settings are the same as in Section 5.3.6. Note that where applicable, only Scenario 4 is employed when comparing our scheme with the UCS scheme of [44]. This is due to the fact that the latter cannot be implemented if the overhead time is not shorter than the cycle time. Hence with the existence of legacy ONUs (i.e., GR-ONU-1) the UCS protocol cannot be utilized, which highlights the advantage of our proposed framework over UCS in being operational on top of any deployed ONU architecture.

We first compare in Fig. 5.9 the total sleep time allocated using SAS under Scenario 1, for three tagged ONUs of different types, versus the assigned sleep time

Table 5.2: Simulation scenarios

ONU Set	Scenario 1		Scenario 2		Scenario 3		Scenario 4	
	Load	ONU Arch.	Load	ONU Arch.	Load	ONU Arch.	Load	ONU Arch.
{1 → 4}	20%	GR-ONU-1/C	25%	GR-ONU-1/C	20%	GR-ONU-1/C	25%	GR-ONU-3
{5 → 8}	32%	GR-ONU-1/A		GR-ONU-1/A	32%			
{9 → 11}	36%	GR-ONU-2		GR-ONU-2	36%			
{12 → 16}	12%	GR-ONU-3		GR-ONU-3	12%			

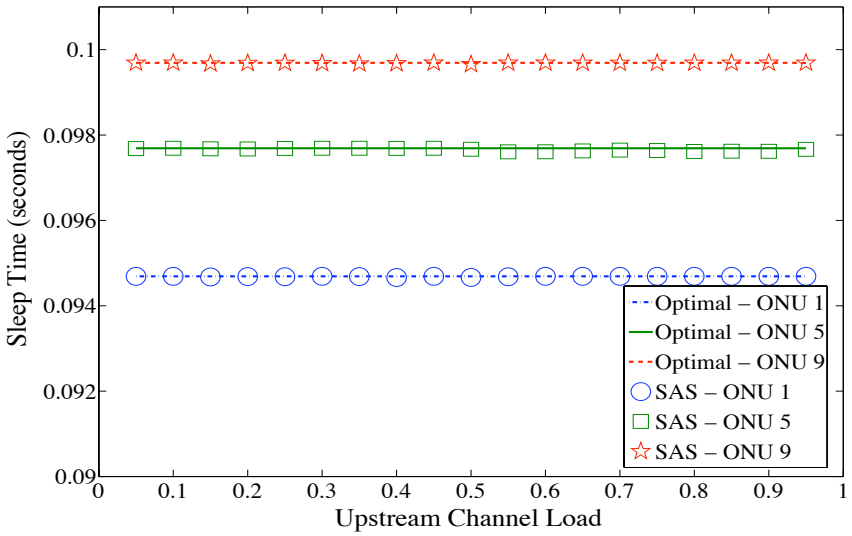

Figure 5.9: Measured total sleep time versus assigned sleep time (i.e., optimal value)

values (i.e., the optimal values). As shown, despite the fact that the sleep time is divided into two parts, SAS still allocates the maximum sleep time for an ONU and hence ensures that the maximum possible energy is saved in the network. Note that a tagged ONU from the final set (e.g., ONU 12) exhibits the same behavior as ONU 9, due to the same displayed overhead time and hence the same computed sleep time.

Fig. 5.10 shows the sleep time behavior of different types of ONUs under SAS. As observed, both the OLT-based and ONU-based sleep times of ONUs with longer sleep times (e.g., ONU 9 and 12) show a similar behavior under both scenarios, whereas ONUs 1 and 5 which have shorter sleep times exhibit different sleep times behaviors depending on the network load. Notably at moderately high network loads (e.g., 0.5 → 0.65), the sleep times of ONUs 1 and 5 are almost evenly dis-

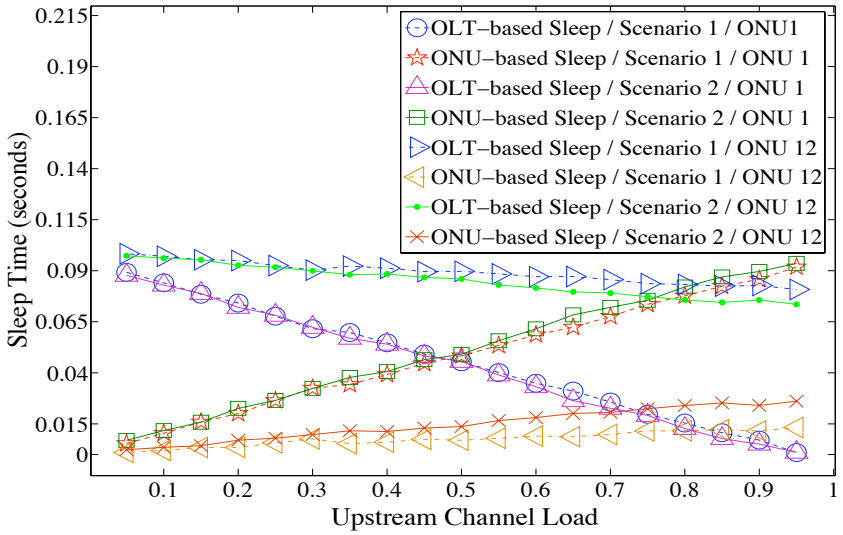

(a) ONUs 1 and 12

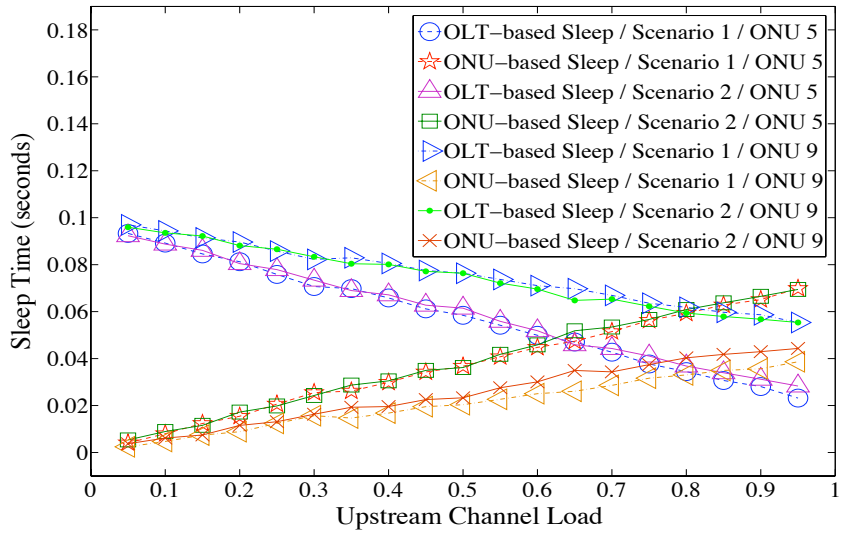

(b) ONUs 5 and 9

Figure 5.10: Sleep time behavior

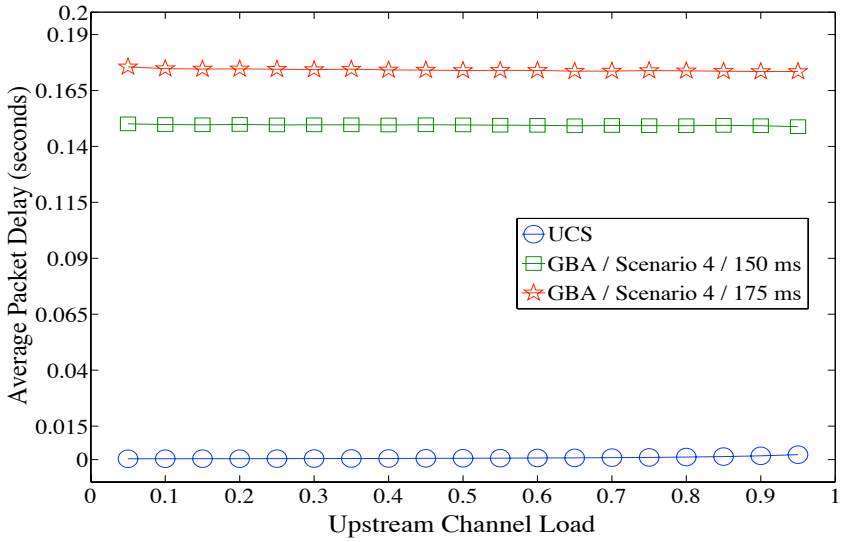

Figure 5.11: Comparison of average packet delay

tributed between their ONU-based and their OLT-based sleep times, respectively; whereas the OLT-based sleep time value outweighs the ONU-based one at lower loads, and vice versa at higher loads. This behavior is due to the way SAS adaptively sorts the sleep times of all ONUs so as the remaining residual time between the end time of the last ONU and the end time of each ONU is taken as credit for the OLT-based sleep time in the next GBA cycle.

Figs. 5.11 and 5.12 highlight the tradeoff between "better network performance" and "higher energy saving" by depicting the average packet delay and the energy consumption of a tagged ONU under both the UCS scheme and the proposed GBA, respectively. As observed with GBA, in contrast to both the UCS scheme and the fully active NG-PON system, although the delay is being sacrificed, the energy consumption for every ONU is significantly decreased. However as shown in Fig. 5.11, the delay performance under GBA depends on the maximum delay requirement. On the other hand, it is noticed in Fig. 5.12 that the energy consumption under UCS is high at low loads, and it decreases at high loads. This is due to the fact that at low loads, the amount of traffic that needs to be transmitted by the ONUs is little. Hence the ONU sleep time (which occurs while other ONUs are transmitting) is either small or null in case the cycle time is smaller than the ONU overhead

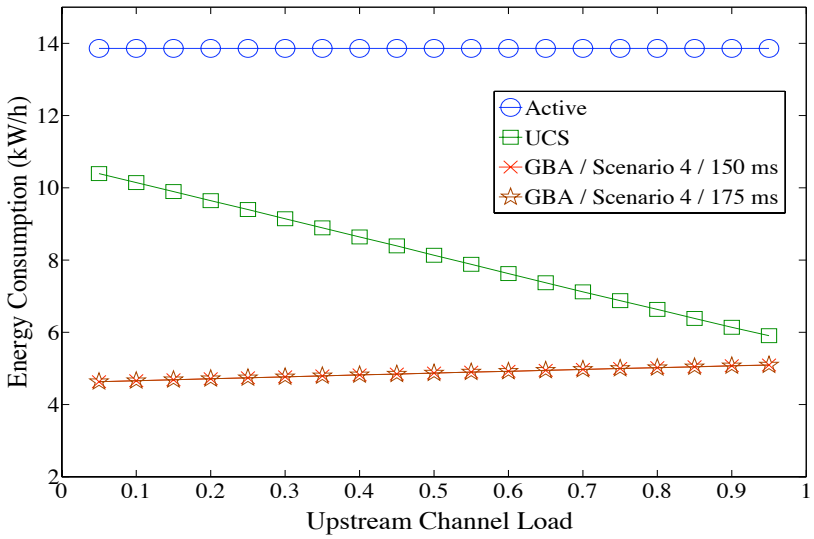

Figure 5.12: Comparison of energy consumption

time, thereby having the ONU most of the times in the active mode. On the other hand with GBA, the ONU sleep time is mainly based on the maximum delay requirement, and hence only a small increase in the energy consumption is witnessed as the load increases. Finally, it is observed in Fig. 5.11 that the delay barely varies as the load increases (under both UCS and GBA) which is, as mentioned earlier, due to the gated service discipline.

In Fig. 5.13, we show how the UCS mechanism may impact the downstream traffic performance if the rates are not controlled as per Eq. 5.13. More specifically, when the downstream traffic load is lower than the upstream traffic load, the downstream packet delay is low; whereas it can no longer be controlled if the downstream traffic load is higher than the upstream one. This also motivates our aforementioned proposition to compute the ONU sleep time based on both the upstream and downstream delays, and then select the minimum value between them. Although this may enable lower energy saving than with the current GBA scheme, it can ensure controlled and guaranteed network performance in the upstream and downstream directions.

We plot in Fig. 5.14 the energy consumption of different types of ONUs un-

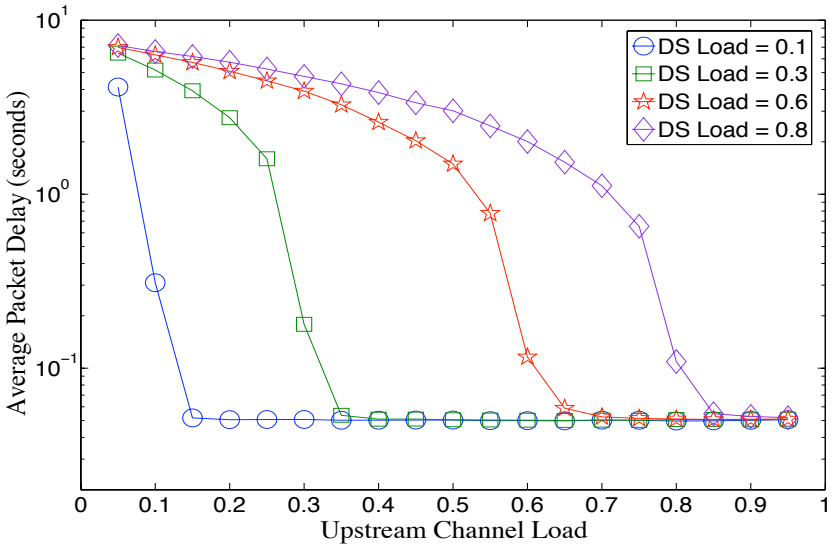

Figure 5.13: Average downstream packet delay

der GBA. As expected, STD-ONU always consumes maximum power as it never sleeps. With efficient sleep time management employing maximum ONU sleep time approximation, GR-ONU-1 can achieve much lower energy consumption than GR-ONU-2 and GR-ONU-3, although it carries the longer overhead time disadvantage. In comparison with the legacy transmission mode (i.e., under STD-ONU), the figure also shows that GBA can achieve almost 90% energy reduction. This proves that the design of a robust sleep control protocol can foster the availability and low-cost deployment of legacy ONUs, and alleviate their long overhead time to build a greener NG-PON.

Finally, to test resilience of the proposed model in achieving the desired energy saving plan under different scenarios, we show in Table 5.3 the network loads in which the employed GBA model (i.e., GBA with gated service) can no longer operate. As observed, with high delay requirements (e.g., 150 ms which is the typical voice delay requirement), the proposed model can fully meet the energy saving requirement and maintain the desired QoS performance. Conversely for lower delay requirements and under different scenarios, GBA's operation is bounded by certain network load thresholds. At these thresholds (which are checked using Eq. 5.9), as mentioned earlier, the OLT can either put the PON system into fully

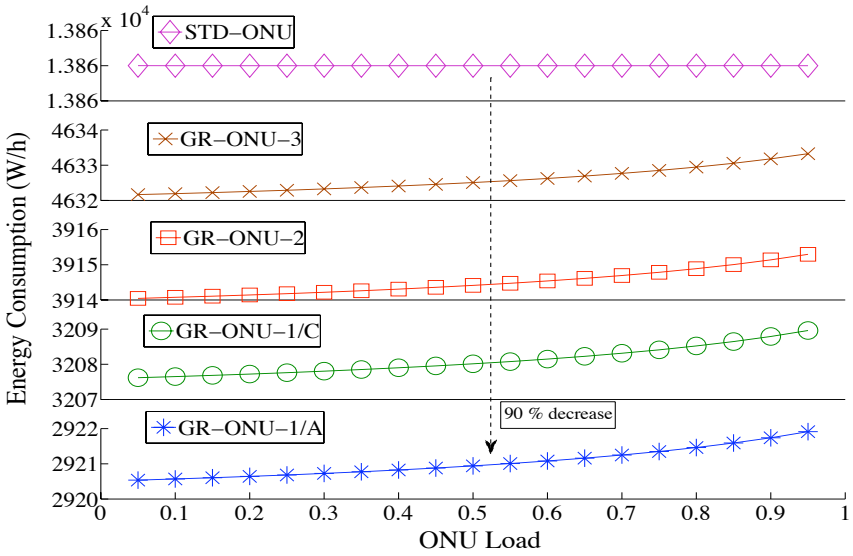

Figure 5.14: Energy consumption of different ONU architectures

Table 5.3: Network loads that break Eq. (5.9).

Scenario	**Maximum Delay Requirement ($\mathbb{D}_c$)**			
	50 ms	100 ms	150 ms	175 ms
1	$\rho > 0.8$	$\rho > 0.9$	N/A	N/A
2	$\rho > 0.6$	$\rho > 0.8$	N/A	N/A
3	$\rho > 0.8$	$\rho > 0.9$	N/A	N/A
4	$\rho > 0.6$	$\rho > 0.8$	N/A	N/A

active mode, or it may employ a different scheduling discipline (e.g., limited service) to compute the ONU sleep time so as to meet the energy saving requirements.

5.6 Summary

Energy saving in telecom IP networks in general and in optical access networks in particular has been gaining massive attention in both the industry and academia. Putting the ONU into sleep is currently the most promising solution to reduce the power consumption in NG-PONs.

In this chapter, we introduce a novel green bandwidth allocation framework, which is characterized by a novel batch-mode transmission mechanism that can incorporate any ONU sleep time computation scheme. An analytical model is proposed to compute the maximum sleep time of each ONU based on the maximum delay requirement of each CoS. Numerical and simulation results prove the correctness of the presented model, and highlight the advantages of our proposed solution. Our results also show that the proposed framework can take advantage of the sleep mode functionality at the ONUs to achieve maximum energy saving while maintaining the users' requirements.

We then address the collision problem that emerges from assigning different sleep time values to the ONUs that are expected to access the shared media directly upon waking up. A new sleep time sizing mechanism, namely Sort-And-Shift, is proposed to effectively synchronize the sleep times of all ONUs without compromising their total assigned sleep time values. Our simulation results verify the effectiveness of the proposed scheme and prove its optimality.

Chapter 6

Conclusion and Future Work

6.1 Conclusion

The integration of EPON and WiMAX has been lately presented as a promising candidate for the realization of high-speed and mobile fiber-wireless backhaul-access networks. However, the integration carries several research challenges such as, but not limited to, integrated resource management, QoS mapping and support, mobility management, and handover, which require effective solutions.

Meanwhile, mission-critical networks have been attracting researchers from both the academia and industry. These types of networks currently suffer from having the employed MC solutions (e.g., TETRA networks) incapable of supporting the emerging MC applications. Thus, alternative solutions are required to address this challenging problem.

Recently, energy efficiency has been considered as one of the biggest challenges in the operation of modern telecom networks. Although it has been well investigated in wireless networks, energy efficiency in optical networks (access and backbone) in general and in NG-PON in specific, is currently being investigated and standardized.

In this thesis, we address all these challenges and porpose effective solutions.

More specifically, after presenting the introduction, background, and related work in Chpaters 1 and 2, we propose in Chapter 3 a new architecture, namely MC-FiWiBAN, to support mission-critical services over the EPON-WiMAX integration. This is mainly achieved via building Layer-2 VPNs over the integration. With MC-FiWiBAN, we define various MC operational themes such as fault-tolerance and error recovery. We also offer a resource management platform to facilitate the design and implementation of bandwidth allocation and admission control schemes.

In Chapter 4, we address the resource management problem that arises from the construction of VPNs over a shared infrastructure. A new framework is proposed, namely WiMAX-V**P**ON, which consists of a new QoS-provisioning paradigm, two new AC schemes (involving the collaboration of the SS, ONU-BS, and OLT), and a novel DBA mechanism. The first AC scheme is measurement-based, and it admits a real-time flow it there is enough bandwidth in both the optical and wireless domains to accommodate its data rate. The second scheme is delay-based, and it admits a real-time flow if its expected delay (which is computed via a new analytical model) is less than the maximum delay requirement. Best-effort traffic is always admitted under both schemes, and it is guaranteed a minimum per-VPN throughput. The framework provides E2E bandwidth and delay guarantees for admitted VPN services. Simulation results prove the effectiveness of the proposed solutions and highlight their benefits.

Finally in Chapter 5, we address the energy efficiency problem in optical access networks. We propose a new green bandwidth allocation (GBA) scheme which enables batch-mode transmissions at the OLT and ONUs so as to minimize the total overhead time caused by switching the ONU from the sleep state to the active state. With GBA, we also propose a new sleep sizing mechanism which eliminates any possible collision caused by scheduling multiple ONUs to wake up and transmit/receive traffic simultaneously. The ONU sleep time computation is done via a new analytical model which computes the ONU sleep time based on the maximum delay requirements so as to achieve maximum energy saving.

6.2 Future Work

6.2.1 MC-FiWiBAN-related Future Work

With the new architecture, mobility management emerges as a crucial theme that requires efficient solutions. Namely, not only seamless handoff/handover techniques are required, but also scenarios where PSDR users roam between TETRA and MC-FiWiBAN coverage zones, will require special handover protocols that consider the physical layer heterogeneity of both networks. Furthermore, important VPN related issues such as VPN gateway design and configuration, require special attention and effective solutions. Finally, advanced VPN resource management paradigms can be designed to improve the network utilization while maintaining the desired MC service performance. More specifically, the following resource management themes may be investigated:

Adaptive Bandwidth Reservation

A new bandwidth allocation/reservation scheme can be designed to adaptively set the value of α according to the bandwidth demand and availability, as well as the stream's delay-tolerance. In some cycles, more bandwidth may be allocated (depending on the value α) for lower priority traffic (e.g., BE) in order to increase its throughput and the overall network utilization, while maintaining the QoS performance of admitted real-time VPN services.

Channel-Aware Bandwidth Management

Our proposed WiMAX-V**P**ON framework guarantees bandwidth for supported VPN services of a certain user/SS, as long as the PHY rate of the SS does not go below the total admitted guaranteed rate.

To resolve this problem, the idea of *backup* bandwidth which has gained tremendous success in optical backbone WDM networks [80], may be applied. More specif-

ically, a portion of the OFDM frame (denoted ψ) may be reserved and used to provide bandwidth guarantees for "unstable" mobile users. However, the bandwidth of current WIMAX networks is considered *modest*. Therefore, the idea of backup bandwidth should be customized to fit the limited network resources of wireless networks. In addition, due to this bandwidth limitation, such a realization is considered almost impossible when the network load is high. Therefore, a certain *degree* of throughput (denoted ξ) may be claimed for the unstable users. As a result, the following research questions need to be answered:

- How much backup should be reserved for the unstable users, while achieving fairness among users belonging to different VPNs. In other words, what is the optimal value of ψ?
- What is the portion of ψ that should be computed for each unstable user?
- What is the maximum degree value ξ that can be attained while meeting all the QoS requirements?

To answer those questions, a new channel-aware bandwidth management scheme should be designed to compute the optimal backup percentage value required for each fluctuating/unstable user, given a certain throughput *degree* requirement.

Service Type-based Admission Control

To efficiently provision MC and non-MC services over the same carrier, a new AC scheme may be designed to admit flows based on the type and requirements of each service request. That is in addition to its QoS requirements, a flow can be categorized as 1) *public* (i.e., belonging to no VPN), 2) *private* (i.e., belonging to a certain supported VPN) or 3) *unknown private* (i.e., belonging to an unsupported VPN).

Preemptive Delay-based Admission Control

The proposed DAC engine computes the expected end-to-end delay for non-preemtipve services and then admits/rejects their flows accordingly. The existence of EGS services in the network requires measuring the expected delay under the assumption that lower-priority services might be preempted, even though such a scenario is envisioned to rarely occur due to the sporadic arrivals of EGS flows.

6.2.2 Green NG-PON-related Future Work

In the future work in this topic, the following areas can be explored:

Sleep Time Bound Analysis

Due to the uncertainty of Internet traffic, bound analysis on the sleep time for ONUs, under both the Direct ONU Transmission and Request After Sleep scenarios, is critical in pushing the proposed framework into practical deployment. Thus, a suite of closed-form expressions can be determined for the upper and lower bounds on the possible ONU sleep time while statitically meeting the user's QoS requirements. Such bounds can provide a design guideline for the ONU sleep time selection, in order to take the best advantage of the advances in ONU architectures and explore the user's QoS tolerance while achieving maximum power efficiency.

OLT Sleep under GBA

As mentioned in Section 5.2, GBA can allow the OLT to go into the sleep mode while other ONUs are sleeping, which will introduce significant energy saving in the system. However, new OLT architectures and sleep control mechanisms will be required to allow the OLT to go into the sleep mode without interrupting the system's operation.

Renewable Energy in NG-PONs

Renewable energy is being envisaged to replace traditional hydrocarbon energy that currently feeds most existing networks. This will not only reduce the carbon footprint, but will also facilitate the transition towards a sustainable and environment-friendly world [21]. In NG-PONs, this can be achieved by deploying the network elements (i.e., OLT and ONUs) at locations where renewable energy can exist. Nonetheless, this realization is restricted by some network constraints such as power budget, split ratio, network reach, and high propagation delay. This will implicate new challenges and issues subject to careful investigations.

Energy Saving in Fiber-Wireless Networks

The FiWi network imposes additional challenges and considerations when energy saving is in context. We list few as follows:

- The fact that wireless technologies (e.g., WiMAX) have their own energy saving standards makes the energy saving mechanism implemented in the optical domain dependent on the one implemented in the wireless domain. Therefore an efficient technique that can seamlessly integrate the energy saving schemes in both domains will then be required.
- Putting a FiWi ONU into the sleep mode not only depends on the traffic availability, but also on the channel conditions at the wireless BS and the mobile users.
- In wireless networks, similar to the OLT, the BS does not support the sleep functionality. However when an ONU-BS node is mounted, such an option becomes viable depending on the designed energy saving method.
- Energy-aware routing in the wireless domain (among wireless users) and in the optical domain (among ONU-BSs) also requires special consideration.

Summary of Notations

K : Number of VPNs

V_k : VPN k ($k = 1, \ldots, K$)

$\mathbf{M}$: Set of all ONUs/ONU-BSs (of size $|\mathbf{M}|$)

$\mathbf{M}^k$: Set of ONU-BSs provisioning V_k (of size $|\mathbf{M}^k|$)

$\mathbf{N}$: Set of all SSs (of size $|\mathbf{N}|$)

$\mathbf{N}_j^k$: Set of SSs connecting to V_k through ONU-BS j (of size $|\mathbf{N}_j^k|$)

n : Number of supported CoSs

c : class of service (CoS) index ($c = 1, \ldots, n$)

i : SS/User/Client index ($i \in \mathbf{N}$)

j : ONU/ONU-BS index ($j \in \mathbf{M}$)

$\sigma_{c,i}$: Peak arrival data rate of user i and CoS c

$\delta_{c,i}$: Maximum Burst Size of user i and CoS c

$\theta_{c,i}^k$: Queuing delay bound of user i, CoS c and VPN k

$\overline{\lambda}_{c,i}$: Mean data rate of user i and CoS c

$\lambda_{c,i}$: Guaranteed data rate of user i and CoS c

λ_j^{ds} : Downstream traffic data rate for ONU j

$\mu_{c,i}$: Service rate of CoS c and user i

μ_i : Service rate of user i

MS : MSDU Size

S_b : DTLB bucket size

S_q : Buffering queue size

$P_{error,i}$: Frame error probability pertaining to user i

$\mathcal{C}_{pon}$: PON transmission speed

α^k : V_k's BE traffic portion

β : Non-VPN services' bandwidth portion

B^k_{min} : Minimum bandwidth reserved for V_k

T^{pon}_{eff} : Effective PON upstream cycle time

T^{up}_{fi} : Upstream fiber/optical cycle time

T^{up}_{wi} : Uplink wireless cycle time

w_k : Weight of V_k

rs_i : Received signal at user i

g_i : Channel gain at user i

ts_i : Transmitted signal by user i

bn_i : Background noise at user i

me_i : Multi-path fading effect at user i

d_i : Distance between client/SS/ONU i and Server/ONU-BS/OLT

fe_i : Shadow fading effect at user i

SNR_i : Signal-to-noise ratio for user i

$\mathcal{P}_i$: Receiving power at user i

$\mathcal{V}_{bn}$: Background noise variance

O_d : Number of OFMD data subcarriers

T_{sym} : OFDM symbol duration

$CR(x)$: Coding rate pertaining to AMC mode x

$\mathcal{W}_{sc}(x)$: Number of coded bits per subcarrier pertaining to AMC mode x

$\mathcal{B}(x)$: Bits per OFDM symbol pertaining to AMC mode x

$\mathcal{C}_i(x)$: User i's transmission speed pertaining to AMC mode x

$\overline{\mathcal{C}}$: Average transmission rate in the wireless domain

w_j^k : Weight of ONU-BS j on V_k

$w_{i,j}^k$: Weight of SS i on V_k, connecting through ONU-BS j

$\mathcal{R}_j^{k,be}$: Reserved rate of V_k's BE traffic at ONU-BS j

$\mathcal{R}_{i,j}^{k,be}$: Reserved rate of V_k's BE traffic at SS i through ONU-BS j

$\mathcal{R}_{be}$: Total reserved BE traffic rate

$np_{f,i}$: Number of packets required to satisfy flow f of user i

T_{wi}^{rt} : Wireless real-time sub-cycle time period

T_{fi}^{rt} : Fiber/optical real-time sub-cycle time period

$T_{wi}^{k,be}$: Wireless V_k BE sub-cycle time period

$T_{fi}^{k,be}$: Fiber/optical V_k BE sub-cycle time period

T_i^{rt} : SS i time share in the wireless real-time sub-cycle

T_j^{rt} : ONU-BS j time share in the optical real-time sub-cycle

$T_i^{k,be}$: SS i time share in V_k's wireless BE sub-cycle

$T_j^{k,be}$: ONU-BS j time share in V_k's optical BE sub-cycle

$B_{f,i}^{g}$: Guaranteed bandwidth for flow f of user i

$F_{f,i}$: Number of OFMD symbols allocated for flow f of user i

$B_{be,i}^{alloc}$: Allocated bandwidth for BE traffic of user i

NBR : Nominal bandwidth ratio

T_{ir} : Initial ranging period

T_{dl} : Downlink frame length

T_{wi}^{f} : Total wireless frame size ($T_{wi}^{f} = T_{wi}^{up} + T_{dl}$)

T_{cp} : Request contention period

T_i^{prop} : Message propagation time to user i

T_{dba} : DBA computation time

T_{gba} : GBA computation time

T_{gr}^{proc} : Grant message processing time

T_{gr}^{tran} : Grant message transmission time

T_g^a : Guard time/Preamble in the active period between two nodes

T_g^{gr} : Guard time between two grants

T_{br}^{tran} : Request message transmission time

T_{br}^{proc} : Request message processing time

T_j^s : Total sleep time of ONU j

$T_j^{s,1}$: OLT-based sleep time of ONU j

$T_j^{s,2}$: ONU-based sleep time of ONU j

T_j^{tran} : Data transmission time of ONU j

T_j^{recv} : Data receiving time of ONU j

T_j^{idle} : Idle time of ONU j

T_j^{o} : Total overhead time of ONU j

$T_j^{o,1}$: *Cyclic* overhead time of ONU j

$T_j^{o,1}$: *Doze* overhead time of ONU j

T_j^{rec} : Clock recovery time of ONU j

T_j^{sync} : Clock synchronization time of ONU j

T_j^{laser} : Time spent by the transceiver's laser to be ready for ONU j

E_{pon} : Energy spent by a single PON system

E_{olt} : Energy spent by the OLT

E_j : Energy spent by ONU j

E_j^a : Energy spent by ONU j in the active state

E_j^s : Energy spent by ONU j in the sleep state

E_j^o : Energy spent by ONU j in the overhead period

P_j^a : Power consumed by ONU j in the active state

P_j^s : Power consumed by ONU j in the sleep state

t_j^0 : Instant time when the grant message is received and processed by ONU j

t_j^{st} : Instant time of ONU j's transmission start time

t_j^{end} : Instant time of ONU j's transmission end time

h_j : Shifted sleep time for ONU j

C_j : ONU j sleep cycle

AI_i : Active/Access interval of client i

I : Wireless uplink sub-frame idle time

U : Wireless Uplink sub-frame utilization

v_c : Client/control vacation time

$v_{s,i}$: Vacation time spent serving user i

v_{be} : Best-effort vacation time

v_i : Total vacation time for user i

m : Number of clients connecting to one server (wireless or wired)

$\rho_{c,i}$: Utilization factor per class c at client i

ρ_i : Utilization factor per client i

D_c^k : End-to-End delay of CoS c belonging to V_k

$\mathbb{D}_c^k$: End-to-End delay bound of CoS c belonging to V_k

$\overline{X_{c,i}}$: The first moment of a CoS c packet's transmission time of client i

$\overline{X_{c,i}^2}$: The second moment of a CoS c packet's transmission time of client i

$S_{c,i}$: Number of CoS c packets serviced for client i

$L_{c,i}$: Number of vacation intervales seen by a packet of CoS c and client i

L_i : Number of vacation intervales seen by a packet of client i

$W_{c,i}$: Waiting time in queue of CoS c and client i

$N_{c,i}$: Total number of backlogged CoS c packets at client i

N_i : Total number of backlogged packets at client i

R_i : Residual service time seen by a packet arriving to client i

$R_{c,j}$: Residual service time seen by a packet arriving to CoS c of ONU j

Y_i : The reservation/gap interval seen by a packet arriving to client i

$Q_{c,i}$: Queue size of CoS c and client i

$Z_{c,j}$: The amount of work spent by the server for CoS c of ONU j

$\overline{V_j}$: The first moment of the vacation time for ONU j

$\overline{V_j^2}$: The second moment of the vacation time for ONU j

Glossary

A

ABC - Always Best Connected

AC - Admission Control

ACU - Admission Control Unit

AF - Assured Forwarding

ALR - Adaptive Link Rate

AMC - Adaptive Modulation and Coding

AP - Access Point

APON - ATM Passive Optical Network

AR - Access Router

ARP - Address Resolution Protocol

ARQ - Automatic Repeat reQuest

ATM - Asynchronous Transfer Mode

B

BE - Best Effort

BER - Bit Error Rate

BPSK - Binary Phase Shift Keying

BS - Base Station

BWA - Broadband Wireless Access

C

CBR - Constant Bit Rate

CE - Customer Edge

CM - Cable Modem

CO - Central Office

CoS - Class of Service

CSI - Channel State Information

D

DBA - Dynamic Bandwidth Allocation

DCS - Downstream Centric Scheme

DiffServ - Differentiated Services

DL - Downlink

DL-MAP - Downlink MAP message

DSL - Digital Subscriber Loop

DTLB - Dual Token Leaky Bucket

E

ECG - Electrocardiogram

EF - Expedited Forwarding

EGS - Emergency Grant Service

EPON - Ethernet Passive Optical Network

ertPS - extended real-time Polling Service

ETSI - European Telecommunications Standards Institute

F

FBA - Fixed Bandwidth Allocation

FDD - Frequency Division Multiplexing

FEC - Forward Error Correcting

Fi - Fiber

FiWi - Fiber-Wireless

FMC - Fixed Mobile Convergence

FTP - File Transfer Protocol

FTTB - Fiber To The Building

FTTC - Fiber To The Curb

FTTH - Fiber To The Home

FTTW - Fiber To The Wireless

FTTX - Fiber To The X

G

GBA - Green Bandwidth Allocation

G-EPON - Gigabit Ethernet Passive Optical Network

GPC - Grant Per Connection

GPON - Gigabit Passive Optical Network

GPSS - Grant Per Subscriber Station

GR-ONU - Green ONU

GSM - Global Systems for Mobile Communications

H

HDTV - High Definition Television

I

ICT - Information and Communications Technology

IEEE - Institute of Electrical and Electronics Engineers

IGW - Internet Gateway

IntServ - Integrated Services

IP - Internet Protocol

ISDN - Integrated Services Digital Network

J,K

L

LAN - Local Area Network

Layer 2 - Data Link (MAC) Layer

LOS - Line of Sight

LR-PON - Long Reach Passive Optical Network

LTE - Long Term Evolution

M

MAC - Medium Access Control

MAN - Metropolitan Area Network

MC - Mission-Critical

MoF - Microwave over Fiber

MPCP - Multi-Point Control Protocol

MPLS - Multi-Protocol Label Switching

MS - Mobile Station

MSDU - MAC Service Data Unit

N

NG-PON - Next-Generation Passive Optical Network

NLOS - Non-Line of Sight

nrtPS - non-real-time Polling Service

O

ODN - Optical Distribution Network

OFDM - Orthogonal Frequency Division Multiplexing

OFDMA - Orthogonal Frequency Division Multiple Access

OLT - Optical Line Terminal

ONU - Optical Network Unit

P

P2MP - Point-to-Multipoint

P2P - Point-to-Point

PCU - Policy Control Unit

PDU - Protocol Data Unit

PE - Provider Edge

PHY - Physical

PI - Polling Interval

PLOAM - Physical Layer Operations and Maintenance

PON - Passive Optical Network

PQ - Priority Queue

PSDR - Public Safety and Disaster Relief

Q

QAM - Quadrature amplitude modulation

QoS - Quality of Service

QPSK - Quadrature Phase Shift Keying

R

ROF - Radio Over Fiber

RR - Round Robin

rtPS - real-time Polling Service

RT - Real-Time

RTT - Round Trip Time

S

SAP - Service Access Point

SAS - Sort-And-Shift

SBA - Static Bandwidth Allocation

SLA - Service Level Agreement

SNR - Signal-to-Noise Ratio

SP - Strict Priority

SS - Subscriber Station

T

TDD - Time Division Duplex

TDM - Time Division Multiplexing

TDMA - Time Division Multiple Access

TETRA - TErrestrial Trunked RAdio

TSPEC - Traffic SPECifications

TW - Transmission Window

U

UCS - Upstream Centric Scheme

UGS - Unsolicited Grant Service

UL - Uplink

UL-MAP - Uplink MAP message

V

VBR - Variable Bit Rate

VoD - Video on Demand

VoIP - Voice over IP

VPN - Virtual Private Network

VPON - VPN-PON

W

WAN - Wide Area Network

WDM - Wavelength Division Multiplexing

WDM-PON - WDM Passive Optical Network

Wi - Wireless

WLAN - Wireless Local Area Network

WiMAX - Worldwide Interoperability for Microwave Access

WMAN - Wireless Metropolitan Area Network

WRR - Weighted Round Robin

X,Y,Z

References

[1] M. Garcia, D. F. Garcia, V. G. Garcia, and R. Bonis, "Analysis and Modeling of Traffic on a Hybrid Fiber-Coax Network," *IEEE Journal of Selected Areas in Communications (JSAC)*, vol. 22, no. 9, pp. 1718–1730, Nov. 2004. 2

[2] "Organization For Economic Co-Operation and Development." [Online]. Available: http://www.oecd.org 2

[3] J.-I. Kani, F. Bourgart, A. Cui, A. Rafel, and S. Rodrigues, "Next-Generation PON—Part 1: Technology Roadmap and General Requirements," *IEEE Communications Magazine*, vol. 47, no. 11, pp. 43–49, Nov. 2009. 3, 4, 9, 35

[4] G. Shen, R. S. Tucker, and C.-J. Chae, "Fixed Mobile Convergence Architectures for Broadband Access: Integration of EPON and WiMAX," *IEEE Communications Magazine*, vol. 45, no. 8, pp. 44–50, Aug. 2007. 5, 21, 22, 28, 46, 64, 66

[5] S. Sarkar, S. Dixit, and B. Mukherjee, "Hybrid Wireless-Optical Broadband-Access Network (WOBAN): A Review of Relevent Challenges," *IEEE/OSA Journal of Lightwave Technology (JLT)*, vol. 25, no. 11, pp. 3329–3340, Novemeber 2007. 5, 21, 28, 50

[6] J. She and P.-H. Ho, "Cooperative Coded Video Multicast for IPTV Services under EPON-WiMAX Integration," *IEEE Communications Magazine*, vol. 46, no. 8, pp. 104–110, Aug. 2008. 5

[7] M. Vrdoljak, S. I. Vrdoljak, and G. Skugor, "Fixed-Mobile Convergence Strategy: Technologies and Market Opportunities," *IEEE Communications Magazine*, vol. 38, no. 2, pp. 116 – 121, Feb. 2000. 5

[8] *Terrestrial Trunked Radio (TETRA); Voice plus Data (V+D); Part 2: Air Interface (AI)*, Online, ETSI EN 300 392-2 V2.5.2, May 2006. 6, 44

[9] "TETRA." [Online]. Available: http://www.tetramou.com/ 6

[10] A. K. Salkintzis, "Evolving Public Safety Communication Systems by Integrating WLAN and TETRA Networks," *IEEE Communications Magazine*, vol. 44, no. 1, pp. 38–46, Jan. 2006. 7, 44

[11] Project MESA. [Online]. Available: www.projectmesa.org 7, 45

[12] "MOTOA4." [Online]. Available: http://business.motorola.com/MOTOA4/index.html 7

[13] "International Energy Outlook 2010." [Online]. Available: http://www.eia.doe.gov/oiaf/ieo/world.html 7

[14] "GreenTouch." [Online]. Available: http://www.greentouch.org 8

[15] M. Gupta and S. Singh, "Greening of the Internet," in *Proceedings of ACM SIGCOMM'03*, Karlsruhe, Germany, Aug. 2003, pp. 19–26. 8

[16] K. J. Christensen, C. Gunaratne, B. Nordman, and A. D. George, "The Next Frontier for Communications Networks: Power Management," *Elsevier Computer Communications*, vol. 27, no. 18, pp. 1758–1770, Dec. 2004. 8

[17] "IEEE Standard for Local and Metropolitan Area Networks Part 16: Air Interface for Fixed Broadband Wireless Access Systems," Online, 2004. 9, 14, 20, 53, 54, 75, 80

[18] K. Christensen, P. Reviriego, B. Nordman, M. Bennett, M. Mostowfi, and J. A. Maestro, "IEEE 802.3az: The Road to Energy Efficient Ethernet," *IEEE Communications Magazine*, vol. 48, no. 11, pp. 50–56, Nov. 2010. 9

[19] M. Gupta and S. Singh, "Using Low-power Modes for Energy Conservation in Ethernet LANs," in *Proceedings of IEEE INFOCOM'07*, Anchorage, Alaska, USA, May 2007. 9

[20] J. Baliga, R. Ayre, K. Hinton, W. V. Sorin, and R. S. Tucker, "Energy Consumption in Optical IP Networks," *IEEE/OSA Journal of Lightwave Technology*, vol. 27, no. 13, pp. 2391–2403, July 2009. 9

[21] Y. Zhang, P. Chowdhury, M. Tornatore, and B. Mukherjee, "Energy Efficiency in Telecom Optical Networks," *IEEE Communications Surveys & Tutorials*, vol. 12, no. 4, pp. 441–458, Nov. 2010. 9, 155

[22] G. Shen and R. S. Tucker, "Energy-Minimized Design for IP over WDM Networks," *IEEE/OSA Journal of Optical Communications and Networking*, vol. 1, no. 1, pp. 176–186, June 2009. 9

[23] ITU-T, "GPON power conservation." [Online]. Available: http://www.catr.cn/radar/itut/201007/P020100707531463472537.pdf 9, 31, 34, 36, 121

[24] J. Mandin, "EPON Power Saving via Sleep Mode." [Online]. Available: http://www.ieee802.org/3/av/public/2008-09/3av_0809_mandin_4.pdf 9, 31, 34, 41

[25] G. Kramer and G. Pesavento, "Ethernet Passive Optical Network (EPON): Building A Next-Generation Optical Access Network," *IEEE Communications Magazine*, vol. 40, no. 2, pp. 66–73, February 2002. 12

[26] IEEE 802.3ah Task Force Home Page. [Online]. Available: http://www.ieee802.org/3/efm 12, 53, 54

[27] G. Kramer, B. Mukherjee, and G. Pesavento, "IPACT A Dynamic Protocol For An Ethernet PON (EPON)," *IEEE Communications Magazine*, vol. 40, no. 2, pp. 74–80, February 2002. 13, 14, 26, 27, 68, 95, 128

[28] N. Ghani, A. Shami, C. M. Assi, and Y. Raja, "Intra-ONU Bandwidth Scheduling in Ethernet Passive Optical Networks," *IEEE Communications Letters*, vol. 8, no. 11, pp. 683 – 685, Nov. 2004. 14

[29] A. R. Dhaini, C. M. Assi, A. Shami, and N. Ghani, "Adaptive Fairness through intra-ONU Scheduling for Ethernet Passive Optical Networks," in *Proceedings of IEEE International Conference on Communications (ICC'06)*, Istanbul, Turkey, June 2006. 14

[30] M. P. McGarry, M. Maier, and M. Reisslein, "Ethernet PONs: A Survey of Dynamic Bandwidth Allocation (DBA) Algorithms," *IEEE Communications Magazine*, vol. 42, no. 8, pp. S8–15, August 2004. 14

[31] C. So-In, R. Jain, and A.-K. Tamimi, "Scheduling in IEEE 802.16e Mobile WiMAX Networks: Key Issues and a Survey," *IEEE Journal of Selected Areas in Communications (JSAC)*, vol. 27, no. 2, pp. 156–171, February 2009. 19, 25

[32] Y. Luo, S. Yin, T. Wang, Y. Suemura, S. Nakamura, N. Ansari, and M. Cvijetic, "QoS-Aware Scheduling over Hybrid Optical Wireless Networks," in *Proceedings of Optical Fiber Communication and the National Fiber Optic Engineers Conference (OFC/NFOEC'07)*, March 2007, pp. 1–7. 21, 27, 49, 62, 95

[33] H.-T. Lin, Y.-Y. Lin, W.-R. Chang, and S.-M. Chen, "A Game-Theoretic Framework for Intra-ONU Scheduling in Integrated EPON/WiMAX Networks," in *Proceedings of IEEE GLOBECOM'09*, Hawaii, USA, Dec. 2009. 21, 26

[34] M. Luo, H. Li, Y. Lu, and Y. Ji, "QoS-Aware Scheduling in Emerging Novel Optical Wireless Integrated Networks," in *Challenges for Next Generation Network Operations and Service Management*. Springer Berlin / Heidelberg, October 2008, pp. 445–448. 21, 26, 49, 62, 95

[35] B. Jung, J. Choi, Y.-T. Han, M.-G. Kim, and M. Kang, "Centralized Scheduling Mechanism for Enhanced End-to-End Delay and QoS Support in Integrated Architecture of EPON and WiMAX," *IEEE/OSA Journal of Lightwave Technology (JLT)*, Early Access 2010. 21, 26

[36] Y. Yan, H. Yu, H. Wang, and L. Dittmann, "Integration of EPON and WiMAX Networks: Uplink Scheduler Design," in *Proceeding of Asia-Pacific Optical Communications (APOC)*, Hangzhou, China, Oct. 2008. 21, 27, 49, 62, 95

[37] K. Yang, S. Ou, G. Ken, and H.-H. Chen, "Convergence of Ethernet PON and IEEE 802.16 Broadband Access Networks and its QoS-Aware Dynamic Bandwidth Allocation Scheme," *IEEE Journal of Selected Areas in Communications*, vol. 27, no. 2, pp. 101–116, Feb. 2009. 21, 25, 26, 49, 62, 66, 92, 95, 96

[38] C. M. Assi, Y. Ye, S. Dixit, and M. Ali, "Dynamic bandwidth Allocation for Quality-of-Service Over Ethernet PONs," *IEEE Journal of Selected Areas in Communications (JSAC)*, vol. 21, no. 9, pp. 1467–1477, Novemeber 2003. 26, 95, 134

[39] G. Kramer, B. Mukherjee, S. Dixit, Y. Ye, and R. Hirth, "Supporting Differentiated Classes of Service in Ethernet Passive Optical Networks," *OSA Journal of Optical Networking*, vol. 1, no. 8/9, pp. 280–298, Aug. 2002. 28, 134

[40] S. Wong, L. Valcarenghi, S. Yen, D. R. Campelo, S. Yamashita, and L. Kazovsky, "Sleep Mode for Energy Saving PONs: Advantages and Drawbacks," in *Proceedings of IEEE GLOBECOM'09*, Hawaii, USA, Dec. 2009. 33, 34

[41] B. Schrenk, F. B. Bo, J. Bauwelinck, J. Prat, and J. A. Lazaro, "Energy-Efficient Optical Access Networks Supported by a Noise-Powered Extender Box," *IEEE Journal of Selected Topics in Quantum Electronics*, Aug. 2010, to appear, early access: DOI 10.1109/JSTQE.2010.2053839. 33, 35

[42] S. S. W. Lee and A. Chen, "Design and Analysis of a Novel Energy Efficient Ethernet Passive Optical Network," in *Proceedings of ICN'10*, French Alps, France, April 2010. 33, 37, 40

[43] S.-W. Wong, S.-H. Yen, P. Afshar, S. Yamashita, and L. G. Kazovsky, "Demonstration of Energy Conserving TDM-PON with Sleep Mode ONU using Fast Clock Recovery Circuit," in *Proceedings of OFC/NFOEC'10*, ser. OthW7, San Diego, CA, USA, March 2010. 33, 38, 40

[44] Y. Yan, S.-W. Wong, L. Valcarenghi, S.-H. Yen, D. R. Campelo, S. Yamashita, L. Kazovsky, and L. Dittmann, "Energy Management Mechanism for Ethernet Passive Optical Networks (EPONs)," in *Proceedings of IEEE International Conference on Communications (ICC'10)*, Cape Town, South Africa, May 2010. 33, 38, 40, 122, 125, 142

[45] L. Valcarenghi, S.-W. Wong, D. R. Campelo, S.-H. Yen, S. Yamashita, P. G. Raponi, L. Kazovsky, and P. Castoldi, "Energy Efficiency in Optical Access Networks," in *Italian Networking Workshop*, Cavalese, Italy, Jan. 2011. 33, 38, 40

[46] J. Zhang and N. Ansari, "Toward Energy-Efficient 1G-EPON and 10G-EPON with Sleep-Aware MAC Control and Scheduling," *IEEE Communications Magazine*, vol. 49, no. 2, pp. S33–S38, Feb. 2011. 33, 39, 40, 131

[47] R. Kubo, J.-I. Kani, H. Ujikawa, T. Sakamoto, Y. Fujimoto, N. Yoshimoto, and H. Hadama, "Study and Demonstration of Sleep and Adaptive Link Rate Control Mechanisms for Energy Efficient 10G-EPON," *IEEE/OSA Journal of Optical Communications and Networking*, vol. 2, no. 9, pp. 716–729, Sep. 2010. 33, 39

[48] L. Shi, S.-S. Lee, H. Song, and B. Mukherjee, "Energy-Efficient Long-Reach Passive Optical Network: A Network Planning Approach Based on User Behaviors," *IEEE Systems*, vol. 4, no. 4, pp. 449–457, Dec. 2010. 33, 41

[49] "IEEE 802.3az Energy Efficient Ethernet Task Force." [Online]. Available: http://www.ieee802.org/3/az/index.html 31

[50] S. Electric, "Technical Specification for Optical Transceiver Module." [Online]. Available: http://www.coretk.com/CataLog/cata_img/FILE/1524076778/SEI/57/72/57_72_1061773162.pdf 34

[51] B. Skubic and D. Hood, "Evaluation of ONU Power Saving Modes for Gigabit-Capable Passive Optical Networks," *IEEE Network*, vol. 25, no. 2, pp. 20–24, Mar./Apr. 2011. 37, 120, 122

[52] W. Luo, C. Pignataro, A. Y. H. Chan, and D. Bokotey, *Layer-2 VPN Architecture*. CISCO Press, 2005. 42, 45, 46

[53] N. Nadarajah, E. Wong, and A. Nirmalathas, "Implementation of Multiple Secure Virtual Private Networks Over Passive Optical Networks Using Electronic CDMA," *IEEE Photonics Technology Letters*, vol. 18, no. 3, pp. 484–486, February 2006. 45

[54] R. Isaacs and I. Leslie, "Support for Resource-Assured and Dynamic Virtual Private Networks," *IEEE Journal of Selected Areas in Communications (JSAC)*, vol. 19, no. 3, pp. 460–472, March 2001. 46

[55] X. Bai, A. Shami, and Y. Ye, "Robust QoS Control for Single Carrier PMP Mode IEEE 802.16 System," *IEEE Transactions on Mobile Computing*, vol. 7, no. 4, pp. 416–429, April 2008. 49, 62

[56] S. Spadaro, J. Solé-Pareta, D. Careglio, K. Wajda, and A. Szymanski, "Positioning of the RPR Standard in Contemporary Operator Environments," *IEEE Network*, vol. 18, no. 2, pp. 35–40, Mar. 2004. 50

[57] S. Sarkar, H.-H. Yen, S. Dixit, and B. Mukherjee, "A Novel Delay-Aware Routing Algorithm (DARA) for a Hybrid Wireless-Optical Broadband Access Network (WOBAN)," *IEEE Network*, vol. 22, no. 3, pp. 20–28, May 2008. 50

[58] S.-E. Elayoubi and B. Fourestié, "Performance Evaluation of Admission Control and Adaptive Modulation in OFDMA WiMax Systems," *IEEE/ACM Transactions on Networking*, vol. 16, no. 5, pp. 1200–1211, Oct. 2008. 56, 58

[59] C.-T. Chou, S. S. N, and K. G. Shin, "Achieving Per-Stream QoS with Distributed Airtime Allocation and Admission Control in IEEE 802.11e Wireless LANs," in *Proceedings of IEEE INFOCOM'05*, Miami, FL, Mar. 2005, pp. 1584–1595. 57, 69, 95

[60] A. R. Dhaini, C. M. Assi, M. Maier, and A. Shami, "Per-Stream QoS and Admission Control in Ethernet Passive Optical Networks (EPONs)," *IEEE/OSA Journal of Lightwave Technology (JLT)*, vol. 25, no. 7, pp. 1659–1669, July 2007. 57, 67, 75, 134

[61] A. Elwalid and D. Mitra, "Traffic Shaping at a Network Node: Theory, Optimum Design, Admission Control," in *Proceedings of IEEE INFOCOM'97*, Kobe, Japan, April 1997. 58

[62] D. Niyato and E. Hossain, "Queue-Aware Uplink Bandwidth Allocation and Rate Control for Polling Service in ieee 802.16 Broadband Wireless Networks," *IEEE Transactions on Mobile Computing*, vol. 5, no. 6, pp. 668–679, June 2006. 59, 73

[63] A. S. Reaz, V. Ramamurthi, S. Sarkar, D. Ghosal, S. Dixit, and B. Mukherjee, "CaDAR: An Efficient Routing Algorithm for a Wireless–Optical Broadband Access Network (WOBAN)," *IEEE/OSA Journal of Optical Communications and Networking (JOCN)*, vol. 1, no. 5, pp. 392–403, Oct. 2009. 64

[64] J. G. Andrews, A. Ghosh, and R. Muhamad, *Fundamentals of WIMAX: Understanding Broadband Wireless Networking*. Prentice Hall, 2007. 65, 95, 98

[65] S. Catreux, P. F. Driessen, and L. J. Greenstein, "Data Throughputs using Multiple-Input Multiple-Output (MIMO) Techniques in a Noise-Limited Cellular Environment," *IEEE Transactions on Wireless Communications*, vol. 1, no. 2, pp. 226–234, April 2002. 65

[66] A. Doufexi, S. Armour, M. Butler, A. Nix, D. Bull, and J. McGeehan, "A Comparison of the HIPERLAN/2 and IEEE 802.11a Wireless LAN Standards," *IEEE Communications Magazine*, vol. 37, no. 12, pp. 172–180, May 2002. 66

[67] Q. Liu, S. Zhou, and G. B. Giannakis, "Queuing With Adaptive Modulation and Coding Over Wireless Links: Cross-Layer Analysis and Design," *IEEE Transactions on Wireless Communications*, vol. 4, no. 3, pp. 1142–1153, May 2005. 66

[68] B. O. Obele, M. Iftikhar, S. Manipornsut, and M. Kang, "Analysis of the Behavior of Self-Similar Traffic in a QoS-Aware Architecture for Integrating WiMAX and GEPON," *IEEE/OSA Journal of Optical Communications and Networking*, vol. 1, no. 4, pp. 259–273, Sep. 2009. 73

[69] B. Sikdar, "Queueing Analysis of Polled Service Classes in the IEEE 802.16 MAC Protocol," *IEEE Transactions on Wireless Communications*, vol. 8, no. 12, pp. 5767–5772, Dec. 2009. 73

[70] B.-J. Chang, C.-M. Chou, and Y.-H. Liang, "Markov chain analysis of uplink subframe in polling-based WiMAX networks," *Elsevier Computer Communications*, vol. 31, no. 10, pp. 2381–2390, June 2008. 73

[71] S. Bhatia, D. Garbuzov, and R. Bartos, "Analysis of the Gated IPACT Scheme for EPONs," in *Proceedings of IEEE International Conference on Communications (ICC'06)*, Istanbul, Turkey, 2006, pp. 2693 – 2698. 74, 135

[72] X. Bai, A. Shami, and Y. Ye, "Delay Analysis of Ethernet Passive Optical Networks with Quasi-leaved Polling and Gated Service Scheme," in *Proceedings of AccessNets'07*, Ottawa, ON, Canada, Aug. 2007. 74, 76, 84, 135

[73] D. Bertsekas and R. Gallager, *Data Networks*. Prentice-Hall, 1992. 76, 84, 88, 128, 130, 131

[74] O. J. Boxma and B. W. Meister, "Waiting-Time Approximations in Multi-Queue Systems with Cyclic Service," *Elsevier Performance Evaluation*, vol. 7, no. 1, pp. 59–70, Feb. 1987. 81

[75] A. Vargas. Omnet++. [Online]. Available: http://www.omnetpp.org/ 93, 131, 142

[76] Mindspeed, "Using Mindspeed Laser Drivers in PON burst-Mode Applications." [Online]. Available: http://www.mindspeed.com/web/download/download.jsp?docId=24461 122, 124

[77] O. J. Boxma and W. P. Groenendijk, "Pseudo-Conservation Laws in Cyclic-Service Systems," *Journal of Applied Probability*, vol. 24, no. 4, pp. 949–964, Dec. 1987. 129

[78] "ITU-T Recommendation G.1010: End-User Multimedia QoS Categories." [Online]. Available: http://www.catr.cn/radar/itut/201007/P020100707569992120755.pdf 134

[79] S. Bharati and P. Saengudomlert, "Analysis of Mean Packet Delay for Dynamic Bandwidth Allocation Algorithms in EPONs," *IEEE/OSA Journal of Lightwave Technology*, vol. 28, no. 23, pp. 3454–3462, Dec. 2010. 135

[80] P.-H. Ho and H. T. Mouftah, "A Framework of Service Guaranteed Shared Protection for Optical Networks," *IEEE Communications Magazine*, vol. 40, pp. 97–103, Feb. 2002. 152